THE
PHYSICAL REVIEW
A Journal of Experimental and Theoretical Physics
VOL. 45, NO. 11 JUNE 1, 1934 SECOND SERIES

The Scattering of a Beam of Potassium Atoms in Various Gases[1]

WALTER H. MAIS, *Columbia University*

(Received March 31, 1934)

A narrow beam of neutral K atoms was scattered in H_2, He, Ne, N_2, A and CO_2 at low pressures. The distribution of the scattered K atoms about the original beam was measured by the Langmuir-Taylor surface ionization detector. The experimental conditions were sufficiently refined that K atoms suffering very small angular deviations (down to about 4.5′ of arc) were counted as scattered atoms. The computed "effective collision radii" when compared with the values expected from the quantum theory of elastic sphere collisions show good agreement for H_2 and He. For the other gases, the experimental values are much larger, indicating the existence of considerable interatomic attractive forces even for Ne and A.

INTRODUCTION

THE kinetic theory of the collision of molecules treated as elastic spheres predicts a scattering function $I(\theta)$ which gives a uniform scattering per unit solid angle with respect to the centroid of the system composed of the two colliding molecules. In other words, all angles of scattering are equally probable. By the angle of scattering we mean the angle through which the relative velocity vector of the colliding molecules is turned. If the simple elastic sphere model is improved by the addition of a force field the scattering function will no longer be uniform but will give preference to scattering in the forward direction. This model will thus increase the probability of small angle scattering. However, if we attempt to use this revised model for computing collision cross sections it turns out that, as we define smaller and smaller deviations as collisions, the mean free path tends to zero and the collision cross section tends to become infinitely great.

The quantum theory[2,3] for the collision of elastic spheres at velocities corresponding to ordinary thermal agitation gives a marked preference for small angle scattering, in many respects similar to that of the classical theory of the scattering of elastic spheres, plus an attractive field of force. (See Fig. 1.) However, in the quantum theory, the total scattering even down to the smallest angles still remains finite. This is also true if we add an attractive field of force to the quantum theory of elastic spheres provided the interaction energy $V(r)$ vanishes at infinity faster than r^{-3}. Furthermore, since the large angle scattering is practically the same on both theories the extra scattering comes almost entirely from the small angle region. Small angles are defined as those for which $\theta \ll \pi/k\sigma_{12}$ where $k=2\pi\mu v/h$; μ being the reduced mass and v the relative velocity of the colliding molecules. Another result is that the total scattering on the basis of the quantum theory of elastic spheres is about twice the

[1] Mais and Rabi, Phys. Rev. **43**, 378 (1933).

[2] Mizushima, Phys. Zeits. **32**, 798 (1931).

[3] Massey and Mohr, Proc. Roy. Soc. **A141**, 434 (1933).

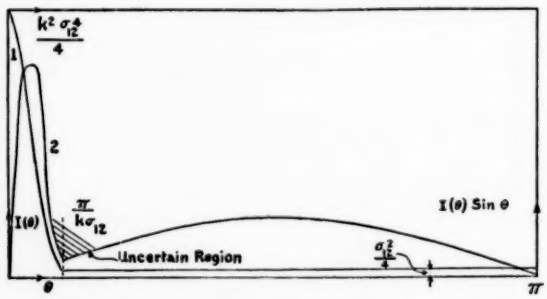

FIG. 1. Curve 1 is a modified form of the curve given by Massey and Mohr (Fig. 2), obtained by using a more exact expression for $I(\theta)$ which was worked out by Dr. Harvey Hall. The expression is: $I(\theta)=(x^4/k^2)[J_1(x\tan\theta)/x\tan\theta]^2$ where $x=k\sigma_{12}$. I wish to thank Dr. Hall for permitting me to use his results before publication. Curve 2 is $I(\theta)\sin\theta$ plotted on a different scale.

classical theory result for elastic spheres, provided $k\sigma_{12}$ is about 20 or greater. For very small relative velocities, $k\sigma_{12}$ approaches zero and the total scattering is then four times what it is on the classical theory. The larger values of $k\sigma_{12}$ thus give an effective collision radius of $\sigma_{eff.}=1.5\sigma_{12}$, which increases to $\sigma_{eff.}=2\sigma_{12}$ for the smaller values of $k\sigma_{12}$.

The object of the experiments which are to be described was to obtain data on the scattering of a narrow beam of potassium atoms in a variety of gases. The gases chosen were: firstly, the more available inert gases namely helium, neon and argon; and secondly, as examples of more complex gases, hydrogen, nitrogen and carbon dioxide. These six gases give a considerable range in mass and consequently considerable variation in the value of the important quantity k. The experiments were designed to investigate the scattering down to about 4.5′ of arc, which is well within the interesting angular region from 0 to $\pi/k\sigma_{12}$. The theoretical scattering curves presented in Fig. 1 show the kind of scattering to be expected in this region from pure hard sphere scattering.

A number of investigators have used the molecular ray method to determine mean free paths and collision radii.[4–12] In none of these experiments were measurements made at angles as small as those used in the experiments to be described.

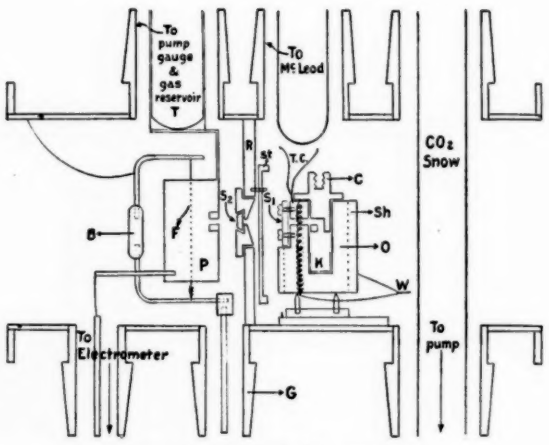

FIG. 2. Diagram of apparatus.

APPARATUS

The source of the beam was the oven O (Fig. 2) which contained a small quantity of potassium K. The potassium was cleaned under petroleum ether by cutting off the hydroxide coating and was then introduced into the oven in a small nickel cup filled with the petroleum ether. The oven was constructed of a single piece of nickel which could be closed at the top, after the introduction of the potassium, by means of a close fitting cylinder of monel metal C. The coefficient of expansion of nickel is less than that of monel metal and therefore when the oven was heated the two metals formed a very tight joint. The oven was mounted on three pointed nickel pegs, fixed in a dove-tailed slide, so that it could be removed from the apparatus after being lined up and then subsequently replaced without any difficulty. The sharply pointed pegs also served to prevent the conduction of heat away from the oven. The oven was heated by two 10 mil tungsten spirals W which were contained in quartz tubes embedded in the copper shield Sh, which surrounded the oven. One end of these heating filaments was grounded. The temperature of the oven and potassium beam was determined by a chromel-alumel thermocouple $T.C.$ located near the oven slit S_1. The temperature was kept constant by two rheostats connected in parallel. Changes in temperature amounting to 0.1°C were easily

[4] Born, Phys. Zeits. **21**, 578 (1920).
[5] Bielz, Zeits. f. Physik **32**, 81 (1925).
[6] Knauer and Stern, Zeits. f. Physik **53**, 766 (1929).
[7] Ellett and Zabel, Phys. Rev. **37**, 1112 (1931).
[8] Knauer, Zeits. f. Physik **80**, 80 (1933).
[9] Knauer, Naturwiss. **21**, 366 (1933).
[10] Zabel, Bull. Am. Phys. Soc. Vol. 8, No. 7, page 10.
[11] Zabel, Phys. Rev. **44**, 53 (1933).
[12] Fraser and Broadway, Proc. Roy. Soc. **A141**, 626–641 (1933).

observed and the oven was usually kept constant within these limits. The height of the oven slit was limited to 2 mm by a hole drilled in the body of the oven. The width of the oven slit was limited to 0.01 mm by two nickel slit jaws which were screwed on the face of the oven. The beam was then defined by a collimating slit S_2 which was also limited to 2 mm in height. These slit jaws ran in a dove-tailed slide, were made of phosphor bronze and were set to a width of 0.013 mm. The beam could be screened by the magnetically operated shutter (*St*). The collimating slit holder was kept cool by a large water jacket on the outside of the tube.

The potassium beam formed by this slit system was detected[13] by the tungsten line filament (*F*) of diameter 0.01 mm, which could be rotated by means of the ground joint (*G*) about an axis passing through the collimating slit in the direction of its length. The filament was mounted on a rigid nickel frame, the two halves of which were insulated by the glass bead (*B*). A two mil tungsten spiral served to keep the 0.01 mm filament taut. This detecting filament rotated inside the semi-cylindrical sheet nickel plate (*P*) which was cooled by carbon dioxide snow contained in the trap (*T*). The potassium positive ion current was measured by an FP-54 vacuum tube electrometer (sensitivity 3×10^{-14} amp./mm). A potential of 45 volts applied between the filament and plate was more than sufficient to give saturation. The position of the filament with respect to the beam was then determined by a glass micrometer stage mounted on the ground joint *G* and a microscope focussed on this scale. This 0.01 mm filament subtended an angle of about 3′ at the collimating slit.

After the oven had reached equilibrium the procedure adopted was to investigate the "vacuum beam"; that is the beam obtained when the McLeod gauge registered "flat" for both the oven and detecting chambers. A typical "vacuum curve" is shown in Fig. 3 where intensity is plotted against scale-divisions. (1 scale division $=2.17'$.) Before running through a curve the residual positive-ion current, due to the filament itself, was measured by cutting off the beam with the shutter. This residual current was then subtracted from the observed beam intensity. It never amounted to more than a few millimeters deflection. The absence of any considerable tails close to the "vacuum beam" indicates that the residual pressure was negligible as far as this experiment is concerned. The small tails close to the beam itself are due chiefly to the finite width of the detecting filament. The "vacuum beam" background further out is due to K atoms scattered from various parts of the apparatus.

The scattering gas was stored in a 5 liter bulb as a reservoir and admitted to the detecting chamber through a stopcock plugged with plaster of paris. The pressure of gas in the detecting chamber was then varied by changing the pressure of gas in the reservoir and was maintained at a given pressure by the diffusion pump. The pressure of the scattering gas was measured by a carefully calibrated McLeod gauge connected at a point such that a considerable pressure gradient could not occur. Under the above conditions the pressure in the oven chamber was always 10^{-5} mm or lower. The intensity distribution in the scattered beam was then obtained by moving the detector on its ground joint. Typical experimental curves for the different gases are given in Figs. 3–8. In each case the upper curve represents the "vacuum" beam, the lower the "gas" beam.

At low pressures it becomes difficult to distinguish between residual gases and vapors and the scattering gas. It therefore became advisable in the interest of accuracy to work with relatively high pressures (10^{-4} mm to 5×10^{-4} mm). The dimensions of the beam were made small so as to reduce the possibility of multiple collisions, the distance from collimating slit to detector being 1.3 cm.

Results

A total of 30 sets of runs were made on the various gases yielding scattering curves of which those shown in Figs. 3–8 are typical. A convenient and instructive way of expressing results of scattering experiments is by means of an effective collision radius. This gives a measure of the total scattering per atom under the defined conditions. The relation

$$I = I_0 e^{-d/\lambda} \qquad (1)$$

[13] Taylor, Zeits. f. Physik **57**, 242 (1929).

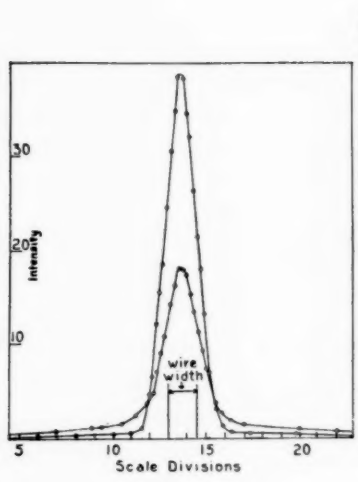

FIG. 3.

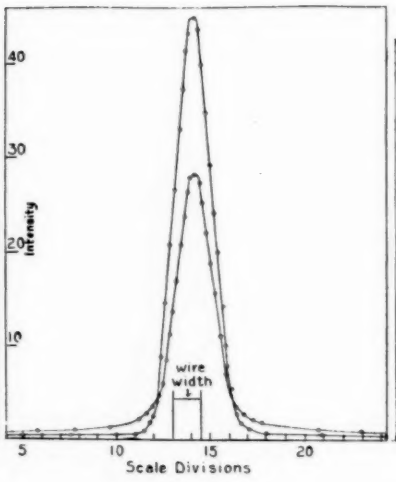

FIG. 4.

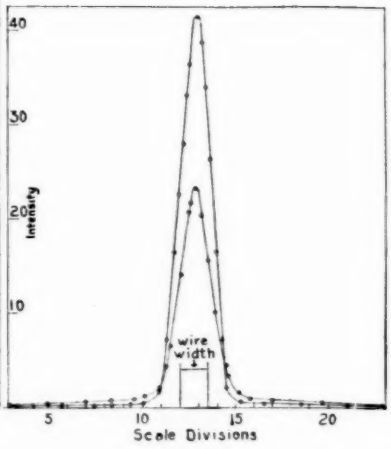

FIG. 5.

FIG. 3. CO_2, pressure -2.59×10^{-4} mm, oven temperature 443°K, wire width 0.01 mm, one scale division is 2.17′.
FIG. 4. Neon, pressure 2.85×10^{-4} mm, oven temperature 436°K.
FIG. 5. Helium, pressure 3.76×10^{-4} mm, oven temperature 446°K.

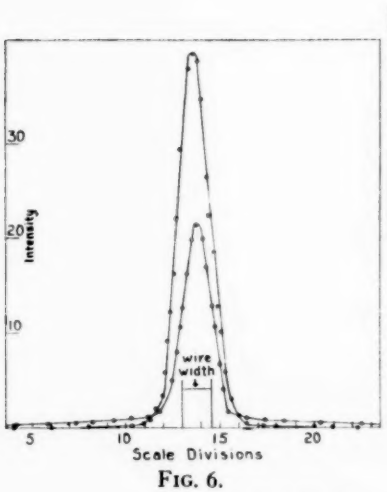

FIG. 6.

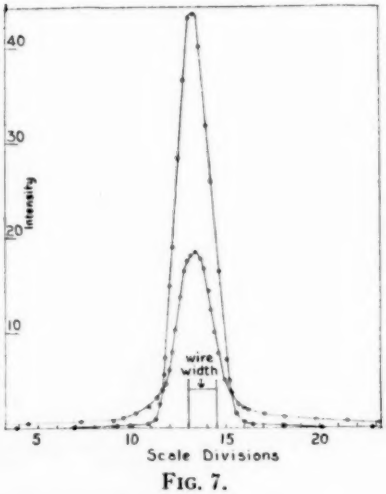

FIG. 7.

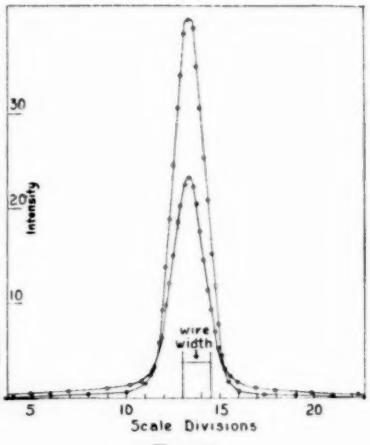

FIG. 8.

FIG. 6. Hydrogen, pressure 2.46×10^{-4} mm, oven temperature 445°K.
FIG. 7. Nitrogen, pressure 2.55×10^{-4} mm, oven temperature 444°K.
FIG. 8. Argon, pressure 1.70×10^{-4} mm, oven temperature 430°K.

defines an effective mean free path λ. Here d is the distance from the collimating slit to the detector expressed in cm, I_0 is the integrated intensity of the vacuum beam within certain angular limits (in arbitrary units), and I the integrated intensity of the scattered beam within the same angular limits. We will thus obtain values for λ depending on the angular limits we choose in the calculation of I and I_0 or in other words depending on what deviation we define as constituting a collision. We will consider two extreme cases.

Case I

We take I to be the peak reading of the "gas curve." The corresponding value of I_0 is the peak reading of the "vacuum curve." Using the ratio I/I_0 and Eq. (1) one can then compute an effective mean free path.

Case II

We take I to be the integrated intensity under the "gas curve" out to 10.5 detector wire-widths (0.105 mm) from the peak; and then get the corresponding value of I_0 from the in-

tegrated intensity under the "vacuum curve." We then compute another λ corresponding to these larger angular deviations.

The λ's obtained in this way are shown in sections I and II of Table I; together with the product $(p\lambda)$, p being the pressure of the scattering gas expressed in mm of mercury. If multiple collisions are infrequent this product should be constant for any one gas. It is evident that this is very nearly the case. The deviations from constancy are not greater than the errors in the pressure measurements.

From these λ's we obtain the effective collision cross sections or collision radii. The mean free paths obtained in experiments of this type are obviously analogous to Tait's mean free path, except that the colliding atoms have different masses, and that the potassium beam and scattering gases are at different temperatures. Account must also be taken of the fact that the detecting wire measures a quantity which is proportional to the number of potassium atoms received per sq. cm per sec., instead of the number present in unit volume. The distribution to be used for the K atoms is therefore not the ordinary Maxwellian distribution of velocities, but:

$$Ae^{-mc^2/2kT}c^3dc. \tag{2}$$

We then obtain[14]

$$\sigma_{12}^2=\frac{2}{\pi^{\frac{1}{2}}\nu\lambda}\left(\frac{T_xm_k}{T_km_x}\right)^2\int_0^\infty xe^{x^2(1-T_xm_k/T_km_x)}\frac{x^4e^{-x^2}}{\psi(x)}dx, \tag{3}$$

where ν is the number of molecules per cc of the scattering gas, T_k, T_x, m_k, m_x, are the temperatures and masses of the potassium and the scattering gases, and

$$\psi(x)=xe^{-x^2}+(2x^2+1)\int_0^x e^{-y^2}dy.$$

The integral in the above expression was evaluated by the method of quadratures by using Tait's tables for values of x from 0.1 to 3.0. For the heavier gases it became necessary to extend his tables to $x=5.0$ before the integral became sufficiently convergent.

The effective collision radii computed in this way are given in sections I and II of Table I. If the detecting wire and beam had been infinitesimally thin, the σ_{12} values obtained from the peak readings would have represented the total effective collision radius. In any actual experiment, however, both beam and detector must have a finite width and the σ_{12} values in section I therefore represent minimum values; because some of the atoms which are scattered through small angles can still reach the detector due to its finite angular width. The difference between the σ_{12}'s listed in sections I and II is due to the fact that the angular width in case II is 21 times as great as in case I. In order to determine the angular limits for cases I and II we must remember that the beam is being scattered along its entire length and therefore the detecting wire subtends different angles at different scattering points. However, if we weight all parts of the length of the beam equally we can compute an average angle of scattering. For case I this average angle is about 4.5′ and for case II it is about 1.5°.

Since the only theory of atomic scattering which has been worked out in any detail is the "hard sphere theory," we shall proceed to discuss the experimental data in the light of that theory. As previously stated, an important quantity in the theory is $k\sigma_{12}$. The k used was obtained by averaging over the distributions of relative velocities of the colliding particles. The radii of the scattering gases were computed from Chapman's viscosity formula[15] derived from an elastic sphere model; but since no viscosity or diffusion measurements exist for potassium we are forced to estimate the size of its radius from other considerations. The packing radius of potassium in the solid state is known to be about 2.3A.[16] Hartree[17] finds that the radius at which the ψ function for the series electron has its large maximum is 2.01A and the radius at which $|r\psi|^2$ has its maximum is 2.66A. This last value would correspond on the old Bohr theory to the radius

[14] Jeans, *Dynamical Theory of Gases*, 4th Ed., p. 255.
[15] Chapman, Phil. Trans. Roy. Soc. Ser. **A216**, 279 (1915).
[16] Neuberger, Zeits. f. Kryst. **80**, 103 (1931).
[17] Hartree, Proc. Roy. Soc. **A141**, 282 (1933).

TABLE I. *Mean free paths and effective collision radii.*

	I CASE I				II CASE II				III	IV	V	VI
Gas	λ	λp	σ_{12}	Aver. σ_{12}	λ	λp	σ_{12}	Aver. σ_{12}	$\sigma_{12}=\sigma_K$ $+\sigma_\theta$	Effect quantum σ_{12}	$k\sigma_{12}$	θ
H_2	1.52	5.88	7.08	7.20	2.64	10.2	5.36	5.67	5.0	7.4	20	8.5°
	2.12	5.43	7.37		4.86	10.6	5.27					
	2.49	5.43	7.36		3.29	8.43	5.91					
	3.83	5.75	7.16		9.29	8.64	5.84					
	4.23	5.92	7.06		9.22	9.32	5.62					
	5.42	5.48	7.34		8.10	12.2	4.93					
	6.40	5.95	7.03		4.58	6.43	6.78					
He	2.04	8.52	6.98	6.91	4.21	17.6	4.86	4.96	4.7	6.9	27	6.8°
	2.24	8.42	6.84		3.84	14.5	5.22					
	2.46	8.56	6.76									
	2.89	8.65	6.80									
	5.89	8.25	6.92		12.2	17.1	4.81					
	5.92	7.70	7.16									
Ne	2.85	8.55	8.80	8.74	6.70	17.3	6.19	5.98	4.8	6.9	56	3.2°
	2.69	8.07	9.06		7.22	21.6	5.53					
	3.10	8.84	8.66		8.04	22.9	5.37					
	3.33	8.60	8.78		5.61	16.9	6.28					
	12.1	9.43	8.38		20.0	15.6	6.52					
N_2	1.68	4.54	12.5	12.6	5.11	13.8	7.19	7.30	5.5	7.8	72	2.5°
	1.74	4.56	12.5		5.51	14.5	7.04					
	3.70	4.58	12.5		12.5	12.4	7.60					
	4.45	4.41	12.7		10.6	13.2	7.36					
A	3.14	5.90	11.3	11.3	5.07	9.55	8.92	8.78	5.4	7.7	79	2.3°
	2.95	5.28	12.0		4.78	8.56	9.41					
	5.28	6.03	11.0		9.96	11.8	8.01					
	6.07	6.68	10.7									
CO_2	1.59	4.08	13.7	13.3	3.37	8.66	9.44	9.63	5.9	8.4	89	2.0°
	1.64	4.25	13.5		3.11	8.06	9.80					
	3.80	4.37	13.3		7.40	8.52	9.53					
	4.25	4.80	12.7		7.23	8.16	9.73					

In the above table λ values are given in cm, σ_{12} values in A units, and the λp values should be multiplied by 10^{-4} when p is in mm of mercury.

of the orbit of the series electron. The quantity $|r\psi|^2$ drops to one-third of its maximum value at a distance of about 3.5A. If we make the very plausible assumption that the collision of a potassium and a helium atom is most like a hard sphere collision because of the symmetry and small polarizability of the helium atom, we can obtain an upper limit for the potassium radius from our data on helium. In case II most of the "extra classical" forward scattering is included in the integrated I. (See Fig. 1.) The correction to be made for classical hard sphere scattering at small angles is less than 1 percent. The σ_{12} value for He and K as given in section II of Table I is about 5A and it should be approximately equal to the kinetic theory value for σ_{12}. If we take the kinetic theory radius of helium to be 1.1A this would give us 3.9A for the potassium radius. This value of 3.9A is probably too high. In all future discussions we shall use the value 3.6A which represents a mean between the values 3.9 and 2.66. It is then possible to compute the kinetic theory values for σ_{12}. They are given in section III of Table I. The computed values of $k\sigma_{12}$ are shown in section V.

A comparison of the σ_{12} values presented in sections I and III shows that the σ_{12} values computed from the small angle scattering (case I) are much larger than the classical kinetic theory values; but when we compute these values from the large angle scattering (case II) they approach the classical kinetic theory values more closely, especially in the case of H_2 and He. This diminution in the "effective collision radius" would be quite large even if we did not go out to angles as large as 1.5°; and it indicates the predominance

of small angle scattering. Multiplying the classical kinetic theory radii by the appropriate factor[2] (approximately 1.5) gives the "effective quantum collision radii." They are presented in section IV of Table I. A comparison of sections I and IV then shows that in the case of H_2 and He the quantum theory values agree with the experimental small angle σ_{12} values within the limit of experimental error.

Accuracy

The accuracy of the σ_{12}^2 values depends on the reliability of the λ's and the pressure measurements. The average error of the pressure measurements amounted to about 2.6 percent; but it should be mentioned that the σ_{12}^2 values obtained from the long mean free paths are not as reliable as the others since their accuracy depends on the accurate determination of small pressures. It is also evident that the σ_{12} values computed from case II show more dispersion than the values obtained from case I. This dispersion arises because the integrated intensities I and I_0 depend on readings along the steep part of the curve, where the intensity varies rapidly over the distance of a wire-width.

In case I the detecting wire covers only a portion of the beam, approximately equal to the width of the central part, which in a "vacuum beam" contains 2/3 of the total beam intensity. It is therefore desirable to find out what the probability is of having atoms from the rest of the beam scattered into this region and being counted as undeviated atoms. It can easily be seen that this probability is small on the hard sphere model. The quantum theory[2] shows that, for the values of $k\sigma_{12}$ under consideration, the "extra scattering" (beyond the amount predicted by classical theory) occurs almost entirely in the region $\theta=0$ to $\theta=\pi/k\sigma_{12}$ and is about equal in amount to the total classical scattering, namely that resulting from an effective collision cross section $\pi\sigma_{12}^2$. The values of $\theta=\pi/k\sigma_{12}$ are tabulated in section VI of Table I. This extra scattering has a form such that the fraction scattered within an angle θ_1 is given quite closely by:

$$\frac{6k^2\sigma_{12}^2}{\pi^2}\left(\frac{\theta_1^2}{2}-\frac{k\sigma_{12}}{\pi}\cdot\frac{\theta_1^3}{3}\right). \qquad (4)$$

The filament and beam used were narrow enough that about 95 percent of the atoms scattered in this extra classical region were scattered through angles sufficiently large to miss the detecting wire entirely. This still holds true when account is taken of the circumstance that the angle θ defines the change in direction of the relative velocity and not the actual change in direction of the K atoms. It is easily shown that for small values of θ, such as occur in this experiment, an angular change θ gives rise to an angular deviation ϕ of the K atoms expressed by: $\phi \cong \theta k/2k'$ where $k'=2\pi m_k \bar{v}_k/h$. This results in an effective contraction of the critical region where the extra quantum scattering takes place; but the wire-width chosen is narrow enough so that 95 percent of the extra scattering is beyond the filament. Of the total scattering on the hard sphere model only 2.5 percent can reach the wire when it is at the central position. This results in a possible 1.6 percent error in calculating the σ_{12}. This is less than the errors due to other causes. No such discussion can be given for the case where the hard sphere model does not seem to fit the data (CO_2, N_2, A, etc.). The values of the σ_{12} in this case are to be regarded as minimum values or as a graphic means of expressing the experimental results.

Conclusions

The experimental results, as is evident from a comparison between cases I and II, show that there is in all gases in question a very striking predominance of small angle scattering. This is better shown by a comparison of the σ_{12}^2's rather than the σ_{12}'s. In the past this effect would have been interpreted as due to attractive forces. However, since the diffraction effects of molecules have been well verified experimentally, this strong forward scattering must be ascribed in part at least to such effects. The agreement of the σ_{12} values for He and H_2 with the hard sphere theory is then something rather to be expected. This agreement is not forced by the choice of the radius for the K atom since we have obtained an experimental upper limit to this quantity. A fair agreement would remain if we made any reasonable assumption. It is then a rather striking fact that this agreement is not maintained for the other gases, not even for

neon and argon. The excess in the σ_{12} values for these cases must be ascribed to an interatomic interaction of considerable range.

Although the σ_{12} values presented are really lower limits for this quantity, in view of the finite total scattering predicted by the quantum theory it is rather likely that they are quite close to the real values.

Acknowledgment

In conclusion I wish to express my appreciation for the guidance and advice provided by Professor I. I. Rabi, under whose direction this investigation was carried out. I also wish to thank Mr. Seymour Rosin for his valuable assistance during the course of the experiments.

Positive Electrons: Focussing of Beams, Measurement of Charge-to-Mass Ratio, Study of Absorption and Conversion into Light

JEAN THIBAUD, *Laboratoire de Physique des Rayons X, Ecole des Hautes Etudes, Paris**

(Received April 12, 1934)

1. Description of a method ("method of the trochoid") of concentrating and focussing weak electron beams so that they form strong sharp lines on a photographic plate. 2. Displacement of the beam thus formed by an additional field, enabling the observer to recognize the sign of the charge and to estimate the charge-to-mass ratio of the particles, with an accuracy thus far brought up to 15 percent. 3. Absorption, in thin films of platinum and a large number of other elements, of the positive and negative electrons proceeding from a source composed of a radioactive substance emitting strong gamma-rays and enclosed in lead; it is shown that the absorption follows an exponential law over a wide range of thicknesses, and the value of the mass absorption-coefficient is obtained from observations on the imprint made upon a photographic plate behind the absorber. 4. When in the foregoing experiments the thickness of the absorber is increased beyond about 500 mg/cm², it becomes evident that the imprint on the plate is partly due to something else than the transmitted electrons. This "something else" is considered to be radiation; with negative electrons it consists entirely of secondary x-rays, with positive electrons there is an additional component ascribed to the merging of positive with negative electrons and their conversion into photons. 5. The absorption-coefficient of these photons implies that their energy is about 0.5 MEV, and the intensity of the radiation implies that there are about two of them per positive electron—two results which agree well with Dirac's theory. 6. Positive electrons have also been observed in conditions where it seems that they proceed directly from radioactive substances.

THE discovery of the positive electron was made by Anderson and confirmed by Blackett and Occhialini, from Wilson-chamber photographs of the tracks of the ionizing particles of the cosmic rays. It was subsequently discovered that gamma-rays have the power of producing these particles when they fall upon matter.[1] However the positive electron is comparatively rare, and all our knowledge of it hitherto has been derived by experiments by the Wilson method. Observations on the curvature of the tracks in a magnetic field, and on the length and the density of ionization of these tracks, have indicated that in charge and mass it is (except for the sign of its charge) much more closely like the negative electron than like the proton or any other known positive particle.

I give here an account of an experimental method particularly suited for forming concentrated beams of charged particles emanating in small numbers from a compact source, and of some results obtained by applying it to positive electrons produced by gamma-rays incident on lead.

THE "METHOD OF THE TROCHOID"

Fig. 1 shows a longitudinal section and Fig. 2 a cross section of the apparatus. The pole-pieces of an electromagnet face each other across a gap, in the center of which the field strength is 10^4 gauss, while in the peripheral parts of the gap it has a considerable radial gradient. In this peripheral region is located the source S (see below); and the charged particles which emerge from S along directions lying close to the plane of Fig. 2 follow "trochoidal" orbits such as are depicted in that figure; and indeed, particles emitted in almost *any* direction in or close to that plane (aperture of almost 2π!) are brought to a narrow region at F, diametrically opposite to S in the peripheral part of the gap. The "yield" of this method of collecting particles

* English version by K. K. Darrow.

[1] Anderson, Science **76**, 238 (1932); Blackett and Occhialini, Proc. Roy. Soc. **A139**, 699 (1933); Anderson and Neddermeyer, Phys. Rev. **43**, 1034 (1933); Curie and Joliot, C.R. **196**, 1581 (1933); Meitner and Philipp, Naturwiss. **24**, 468 (1933); etc. History and references given by Blackett, Nature **132**, 917 (1933); Darrow, Rev. Sci. Inst. **4**, 263, 427 (1933) and **5**, 115 (1934); Scientific Monthly **38**, 1 (1934).

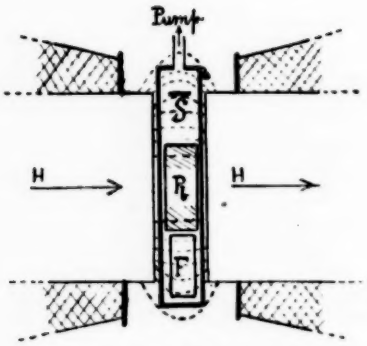

FIG. 1. Longitudinal section of apparatus.

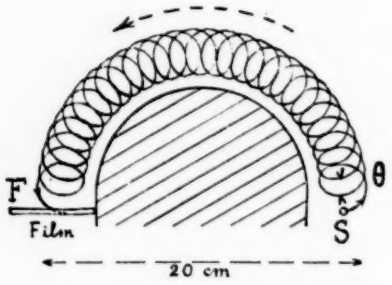

FIG. 2. Cross section of apparatus with diagram of trochoid.

is much (10^2 to 10^3 times) greater than that of any scheme of deflection by a uniform magnetic field.

The source of positive (and negative) electrons is a narrow tube containing some powerful emitter of gamma-rays (radon, salt of radium, or better a salt of RdTh) wrapped in a leaden "radiator" (rolled-up lead foil 0.15 to 0.3 mm thick). The "receiver" F (shielded from the gamma-rays of S by a block of lead 10 to 15 cm thick, Fig. 1) may be a Geiger-Müller counter, an ionization chamber, or a photographic film; I have employed chiefly the last-named. A mere reversal of the direction of the magnetic field brings negative electrons against the film at F instead of positive, or *vice versa*. Either produce on the film *a very compact line* (Fig. 6), *the edge farther from S being especially sharp*, as is brought out by the microphotometer curves (Fig. 3). The lines produced by the two kinds of electrons are identical, if the exposure is 100 to 200 times as long for the positives as for the negatives. The following tests have shown that this line is truly due to the particles which have followed the trochoidal orbits: (*a*) a displacement of S in the plane of Fig. 2 entails a symmetrical displacement of the line; (*b*) the position of the line is (to first approximation) independent of the magnetic field strength; (*c*) the line fades out when S is shifted toward the axis of the system where the magnetic field is uniform; (*d*) films oriented at right angles to H show the expected curves; (*e*) all the particles can be made to pass through a narrow slit in a screen set across the trochoidal orbit of Fig. 2.—Note that the sense of progression of the trochoids in a given magnetic field, and the similarity of the lines produced by the negative electrons and by the new rays, enable us to affirm from the start that the charge-to-mass ratio of the new corpuscle is positive and of the same order as that of the negative electron.

ELECTROSTATIC DEFLECTION OF POSITIVE ELECTRONS

Two grids are installed at right angles to the "direction of progression" of the trochoids and in front of the photographic film at F (Figs. 2, 4); between them is applied a voltage V and consequently an electric field E, parallel to the said direction and at right angles to the magnetic field H; it produces a radial displacement x of the trajectories and consequently of the line upon the film, x being proportional to E/H and to the time t during which any corpuscle is between the grids. This time-interval t depends on the separation θ between successive turns of the trochoidal orbit, which latter quantity is controlled by the gradient of magnetic field strength in the region where the source and the orbits are, and can be varied at will by varying the distance of S from the axis of the system. The

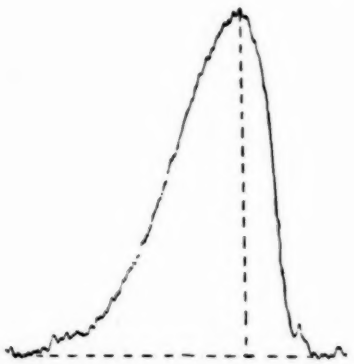

FIG. 3. Microphotometer tracing of the line due to a beam of positive electrons.

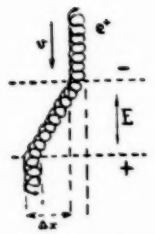

FIG. 4. Displacement of the trochoid by an applied electrostatic field.

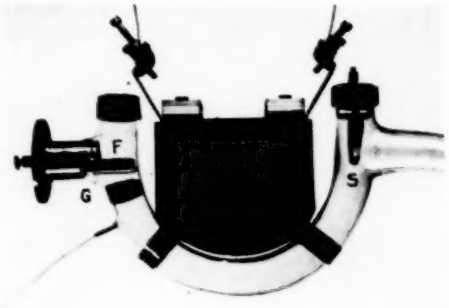

FIG. 5. Photograph of the apparatus prepared for study of positive electrons.

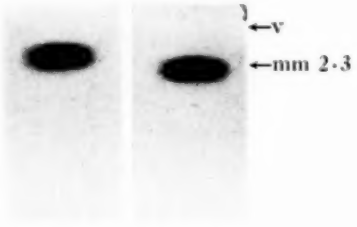

−7500 v + 5000 v

FIG. 6. Line produced on plate by positive electrons, for two values of applied electrostatic field.

first-approximation formulae for θ and x in terms of r the radius of a single turn of the trochoid, ΔH the difference in magnetic field strength at opposite sides of such a turn, and βc the speed of the corpuscles, are the following:

$$\theta = \pi r \Delta H / 2H \tag{1}$$

$$x = 4V/300\beta\Delta H, \tag{2}$$

the units employed being the centimeter, the volt and the gauss.[2]

In the actual experiment, the electromagnet has cylindrical pole-pieces of 20 cm diameter and 3.5 cm gap-width; the electrons travel in a curved tube of Pyrex (Fig. 5); S is seen at the right, F at the left; the two grids G are parallel to the film and 1 cm apart. When the voltage is applied between the grids, the line due to the electrons impinging on the film is displaced by about 1 mm for each 5000 volts; Fig. 6, relating to positive electrons, exhibits the displacement of 2.3 mm due to a change in the voltage from +5000 to −7500. When the magnetic field is reversed, negative electrons instead of positives come to the film, and the displacement produced by the application of the voltage is reversed in sign.

MEASUREMENT OF e/m FOR POSITIVE ELECTRONS

Combining Eq. (2) with the following equation,

$$Hr = (m_0c^2/e)\beta/(1-\beta^2)^{\frac{1}{2}} \tag{3}$$

one sees that it is possible to evaluate e/m and β if r and the values of magnetic field strength at all points of the trochoidal orbits are known. The field strengths are determined by placing a little block of nickel of known susceptibility, suspended from a balance, at various points of the gap; r is determined by photographing the electron tracks. Unfortunately the positive electrons have a distribution-in-energy extending over a wide range, the most probable energy values lying between 800 and 900 electron kilovolts; the measured value of r is only a mean value; the best that can be concluded from this "absolute" determination of e/m_0 for positive electrons is that it is between one-half and twice the value for negative electrons. A more accurate "relative" determination can be made by comparing the values of x observed with positive and negative electrons. A more accurate "relative" determination can be made by comparing the values of x observed with positive and negative electrons. On plotting them against voltage, the two straight lines of Fig. 7 were obtained; their slopes are equal within the uncertainty of experiment, so also must be[3] the products $(m_0/e)\beta^2/(1-\beta^2)^{\frac{1}{2}}$; and comparing the mean radii r of the turns of the trochoids made by the electrons

[2] It has been shown by L. Cartan (C.R. **197**, 1604 (1933)) that the substitution of relativistic for classical mechanics does not impair these formulae.

[3] In expression (2) for the displacement x, ΔH is proportional to the gradient of the magnetic field and to the radius r of the orbit. Thus x will vary inversely as βr, and hence, according to expression (3), inversely as $(m_0/e)\beta^2/(1-\beta^2)^{\frac{1}{2}}$.

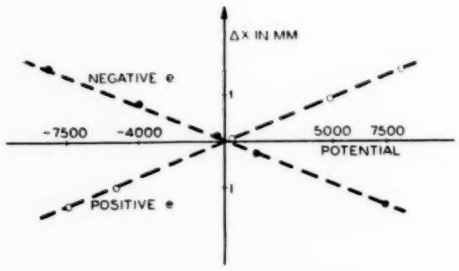

FIG. 7. Illustrating the determination of e/m.

of the two signs, I conclude that the charge-to-mass ratio of the positive electron cannot differ by more than 15 percent from that of the negative electron.

PASSAGE OF POSITIVE ELECTRONS THROUGH MATTER: SCATTERING AND ABSORPTION

The method of the trochoid, combined with a photometric study of the imprint made upon the photographic film (we employ the registering microphometer of Chalonge and Lambert) is well suited for investigating the "absorption" of electrons in matter. The law of the photographic action is the same for positive as for negative electrons,[4] and it has been verified that the density S of the spot is proportional to the number of incident positives all the way up to $S=1$. Fig. 7A exhibits three photometer curves, obtained with three thicknesses of absorbing matter (the absorbing screens are pressed closely against the film): it is seen that the general aspect of the line (especially its dissymmetry) remains the same.

For each of the elements studied, we have plotted the logarithm of the transmitted intensity (or photographic density) against the mass-per-unit-area of the absorbing screens (Fig. 9 shows an example for platinum). In general, the curves are concave toward the axis of abscissae from $x=0$ onward to about $x=50$ mg/cm^2; thenceforward they are linear over a considerable interval (though not indefinitely!), and we may define and measure a "mass-absorption-coefficient" μ/ρ in the customary fashion. For a long list of elements (C, Al, S, Ca, Mn, Ni, Cu, Zn, As, Se, Mo, Pd, Ag, Cd, Sn, Ce, Ta, Pt, Au, Pb) and for the particular distribution of positive electrons emanating from

[4] Thibaud and Dupré la Tour, C.R. **198**, 805 (1934).

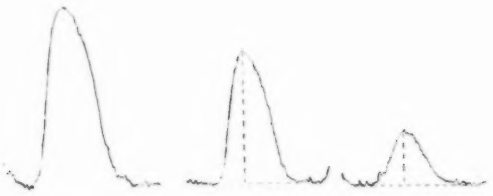

FIG. 7A. Microphotometer tracing of the lines due to the same beam of positive electrons after passage through different thicknesses of absorber.

our source (RdTh), the values of μ/ρ lie between 8 and 10; the differences are probably due in part to errors of measurement,[4] but in part to a periodic variation of μ/ρ with atomic number Z. The negative electrons proceeding from the same source (expelled by the thorium gamma-rays from the atoms of the radioactive substances and of the enclosing lead foil) likewise have an absorption-curve which, when plotted in this semi-logarithmic fashion, exhibits a long straight portion;[5] the example in Fig. 9 (lower curve) yields a value 13.7 for μ/ρ.

The absorption of the positive electrons in air was studied by introducing air at various pressures into the apparatus, measuring the corresponding densities of the spot, and adopting for the total length L of the trochoid the formula $L=4\pi RII/\Delta II$, where R stands for the distance to the source from the axis of the system (Fig. 2). The semi-logarithmic curve is shown in Fig. 8;

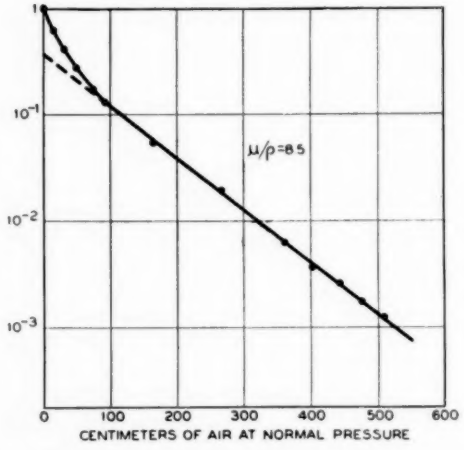

FIG. 8. Absorption-curve of positive electrons in air.

[5] It has long been known that inhomogeneous electron beams, such as ours is, may exhibit an exponential absorption law (which on the semi-logarithmic plot appears as a linear law). Cf. for instance K. W. F. Kohlrausch, *Radioaktivität*, p. 367 (Handbuch der Physik).

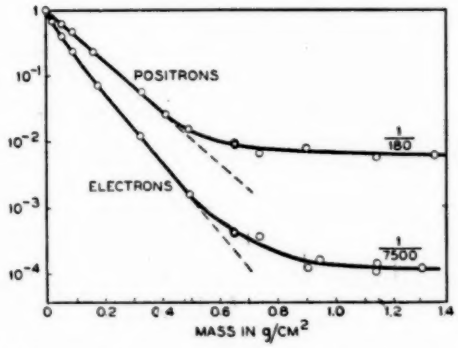

FIG. 9. Absorption-curves of positive and negative electrons in platinum, with extension attributed to photons.

it is convex[6] for low values of x, subsequently straight; the value of μ/ρ is 8.5, in good agreement with those obtained with solid absorbers.

Our general conclusion is, that as they pass through matter up to thicknesses of the order of at least 500 mg/cm², these positive electrons behave like negatives, undergoing a similar scattering and slowing-down by virtue of their interactions with atomic electrons and nuclei.[7] But as the thickness of the screens is further increased, a different phenomenon comes to notice.

RADIATION ASCRIBED TO STOPPING AND TO ANNIHILATION OF POSITIVE ELECTRONS

Returning to Fig. 9, it is seen that the sensibly-straight portion of each of the absorption curves is succeeded by a portion with a notable upward concavity, which approaches a not-quite-horizontal asymptote. This signifies that the effect produced on the film by *photons excited within the metal by the electrons* is becoming comparable with that produced by the electrons which succeed in traversing the whole of the metal and reaching the film. In the case of *negative* electrons, all of these photons are presumed to belong to the well-known x-ray spectrum (both line-spectrum and continuum) evoked whenever fast electrons impinge on matter. Their contribution to the blackening of the film is actually very slight, only 1/7500 of the effect of the primary beam when no absorber is interposed. This is not surprising in view of the small yield (a few percent) of x-ray emission from platinum evoked by electrons of these speeds. On comparing the two curves of Fig. 9 one sees, however, that the photons produced by the *positive* electrons have a much greater effect. Beyond 500 mg/cm² of Pt (at which thickness more than 1 percent of the incident positives are still transmitted) there is evident an intense and penetrating radiation. Its limiting strength produces a blackening 1/180 of that caused by the undiminished primary beam and some *fifty times* as great as that due to the photons evoked by negative electrons. (The difference is also made obvious by the fact that at 100 mg/cm² the film must be exposed 200 times as long to the positives as to the negatives to get the same blackening, while at 1000 mg/cm² the ratio of exposures is only 4.) Meanwhile, the aspect of the spot on the film is changing; the original fairly sharp "line" of Fig. 3 is replaced by a much broadened area with no definite edge nor sharply-marked central maximum of blackness. We infer that the imprint of the transmitted fraction of the beam of positives is masked by a secondary radiation (photons) emitted in all directions.

The mean frequency of the new radiation can be deduced from the slope of the not-quite-horizontal asymptote of Fig. 9. Most of the photons are presumably produced near the front surface of the absorbing metal,[8] while the major part of their photographic effect is presumably due to secondary electrons produced near the rear surface and springing out of the metal against the film. We therefore kept the rear surface of the metal pressed against the film,

[6] Thibaud, C.R. **198**, 562 (1934). Curves of this shape have been obtained by Crowther with negative electrons (Proc. Roy. Soc. **A80**, 186 (1908)).

[7] Note that the trochoidal trajectories enter the solid absorbing screens almost tangentially, but, owing to the scattering of the positives which commences as soon as they enter the screens, it is proper to assume that the thickness of these screens corresponds to the real path of the corpuscles in metal. This assumption is supported by the identity of the values of μ/ρ obtained with solids and with air.

[8] This is due to the very strong diffusion of the electrons which occurs shortly after they enter the metal; one can thus find, at a very small distance ϵ from the front surface of the metal, corpuscles which have already traversed in the metal a distance L much greater than ϵ and are close to the ends of their courses and to their ultimate annihilation. Our measurements show that in platinum half of the positive electrons have already been diffused laterally at a depth of 0.0035 cm. With the thickness of 0.05 cm or more corresponding to an areal density of 1000 mg/cm², very few electrons will traverse the metal undeflected. The "centroid of emission" of the photons will thus be very close to the surface.

but maintained a constant value of the distance from the film to the front surface; these apparently contradictory requirements were fulfilled by separating, to a greater or less extent, the several sheets constituting the various thicknesses of absorber. It is possible to compute, by use of King's functions, what fraction of the total energy radiated in all directions in the form of photons is absorbed in such a manner as to produce secondary electrons which attain the film; the fraction comes out to about 0.05.

Experiments conducted in this manner, with thicknesses of absorber extending up to 1700 mg/cm², indicate a value of 0.2 for the mass-absorption-coefficient of the photons. This result is confirmed by a direct count of the transmitted photons with a Geiger counter in place of the film (the gamma-rays from the radioactive substances in the source cause much trouble in this case). This value of mass-absorption-coefficient suggests photons of energy about 0.5 MEV. The energy of the x-ray photons produced by the negative electrons is sufficiently near to the foregoing value, to justify us in assuming that the photographic effect per photon is about the same for both types of radiation, and hence that the positive electrons produce about 50 times as many photons altogether as the negatives.

From our general knowledge of the efficiency of production of x-rays by electrons of various energies impinging on various anticathodes, it is possible to make a rough estimate of the number of x-ray photons which the negative electrons of these experiments, with their energies distributed about a mean value of some 0.4 MEV, would be expected to produce in the various absorbers.[9] In the case of platinum it comes out to about 0.04 photons per electron. Multiplying this by 50, we obtain about *two photons per positive electron* as our estimate of the "yield" of the additional process peculiar to positive electrons. To make a closer evaluation it will be necessary to know more accurately the distribution-in-energy of the negative electrons.

It is clear that our two major conclusions—that the energy of these photons is about 0.5 MEV, that the number thereof is about twice the number of the positive electrons—are both compatible with the theory that *these photons arise through the fusion of a positive with a negative electron* (the latter presumably one of those already present in the metal) *every such process producing two photons which share the energy derived from the rest-masses of the electrons.* For if two electrons of opposite sign encounter one another while moving with negligible speeds, and merge and are converted into radiation, then two identical photons must spring off in opposite directions in order to assure conservation of momentum, and each of these must have one-half of the energy originally manifested as the rest-masses of the two electrons, which is to say, one-half of 1.02 MEV. "Negligible speeds" in the foregoing sentence signifies speeds for which the kinetic energy is very small compared with 0.5 MEV; it seems reasonable to suppose that positive electrons and negative electrons are especially likely to combine, when their speeds are small in this sense.

This accordingly appears to be the strongest evidence thus far obtained for *the process of the conversion of electricity*—we may say, *the conversion of matter—into radiation*, often suggested of recent years, and vital to many cosmogonic theories.[10] This is the opposite of the process of conversion of light into electricity, first postu-

[9] These electrons have a continuous spectrum extending beyond 2 MEV, in addition to spectrum-lines of photo-electric origin. The "practical average speed" prevailing after the electrons have traversed the thin surface-layer of the platinum is ascertained from the previously-cited absorption coefficient ($\mu/\rho = 13.7$); we estimate what would be the corresponding coefficient for Al, and then take the corresponding electron-speed from tables of Lenard; it appears that β is a little less than 0.85, the energy therefore about 0.4 MEV. We compute the yield of radiant energy from the expression CZU, putting 78 for Z the atomic number (of Pt) and 0.4 MEV for U the energy of the electrons and 10^{-6} for the constant C; and divide this by an estimated average energy of the photons. This calculation is justified by the results of the measurements of J. A. Gray (Phys. Rev. **25**, 237 (1925)) on the x-ray emission caused by the beta-ray spectra of radioactive substances. We ignore the effect of the $K\alpha$ line of Pt, reduced by absorption to a few percent.

[10] Gray and Tarrant and several others have observed radiation proceeding from metals irradiated by gamma-rays, which they attribute to this process; the positive electrons involved in the process are supposed to be created out of the gamma-ray photons (along with negative electrons) within the metal itself.—Joliot also observed, with the method of the trochoid, radiation of this character springing from metals bombarded by positive electrons (C.R. **197**, 1622 (1933)); he employed a Geiger counter for detection, and a considerable part (86 percent) of the observed radiation seems to have been due to parasitic effects, perhaps the contamination of the laboratory (see my criticism, C.R. **198**, 562 (1934)); the photographic method is exempt from this source of uncertainty.

lated by Dirac, which is supposed to be occurring in many cases where positive electrons are observed—*e.g.*, in the cases where gamma-rays impinge on heavy metals and positive electrons spring forth.[11] However, the process commonly postulated in the latter case is not the exact converse of the one which we postulate to explain the experiments here described. In our experiments it seems that *two* electrons merge to produce *two* equal photons, whereas in the other case it seems that a *single* photon produces two electrons. The conversion of one photon into two electrons would not be compatible with the conservation of momentum, unless the process were to occur in the vicinity of an atom-nucleus which could take up a certain amount of momentum; it is generally assumed that this happens. It therefore appears (from the experiments thus far recorded in the literature) that the conversion of photons into electrons occurs chiefly under conditions where atom-nuclei participate in the process, while the conversion of electrons into photons occurs chiefly as a self-contained process not involving the participation of nuclei.[12]

"Free Path Before Conversion" of Positive Electrons

The positive electron is distinguished from its negative counterpart by its very short "mean life," curtailed by its eventual conversion into light. We point out that this distinction may not be fundamental at all, but simply a result of the vast excess of negative electrons in the universe which we know. Were the orbital electrons of atoms positive instead of negative, it would probably be the negative electron which would have the short life.

From the curves of Fig. 9 we infer that the free path before conversion of a positive electron in platinum is at least 0.03 cm, corresponding to a stratum of metal of areal density 600 mg/cm^2; while our experiments with air suggest a free path corresponding to 640 mg/cm^2 (at least 500 cm of air at N.T.P.). These two figures are so nearly alike as to imply that interactions with negative electrons are responsible both for the slowing-down and for the eventual conversion of positive electrons.

Positive Electrons from Radioactive Substances

We have found that a thin-walled glass tube of radon emits more positive electrons than proceed from a source formed by enclosing the same tube in lead;[13] a like result has been obtained with a tube of RdTh. It is unlikely that the wall of glass, thin as it is and consisting of light elements, should be responsible for this emission. We attribute it to processes occurring in the radioactive substance itself—perhaps conversion of gamma-rays into electrons, perhaps impacts of alpha-particles against nuclei.

Some years ago I observed[14] gamma-ray photons of energy 0.507 MEV proceeding from the two substances Ra C and Th C″—that is to say, the two substances of which the gamma-ray spectrum extends well beyond one MEV. It is not too unplausible to suggest that these gamma-rays may be due to the conversion into light of "natural" positive electrons, emitted by the radioactive substance itself and converted before they escape.

[11] See references given at end of footnote 1; also Oppenheimer and Plesset, Phys. Rev. **44**, 53–55 (1933).

[12] This idea is supported by the observations of Gray and Tarrant, who found in their experiments that 0.5-MEV photons were much more abundant than 1-MEV photons (footnote 10).

[13] Thibaud, C.R. **197**, 915 (1933).

[14] J. Thibaud, Thesis, Paris, 1925; see C.R. **198**, 562 (1933).

Accommodation Coefficient and the Fraction of Current Carried by Ions in a Low Voltage Arc

IVAN A. GETTING,* *Massachusetts Institute of Technology*

(Received November 8, 1933)

The upper limit for the value of the fraction of the current at the cathode of a low-voltage arc carried by positive ions is estimated to be less than 0.5. A method is derived for experimentally determining this fraction from pressure measurements made within the arc plasma. A vane was inserted into the plasma of a helium arc and the force on it was measured with a sensitive torsion balance. A procedure is developed for correcting for radiometric forces and for changing surface conditions. The fraction mentioned above is determined as a function of total arc current. This fraction increased with increasing arc current, but never exceeded 0.2 as long as the arc remained a true low voltage arc. These experiments demonstrate the enormous velocities of the neutralized positive ions coming from the cathode, and show the sensitivity of the accommodation coefficient to changes in surface conditions.

ALTHOUGH knowledge of the fraction of the current carried by positive ions at the cathode of a low voltage arc is important for an understanding of the arc, very little experimental work has been done to determine it. The chief cause for this lack has been the complexity of the phenomena at the cathode, making interpretation of the data uncertain. Dr. K. T. Compton[1] has given a method for a systematic estimate of the fraction of current carried by positive ions from consideration of the energy balance at the cathode. Unfortunately, however, his equation can be evaluated only within rather wide limits of uncertainty on account of terms whose magnitudes are as yet indeterminate.

The fraction f of the current at the cathode carried by positive ions can be estimated within limits. Since the voltage drop across a low voltage arc is never much higher than the ionization potential of the gas, and since the mean kinetic energy of the electrons when emitted from the cathode is small, an average electron cannot ionize more than once on its way to the anode. Actually not every electron will ionize, hence the fraction must be less than one-half.

In the present experiments, the fraction f was determined from momentum relations. If an arc is formed between a filament cathode and a surrounding coaxial cylindrical anode (see Fig. 1) a plasma will form extending from the anode to the boundary of the very thin positive ion sheath around the filament. In this plasma may be inserted a small vane, so mounted that forces acting normally on it may be measured. As the vane is in the plasma, it will be struck on both sides by approximately the same number of

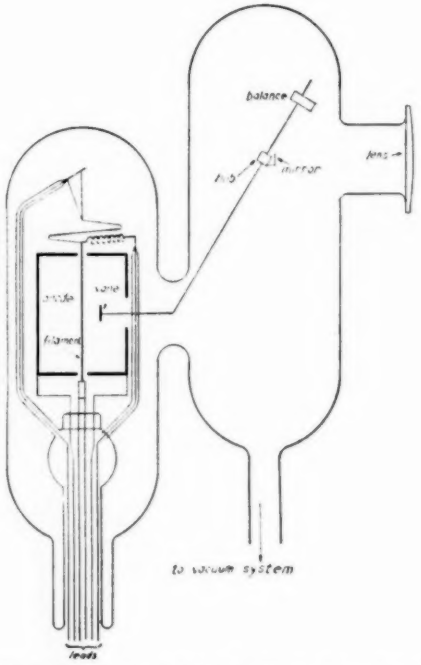

FIG. 1. Diagram of arc tube. (Horizontal section of tube.)

* At present Rhodes Scholar in Merton College, Oxford.

[1] K. T. Compton, Phys. Rev. **37**, 1077 (1931).

random positive ions and electrons. Positive ions drifting into the sheath will fall into the cathode and be neutralized. If after neutralization the particles retain a fraction of the energy gained in the cathode fall, they will spread more or less radially from the filament. A portion of them will strike the vane and again be reflected. The vane will thus undergo a pressure due to the stopping and reflecting of these particles. There is no counterpart to these neutrals on the back of the vane. Thus the vane will tend to move away from the filament.

The fraction of the current carried by positive ions may be calculated as follows, where we consider only the presence of the positive ions and their immediate products after neutralization, leaving till later an analysis of any other forces or disturbing characteristics brought about by the introduction of the vane.

The ions reach the cathode with a kinetic energy corresponding to the cathode fall V_c plus their random energy in the plasma, which is negligible. If v_1 is the velocity of the ions immediately before neutralization,

$$v_1=(2V_ce/m)^{\frac{1}{2}}.$$

A fraction $(1-\alpha)$ of the kinetic energy of the ions is retained after colliding with the cathode, hence the velocity after neutralization, v_2, is given by

$$v_2=v_1(1-\alpha)^{\frac{1}{2}}.$$

In a plane perpendicular to the filament, the particles spread out radially, but in a plane through the filament, the distribution in direction is random. That this is probably the case is suggested by the fact that the ions are striking a surface which consists of particles whose sizes are of the same order of magnitude as those of the impinging ions. Furthermore, in his measurements of the accommodation coefficient of helium on molybdenum using the pressure on an auxiliary electrode, E. S. Lamar[2] had to assume this in order to get results in agreement with the accommodation coefficient as obtained thermally by C. C. Van Voorhis and K. T. Compton.[3]

Under these conditions the normal component of force due to the particles impinging on the vane is:

$$F_1=(2NL/\pi^2l)mv_2\sin\theta_1,$$

where N is the total number of particles leaving the filament per second, L the length of the vane, l the length of the filament, and θ_1 the angle subtended by the vane in a plane perpendicular to the filament.

On rebounding from the vane, the particles will again contribute a normal force component:

$$F_2=(N\theta_1L/\pi l)(mv_2/2)(1-\alpha_V)^{\frac{1}{2}},$$

where $(1-\alpha_V)$ is the fraction of kinetic energy retained after collision at the vane, and where the distribution now is completely random. The total force is, therefore,

$$F=F_1+F_2=\frac{Nmv_2L}{l}\left[\frac{2\sin\theta_1}{\pi^2}+\frac{\theta_1}{2\pi}(1-\alpha_V)^{\frac{1}{2}}\right].$$

If N is replaced by if/e, and the equation be solved for f,

$$f=\frac{Fl}{iL}\left(\frac{e}{m}\frac{1}{2(1-\alpha)V_c}\right)^{\frac{1}{2}}\left(\frac{2\sin\theta_1}{\pi^2}+\frac{\theta_1}{2\pi}(1-\alpha_V)^{\frac{1}{2}}\right)^{-1}.$$

It is at once apparent that the only factors in the equation which are not known are the force F, and the two terms $(1-\alpha)$ and $(1-\alpha_V)$. The force on the vane can be measured; and α and α_V can be identified with the ordinary accommodation coefficients with slight modifications as follows:

The accommodation coefficient has been defined in three ways: by Knudsen,[4] by Blodgett and Langmuir,[5] and by Van Voorhis and K. T. Compton.[6] Knudsen defined the accommodation coefficient as

$$\alpha=(T_2-T_1)/(T_2'-T_1),$$

where T_1 is the temperature of a gas molecule before and T_2 the temperature after striking a surface of temperature T_2'. Langmuir and Blodgett defined the accommodation coefficient in terms of heat exchange. Both definitions

[2] E. S. Lamar, Phys. Rev. **43**, 169 (1933).
[3] C. C. Van Voorhis and K. T. Compton, Phys. Rev. **35**, 1438 (1930).
[4] M. Knudsen, Ann. d. Physik **34**, 593 (1911).
[5] K. D. Blodgett and I. Langmuir, Phys. Rev. **40**, 78 (1932).
[6] C. C. Van Voorhis and K. T. Compton, Phys. Rev. **37**, 1596 (1931).

express the fact that equilibrium is not reached at the surface.

Van Voorhis and K. T. Compton defined the accommodation coefficient for ions as the ratio of measured heating to the expected heating by ions striking a cathode. The expected heating includes two terms, the energy gained by the ion in the cathode fall, and the positive ion work function, itself not definitely known. The possible limits for the positive ion work function, defined as the heating per unit charge when a positive ion of zero kinetic energy is neutralized at a cathode, are $(V_i-\phi_-)$ and zero.

Even if this positive ion work function were known, the α in the above equations would not be the accommodation coefficient as defined for positive ions: for if it were, the factor $(1-\alpha)$ would imply that all kinetic energy that was not consumed in heating remained as kinetic energy of the particles and that none of the excitation energy went into kinetic energy at neutralization. In the case of helium on tungsten, probably a large part of the excitation energy $(V_i-\phi_-)$ goes into heating the cathode. If the remaining goes into radiation, excitation of metastable atoms, and the emission of secondary electrons and ions, the excitation energy can be neglected as far as momentum alone is considered. Lamar and Compton[7] actually found that the excitation energy of argon did not go into kinetic energy at all with an aluminum cathode. Since it is assumed that this excitation energy does not enter into the force equations, α and α_V are identical and may be identified with thermal accommodation coefficients at extremely high temperatures.

In the present experiments, helium gas and a tungsten cathode were used. The Knudsen value of α varies in the literature from 0.06[8] to 0.17.[9] Experiments were performed with the present apparatus, following the procedure developed by Langmuir,[10] which gave Knudsen values ranging from 0.06 to 0.08 with the filament at 2500 degrees Kelvin. It is safe to say that the minimum value to be used here is 0.06, since the ion velocities used are much higher than the thermal molecular values, and should therefore involve a larger number of collisions within the metal. From comparison of data of helium ions on platinum,[11] 0.20 was taken as a safe upper limit; for the velocities used here were smaller, and platinum and tungsten have nearly the same ratios of density to molecular weights, and almost the same molecular weights so that their accommodation coefficients should be of the same order of magnitude.

The tube in which the force was measured consisted essentially of a filament cathode and a concentric cylindrical anode inside of which was a platinum vane attached to an arm of a torsion balance (Fig. 1). The filament was of 15 mil tungsten, 8.65 cm long, and was heated by a 60 cycle alternating current. The heating current was measured through a current transformer to eliminate any direct-current components which might distort meter readings. The anode was of sheet nickel, closed on both ends, 6 cm in diameter, and three inches long. Above the center of the filament was a narrow slit through which the distance between the vane and filament could be measured with a Hilger comparator.

The filament temperature was determined from its resistance which was measured by a Kelvin double bridge. The bridge had a sensitivity sufficient to detect a change of 0.1 percent in the resistance of the filament. Balance was shown by a vibration galvanometer of high sensitivity. As the bridge was balanced only for alternating voltages, no error was introduced by direct-current components in different parts of the bridge.

The vane was made of platinum, nearly one cm square, 0.025 cm thick and located 0.6 cm from the filament. After the arc had been running, the vane became coated with a visible layer of tungsten; hence the vane was in effect tungsten. The force on the vane was measured with a torsion balance whose sensitivity was 0.01 dyne per degree. The effective length of the vane arm was 11.0 cm.

The factors which may produce forces on the vane may be analyzed under five headings: (1) the force due to the neutralized ions coming

[7] E. S. Lamar and K. T. Compton, April Meeting of the National Academy of Sciences (1933).
[8] Roberts, Proc. Roy. Soc. **A135**, 192 (1932).
[9] Michels, Phys. Rev. **40**, 472 (1932).
[10] I. Langmuir, J. Am. Chem. Soc. **37**, 422 (1915).
[11] C. C. Van Voorhis and K. T. Compton, Phys. Rev. **35**, 1438 (1930).

from the cathode; (2) the radiometric forces; (3) electrostatic forces; (4) electromagnetic forces; and (5) electron and positive ion forces.

The force we seek is (1) and has already been discussed. Calculations show that it should be of the order of a dyne. The radiometric force must necessarily be high on account of the high temperature gradient from the filament to the anode. This force depends chiefly upon the temperature of the filament, the thermal accommodation coefficient, the temperature of the vane, and the distortion produced by the presence of the vane. It cannot be calculated, but can be determined experimentally by measuring the force on the vane with the arc turned off and the filament at an equivalent temperature as determined by the resistance. Any additional heating of the vane by electron or ion impact does not produce an unbalanced force on account of the high conductivity and thinness of the vane, and the almost equal distribution of impinging particles.

The electrostatic forces are of two kinds: (a) forces on the vane within the arc, and (b) forces outside of the arc on the vane arm. As long as the vane does not disturb the potential curve of the arc, it will not undergo electrostatic forces. This is true as long as a sheath is formed which does not overlap an anchored electrode. Since the vane was left floating, it assumed a negative potential forming a positive ion sheath. Electrostatic forces on the vane arm were zero also as the vane arm was insulated and assumed along its path the same potential as the surrounding walls.

There could be no magnetic forces as there was no current in the vane or the vane arm, the entire suspension being floating.

Lastly, there are the electron and positive ion forces. The momenta of both the primary electrons from the filament that might strike the vane, and the electrons drifting toward the anode are found to be negligible. The force due to the positive ions is also negligible. Most of the ions were formed between the vane and the filament, hence the ions striking the vane were random ones and as such would strike in nearly equal numbers on both sides of the vane.

When attempts to take data were first made, consistent results could not be obtained. This arose from the fact that the surface conditions of the filament and vane were different when the arc was on or off and when the vane was cleaned by sputtering. Changes in the accommodation coefficient, which is very sensitive to surface conditions, accounted for this initial inconsistency of the results.

A plot of the force as a function of time with the arc on after the vane had been sputtered shows the asymptotic nature of the change of the force (Fig. 2). [It took about a minute to determine the first point.] At first one would imagine that the difference between the values at which the curves straightened out, one curve being with the arc on and the other with the arc off, would give a true value of the force due to the neutralized positive ions. Unfortunately, even at the high temperature of the filament, the cathode surface changed when it was not being bombarded by the positive ion current. Hence the conditions represented by the two asymptotes are not the same. This would not have been so serious had not the radiometric force been so large. Whereas the radiometric force gave a deflection of about 550 degrees, the force due to the neutralized positive particles twisted the fiber only about ten degrees. In other words, a two percent change in the radiometric force completely overshadowed the force being sought! These difficulties could be overcome if measurements were made when both the vane and filament were clean, that is, if the curves could be extrapolated to zero time.

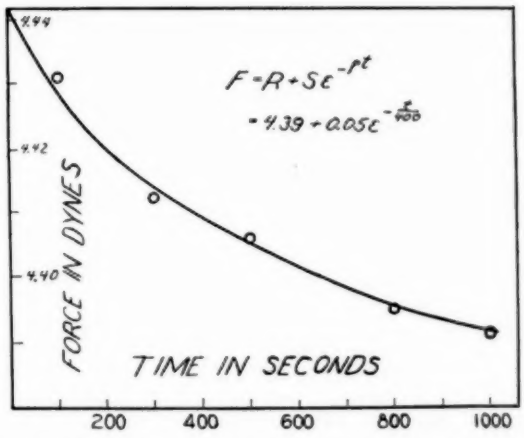

FIG. 2. Force on the vane as a function of time after sputtering of the vane was stopped.

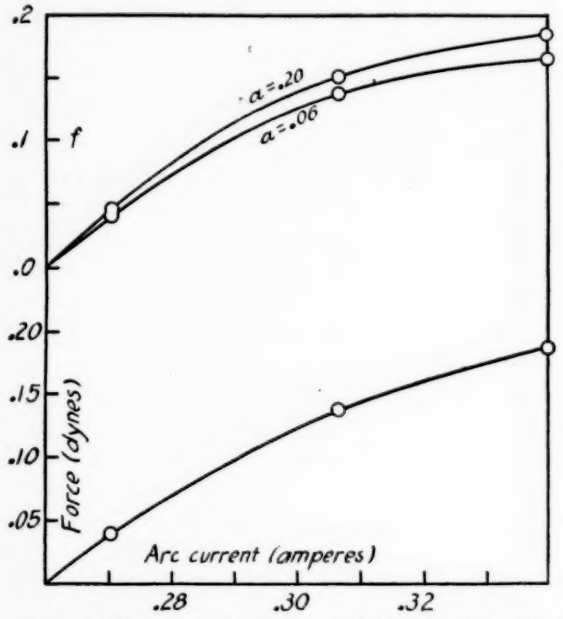

FIG. 3. Force on the vane, and the fraction of the current carried by positive ions at the cathode as functions of total arc current.

The shape of these curves as they approach the axis can be calculated if it is assumed that the change in the force is due to changing surface conditions. Consider the case in which only the vane is affected, that is the arc is kept running. The rate of formation of a layer of adsorbed gas depends upon the rate at which the particles are adsorbed and upon the rate with which they evaporate. If σ is the fraction of the surface covered,

$$d\sigma/dT = A(1-\sigma) - B\sigma$$

for the rate of adsorption depends upon the fraction uncovered, and the rate of evaporation on the fraction covered.

If α for a clean surface is denoted by α_c and for a covered or dirty surface by α_d, the force dependence on the α's can be written

$$F = P[1+\sigma(1-\alpha_d)^{\frac{1}{2}} + (1-\sigma)(1-\alpha_c)^{\frac{1}{2}}].$$

On reduction to the simplest form

$$F = R + S\epsilon^{-\rho t},$$

where

$$R = P\left[1+\left(1-\frac{\alpha_c}{2}\right)+\frac{A}{2(A+B)}(\alpha_c-\alpha_d)\right],$$

$S = [P/2(A+B)](\alpha_c-\alpha_d)$ and $\rho = A+B$.

Fig. 2, shows a plot of a typical curve satisfying the derived equation. Thus the curves may be extrapolated to zero time, in accordance with this equation, and there is no sudden change near the force axis.

By this method, it was possible to measure the force on the vane as a function of the arc current at a pressure of 0.090 mm (Fig. 3). From these measurements the values of f in Table I were calculated.

TABLE I. *Values of f.*

Arc current (amp.)	Twist (deg.)	Force (dynes)	f $\alpha=0.06$	f $\alpha=0.20$	f mean	Arc drop volts
0.340	19.0	0.180	0.165	0.185	0.175	29
.307	14.5	.136	.138	.155	.147	21
.270	4.0	.038	.044	.049	.046	16.8

The point where the fraction goes to zero may be interpreted as the point where the arc goes off. Of course, f really should not go entirely to zero, but smaller forces due to smaller values of f could not be detected by the methods employed. Up to 0.260 ampere, the current was practically all electronic. Table II and Fig. 4 show the variation of the positive ion and electron currents at the cathode with different arc currents.

TABLE II.

i	0.340	0.307	0.270	(0.260)
i_+	.060	.045	.012	(.000)
i_-	.280	.262	.258	(.260)

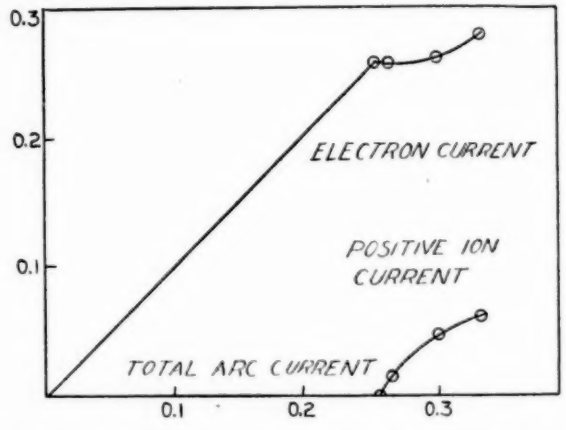

FIG. 4. The electron and positive ion currents at the cathode as functions of total arc current.

It is interesting to note that as long as the arc ran as a low voltage arc, the electron current was almost constant (Fig. 4). The rise when the arc reached 0.34 ampere was due to more secondary emission on account of bombardment by more positive ions, photons, and metastable atoms, and to a change in the field immediately at the cathode.

The accuracy of these experiments is limited by both experimental difficulties and by uncertain assumptions. The greatest experimental error came in through the variation of the radiometric force. Repeated measurements showed that the radiometric force could be matched to within one degree twist with a total deflection of 550 degrees. As the largest force due to the neutrals superimposed on the radiometric force was only about a twist of 20 degrees more, an accuracy of 5 percent is the best that can be expected. All other measurements were far more accurate.

The author is indebted to Dr. K. T. Compton for the subject of this paper as well as for much valuable advice and encouragement. He also wishes to express his appreciation to Dr. E. S. Lamar for his frequent advice and generous assistance. He also extends his thanks to Mr. Ryan for the glass blowing in the construction of the experimental tube.

Electronic Energy Bands in Metals

J. C. SLATER, *Massachusetts Institute of Technology*

(Received April 5, 1934)

The method of Wigner and Seitz is extended to the computation of the excited bands of electrons in a metal, with particular applications to sodium. Instead of using simply one s wave function, as Wigner and Seitz do, a combination of eight separate functions is used, one s, three p, three d, and one f. Boundary conditions for an arbitrary electron momentum are satisfied at the midpoints of the lines connecting an atom with its eight nearest neighbors. The solution is carried out for an arbitrary direction of propagation in one of the principal planes. Energy levels and wave functions are determined as functions of internuclear distance, leading to the following qualitative results: At the observed distance of separation, energy levels are given with remarkable accuracy by the Fermi-Sommerfeld theory, the gaps fall approximately where they should as computed from de Broglie waves, and the wave functions act accurately like plane waves in the region between atoms, but fluctuate violently, like s, p, $\cdots$ functions, near the nuclei. Gaps in energy are precisely filled up, though in each definite direction of propagation there are gaps. As the internuclear distance increases, gaps in energy appear at definite points, the allowed regions shrinking to zero breadth about the atomic energy levels at infinite separation.

INTRODUCTION

WIGNER and Seitz[1] have proposed an important improvement in the methods of finding wave functions for electrons in periodic force fields, such as one encounters in metals. Previous methods had proceeded by perturbation theory; a good account of these methods is found in the excellent article by Sommerfeld and Bethe[2] in the *Handbuch der Physik*. Many of the results quoted in that article will be assumed familiar to the reader, as well as the paper of Wigner and Seitz. The advance of Wigner and Seitz lay in their observation that the potential field acting on an electron in a metal is very approximately spherically symmetrical in the neighborhood of a nucleus, so that the wave equations can be solved by separation of variables, and numerical integration of the equation for the radial function, as in problems of isolated atoms. Only the boundary conditions distinguish the problem from an atomic one. They imagine the crystal to be made up of closepacked cells, one surrounding each nucleus, approximately spheres but bounded by planes so that they exactly fill the space. Then the wave function must satisfy the condition that it be continuous with continuous derivative in going from one cell to the next. Further, they consider only the lowest electron level, for which the wave function is periodic, repeating in each cell. It is easy to see that their conditions then demand that the normal derivative of the wave function be zero around the surface of the cell, which they approximate by using a spherical cell of the same volume as the actual one, and making the radial derivative of the wave function zero on the surface of the sphere. By applying this condition they obtain an energy level as function of internuclear distance (or of radius of the sphere), showing a minimum near the observed internuclear distance, and which they could bring into connection with the heat of dissociation of the crystal. They estimate the excited energy levels, corresponding to electrons having linear momentum of translation through the crystal, from the Fermi distribution, adding the kinetic energy of free electrons to the energy derived for the lowest state, and correctly pointing out that the actual band of energy levels will necessarily be narrower than the band so computed. It is the purpose of the present paper to extend the method of Wigner and Seitz to an actual calculation of these excited energy levels.

[1] Wigner and Seitz, Phys. Rev. **43**, 804 (1933).
[2] Sommerfeld and Bethe, Handbuch der Physik, Vol. XXIV, 2nd Ed.

1. Formulation of Boundary Conditions

Consider a wave which is modulated, in passing through the crystal, according to the plane wave function $\exp(i(\mathbf{k}\cdot\mathbf{r}))$, so that $\mathbf{k}/2\pi$ is a vector along the wave normal, equal numerically to the wave number, and $\mathbf{k}h/2\pi$ would be the mechanical momentum, if the wave represented a free electron. Then according to a theorem of Bloch (for this and similar references, see Sommerfeld and Bethe[2]), if we go from one point in the lattice to an equivalent point in another cell, the wave function is multiplied by the factor $\exp(i(\mathbf{k}\cdot\mathbf{r}_{ij}))$, where $\mathbf{r}_{ij}$ is the vector from the nucleus i of the first cell to the nucleus j of the second. In particular, consider one cell and an adjacent cell, so that $\mathbf{r}_{ij}$ is not only the distance between adjacent nuclei, but the perpendicular distance between the opposite faces of the cell, which are cut at right angles by the line joining the nuclei in question. Going from a point of one of these faces to the perpendicularly (not diametrically) opposite point of the other is then such a translation as we have considered. Our boundary condition then is: in going from a point of the surface of the cell to the perpendicularly opposite point, the wave function must be multiplied by $\exp(i(\mathbf{k}\cdot\mathbf{r}))$, where $\mathbf{r}$ represents the perpendicular distance between faces. Similarly, each of the three components of the gradient must be multiplied by the same factor. The latter condition can be restated. The tangential components of gradient will be automatically taken care of, so that we consider only the normal components. We note that the absolute direction in space which is along the outer normal for one face is along the inner normal for the other. Thus we require that the derivative along the outer normal be multiplied by $[-\exp(i(\mathbf{k}\cdot\mathbf{r}_{ij}))]$ in going from one point to the perpendicularly opposite point. This is the general and exact boundary condition.

Our problem is to solve a spherically symmetrical wave equation, subject to the boundary condition stated above on the surface of a polyhedral cell. The problem is in essence soluble. We may separate variables, and solve the equation in a series of products of spherical harmonics of the angle, multiplied by functions of r, the coefficients of the series being arbitrary. Such a solution can be found for any energy value, and for any energy value we can satisfy the one boundary condition that the function be finite at the origin, though except for the characteristic values of the equation these solutions will become exponentially infinite at infinity. This however does not concern us, since we work in finite cells. It is now in principle possible to choose the infinite number of coefficients so as to satisfy the boundary conditions. The procedure, however, is impracticable, and here we introduce an approximation. We try to get the approximate solution by summing a finite number out of the infinite series of solutions, and consequently we can satisfy the boundary conditions, not at every point of the surface, but only at certain discrete points. In the actual calculations described, we have dealt with a body centered cubic lattice, and we have satisfied the boundary conditions at the eight midpoints of the lines joining an atom to its eight nearest neighbors; that is to say, referring to *W.* and *S.* Fig. 1, at the centers of the eight hexagonal faces of the cell. Corresponding to this, we require only eight wave functions; and using the conventional spectroscopic notation for l values, we find that this demands one s function, three p's, three d's, and one f. It now proves to be the case that we can satisfy the boundary conditions at the centers of faces particularly easily, for then corresponding points are diametrically opposed (at opposite ends of a line passing through the nucleus) as well as perpendicularly.

Let u be the wave function we are considering, a function of three coordinates. Let it be a sum of an even part u_g which is unchanged on going from one point to the diametrically opposite point, and an odd part u_u whose sign changes. Then if the function is u_g-u_u at the midpoint of one face, it will be u_g+u_u at the opposite point, and similarly if its normal derivative is $u_g'-u_u'$ at one midpoint, it will be $u_g'+u_u'$ at the opposite point, where primes indicate normal derivatives. Hence our boundary conditions may be stated as

$$(u_g+u_u)=[\exp(i(\mathbf{k}\cdot\mathbf{r}))](u_g-u_u),$$

$$(u_g'+u_u')=-[\exp(i(\mathbf{k}\cdot\mathbf{r}))](u_g'-u_u'),$$

where the u's are to be computed at the mid-

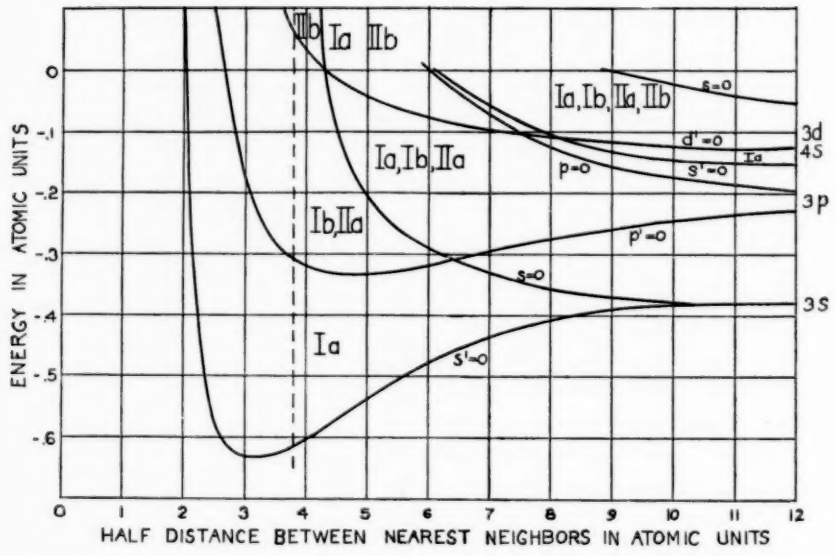

FIG. 1. Energy bands for sodium. Symbols Ia–IIb represent type of state allowed in each band.

points of faces, $\mathbf{r}$ is the vector joining midpoints, and there are in our case four such conditions, for the four pairs of opposite faces.

The equations above can be easily transformed to a more usable form. The first one gives at once

$$\frac{u_g}{u_u}=-\frac{1+\exp(i(\mathbf{k}\cdot\mathbf{r}))}{1-\exp(i(\mathbf{k}\cdot\mathbf{r}))}=-i\cot(\mathbf{k}\cdot\mathbf{r}/2),$$

and the second gives

$$u_g'/u_u'=i\tan(\mathbf{k}\cdot\mathbf{r}/2).$$

Since it is allowable to multiply the whole solution by an arbitrary factor, let us assume that u_g is real. Then the equations demand that u_u be pure imaginary, so long as k is real, which is necessary for real, undamped propagation. If $|u_u|$ is the absolute magnitude of u_u, we then have $u_u=i|u_u|$, so that the equations above may be combined in the form

$$|u_u|/u_g=-u_g'/|u_u|'=\tan(\mathbf{k}\cdot\mathbf{r}/2).$$

The four equations of this sort give eight equations in all to be satisfied for the boundary conditions.

To satisfy these conditions, it proves to be necessary to build up u_g as a sum of four independent functions, and similarly for u_u. Now all the spherical harmonics can be written in such form that they have the same magnitude at each of the eight midpoints in question, differing only in sign. There are then just eight different types of function: (1) a function which has the same value at all eight points; (2) three functions in which there is a change of sign on reflection in one of the three coordinate planes; (3) three functions in which there is a change of sign on reflection in one of the three coordinate lines; (4) one function which changes sign on reflection through the origin. Any one of these types can be set up in an infinite number of ways from the infinite number of wave functions at our disposal. But we assume that, at any rate for states of low energy, we shall get a good approximation by taking in each case only the lowest state of the required symmetry. Thus we take in case (1) an s function, in (2) the three p functions with spherical harmonics x/r, y/r, z/r, in (3) the three d functions with spherical harmonics xy/r^2, yz/r^2, zx/r^2, and in (4) the one f function xyz/r^3. It is obvious that in building up our solution from these functions, we cannot hope to reproduce correctly the energy levels originating in any atomic level except an s or p; for we omit entirely two of the five d, and six of the seven f, functions.

Let $R=r/2$ be the distance from a nucleus to the midpoint where we satisfy boundary conditions. Let s, p, d, f represent the values of the radial parts of the corresponding functions, at this distance R from the nucleus. Then, if we put in the suitable values of x/R, etc., for the corresponding midpoints, we have

$$u_g=As+3(Bxy+Cyz+Dzx)d/R^2,$$

$$|u_u|=3^{\frac{1}{2}}(Ex+Fy+Gz)p/R+H(3)^{\frac{1}{2}}xyz\,f/R^3.$$

In particular, we have four pairs of midpoints. Let us compute the values of the u's in succession for the four points whose coordinates x/R, etc., are $3^{-\frac{1}{2}}$ times (111), (11-1), (1-11), (1-1-1). We have, for instance for the second, $u_g=As+(B-C-D)d$, $|u_u|=(E+F-G)p-Hf$. For setting up the equations, we need also the quantities tan $(\mathbf{k}\cdot\mathbf{R})$. Remembering that the components of R are each $\pm R/3^{\frac{1}{2}}$, the second of these quantities for instance is tan $((k_x+k_y-k_z)R/3^{\frac{1}{2}})$. Let us name the four tangents, in the order stated above, K, L, M, N. Then our eight equations describing the boundary conditions become

$$K(As+(B+C+D)d)-(E+F+G)p-Hf=0,$$

$$L(As+(B-C-D)d)-(E+F-G)p+Hf=0,$$

$$M(As+(-B-C+D)d)-(E-F+G)p+Hf=0,$$

$$N(As+(-B+C-D)d)-(E-F-G)p-Hf=0,$$

$$(As'+(B+C+D)d')+K((E+F+G)p'+Hf')=0,$$

$$(As'+(B-C-D)d')+L((E+F-G)p'-Hf')=0,$$

$$(As'+(-B-C+D)d')+M((E-F+G)p'-Hf')=0,$$

$$(As'+(-B+C-D)d')+N((E-F-G)p'+Hf')=0.$$

These are eight simultaneous linear homogeneous equations for the eight coefficients $A\cdots H$, and as such they have no non-vanishing solutions unless the determinant of their coefficients is zero. This gives a single relation between the four quantities K, L, M, N. A second relation between these quantities arises from the fact that they are derived from only three independent variables, the three components of $\mathbf{k}$. With these two relations between K, L, M, N, only two of them may be taken to be arbitrary. We may for instance assume arbitrarily two variables determining the direction of $\mathbf{k}$, so that for each energy, internuclear distance, and wave normal, the equations determine the magnitude of the electronic momentum or wave-length. The solution corresponds to a real wave, however, only if K, L, M, N are all real. The regions of energy and internuclear distance where this condition is satisfied correspond to the allowed bands of energy, those where some of these quantities are complex correspond to the forbidden bands, in which only damped waves can be propagated.

2. Propagation in the xy Plane

The equations above are too difficult to handle in the general case. However, if we limit ourselves to propagation in an arbitrary direction in the xy plane, they simplify enough so that they can be solved, and at the same time the results are of sufficient generality to indicate the essentials of the general solution. In this case $k_z=0$, from which $K=L$, $M=N$. Now we set up eight new equations, of which the first is half the sum of the first two above, the second half the sum of the third and fourth above, and so on, and the fifth to eighth are half the corresponding differences. These equations are

$$K(As+Bd)-(E+F)p=0,$$

$$M(As-Bd)-(E-F)p=0,$$

$$(As'+Bd')+K(E+F)p'=0,$$

$$(As'-Bd')+M(E-F)p'=0,$$

$$K(C+D)d-Gp-Hf=0,$$

$$M(-C+D)d-Gp+Hf=0,$$

$$(C+D)d'+K(Gp'+Hf')=0,$$

$$(-C+D)d'+M(Gp'-Hf')=0.$$

These equations break up into two groups of four each, the first containing the four variables A, B, E, F, and the second containing C, D, G, H. They can thus be solved separately. For all eight variables to be different from zero demands

that the determinant of coefficients of each of the two sets of equations be zero, giving one more condition than we had before, so that in general we cannot satisfy both conditions. As a result, we must satisfy our equations by letting all variables of one of the two sets be zero, and satisfying the determinantal equation connected with the other set. This divides our solutions into two independent sets: (I) in which A, B, E, F are different from zero, the others equal to zero, and (II) in which C, D, G, H only are different from zero. On looking back at the significance of the constants $A \cdots H$, we see that solutions of the first class are unchanged on reflection in the xy plane, while those of the second class change sign on reflection. We now consider separately the two classes.

Class I

Eliminating A, B, E, F, between the four equations, the determinantal equation by elementary algebraic manipulation can be put in the form

$$[K^2+\tfrac{1}{2}(p/p')(s'/s+d'/d)] \times[M^2+\tfrac{1}{2}(p/p')(s'/s+d'/d)] = [\tfrac{1}{2}(p/p')(s'/s-d'/d)]^2.$$

This determines a single relation between K^2 and M^2, assuming that s, s', etc., are regarded as known, which they are if we first fix the energy and internuclear distance. Plotting M^2 against K^2, it is the equation of a rectangular hyperbola, with the 45 degree diagonal passing through the foci, and the asymptotes at K^2, $M^2=-\frac{1}{2}(p/p')\times(s'/s+d'/d)$, the two intersections with the 45 degree line coming at $K^2=M^2=-(p/p')(s'/s)$, $-(p/p')(d'/d)$.

Let us next consider the other relation between K and M. In the present case, by assuming propagation to take place in the xy plane, we have already fixed one of the two variables determining the direction of the wave normal. Let the other be θ, the angle between this direction and the x axis. Then $k_x=k\cos\theta$, $k_y=k\sin\theta$, where k is the magnitude of the vector, so that

$$K=\tan(k_x+k_y)R/3^{\frac{1}{2}}, \quad M=\tan(k_x-k_y)R/3^{\frac{1}{2}},$$

from which, eliminating k and R by easy trigonometrical manipulation, $(\tan^{-1}M)/(\tan^{-1}K)=\tan(45°-\theta)$. This equation between K and M must be solved simultaneously with the hyperbolic equation above, determining K and M as functions of θ, and hence determining k, the magnitude of the momentum, as a function of direction of the wave normal. The solution is most easily carried out graphically, plotting both equations in the K^2-M^2 plane. The first equation, as we have seen, is that of a hyperbola. The second gives curves, proceeding out from the origin in a more or less radial manner. On account of the symmetry, we can get all possible types of propagation by merely considering angles θ between 0 and 45 degrees. For $\theta=0$, $M=K$, so that the curve is the 45 degree diagonal in the K^2-M^2 space. For $\theta=45$ degrees, $M=0$, so that the curve is the axis of abscissas. For intermediate angles, the curve lies between these values. Further, in order to have real propagation, K and M must be real, so that K^2 and M^2 are positive. Hence we consider only the intersections of the two curves in the first quadrant. With these descriptions of the curves, the following facts become evident. The equations can have no, one, or two real solutions. If both intersections of the hyperbola with the 45 degree diagonal come for negative K^2 and M^2, there are no real solutions. This is the case if $-(p/p')(s'/s)$ and $-(p/p')(d'/d)$ are both negative, or if s'/s, p'/p, and d'/d all have the same sign. If one of these conditions is satisfied, but not the other, there will be one real solution. In this case one branch of the hyperbola cuts the first quadrant. If it cuts both 45 degree line and axis of abscissa, there will be real propagation for all directions; this is true if the asymptotes come for negative K^2 and M^2, or if $-\frac{1}{2}(p/p')(s'/s+d'/d)$ is negative. In the contrary case, however, the hyperbola will cut the 45 degree line but not the axis of abscissas, so that there will be real propagation for a certain range of angles about $\theta=0$, but no real propagation in the neighborhood of 45 degrees. Finally if both intersections of the hyperbola with the diagonal are positive, there will be two real solutions. One of these, coming from the positive branch of the hyperbola, will necessarily have real propagation for a limited range of angles only, while the other, coming

from the negative branch, which must cut both axes, will have propagation for all directions.

Class II

The discussion is throughout similar to that of class I. The determinantal equation is

$$[K^2+\tfrac{1}{2}(d'/d)(p/p'+f/f')] \times[M^2+\tfrac{1}{2}(d'/d)(p/p'+f/f')] = [\tfrac{1}{2}(d'/d)(p/p'-f/f')]^2.$$

The asymptotes come at K^2, $M^2=-\frac{1}{2}(d'/d)\times(p/p'+f/f')$, the intersections with the 45 degree line at $K^2=M^2=-(d'/d)(f/f')$, $-(d'/d)(p/p')$. If these values are substituted for the corresponding ones of class I, the same discussion applies in the present case.

For both cases, once K and M are determined as functions of θ, the linear equations can be solved for the coefficients, A, B, E, F, or C, D, G, H, and the whole wave functions can be set up. Of course, only the ratios of coefficients are determined, the absolute values coming from the normalization condition. The solution is perfectly straightforward, and it is unnecessary to reproduce it here.

3. Results

With the same potential curve for sodium employed by Wigner and Seitz, calculations have been made for s, p, d, f wave functions connected with a variety of energies. From these, we get s'/s, p'/p, etc., as functions of internuclear distance for each energy used. We can then construct Fig. 1, in which energies are plotted as functions of internuclear distance, and in which the curves are those on which $s'=0$, $p'=0$, etc., and $s=0$, $p=0$, etc. The lowest curve $s'=0$ is that of Wigner and Seitz. These curves divide the space into different regions, within each of which the equations have a definite number of real solutions; for it is obvious that such a quantity as $-(p/p')(s'/s)$, whose sign determines the number of solutions, will change sign when either s', p', s, or p changes sign by going through zero. We see that for large distances, the allowed regions are narrow bands surrounding each energy level of the isolated atom, the bands broadening as the atoms come together, until they touch or overlap. As indicated in Fig. 1, it is convenient to divide the solutions into their four types, two of class I, two of class II, in which $-(p/p')(s'/s)$ is positive for class Ia, $-(p/p')(d'/d)$ is positive for classes Ib and IIa, and $-(f/f')(d'/d)$ is positive for class IIb, so that Ib and IIa always occur together in the same region. Then we note the following fact from Fig. 1: as the energy bands broaden, and attempt to overlap, two solutions of different type can overlap without interfering with each other; but two solutions of the same type not only do not overlap, but are forced entirely out of the overlapping part of the band. An example is seen in the overlapping of the $3s$ and $3p$ bands, in which among the three solutions of $3p$, there is one, of type Ia, which has the same symmetry as the $3s$ solution. This type is absent in the overlapping region, only the other two $3p$ functions occurring in this region. Several other examples are evident in the figure. This effect is similar to that found in second order perturbation theory, in which terms of different symmetry do not perturb each other, but terms of the same symmetry repel. Another fact follows from Fig. 1, if it is extended to larger internuclear distances: while one state originates from each atomic s level, three from each p level, as we should suppose, only three originate from each d level, instead of five, and only one from each f level, instead of seven. This was to be expected, as we mentioned earlier, on account of using but eight functions to set up our approximate solution. It means, however, that above the lowest line $d'=0$ we must expect to have missing states, not given by our approximation, so that we can place no great credence in any results of the method for higher energies. At the actual distance of separation, this means that but three states, the $3s$ and two of the $3p$, may be expected to be reliable. A next step in the improvement of the method would consist in using, not eight, but fourteen functions, satisfying conditions at the midpoints of lines to the eight nearest and six next nearest neighbors, or at the center of each face of the cell. This would be quite feasible, and should extend the correct results to decidedly higher energies.

The well-known gaps in energy appear at large distances in Fig. 1, as the gaps between energy levels arising from different atomic

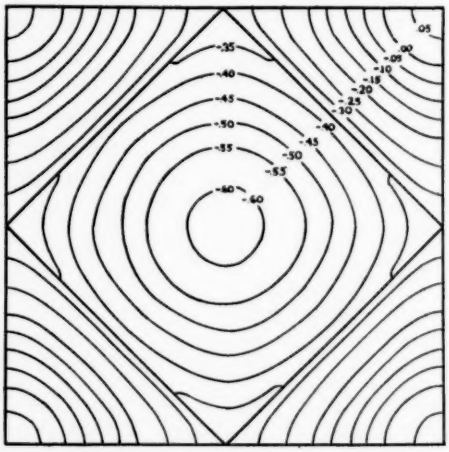

FIG. 2. Two inner Brillouin zones, showing energy contours, approximately normal distance of separation.

states. For smaller distances they are not evident in the figure, the allowed states filling all energy levels without gaps in energy. The gaps come about if we consider only a particular direction of propagation; the allowed bands in this case would not fill up the whole regions in Fig. 1, and in general there would be gaps separating the regions. This situation is indicated in Fig. 2, in which we use a space with k_x as abscissa, k_y as ordinate, essentially a momentum space, and draw contours of constant energy. In this space, as Brillouin has shown (see Sommerfeld and Bethe), certain zones are formed, bounded by straight lines, and the gaps in energy come at the boundaries of the zones. In our case these are three dimensional zones, and in Fig. 2 we give the sections of them made by the plane $k_z=0$. They resemble, but are not identical with, the zones of two-dimensional lattices discussed by Brillouin, Sommerfeld and Bethe. Only two out of our three lowest zones, the $3s$ Ia and $3p$ Ib, prove to be cut by the plane $k_z=0$, when plotted in this way. We shall not go into the method of identifying the polygonal parts of zones with the central zone, since this question is treated in the references mentioned.

In Fig. 2 the gaps of energy are plainly evident: along the 45 degree diagonal, there is no contour for energy -0.35, the energy jumping from about -0.37 to -0.32. If we look at the figure in a broader way, however, we see that the lines of constant energy are roughly circles. If the electrons were free, the lines would be exactly

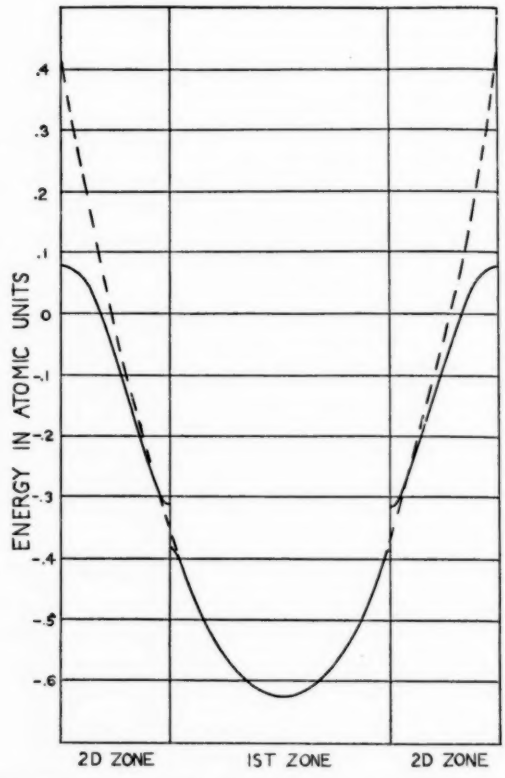

FIG. 3. Energy as function of wave number, for wave in 110 direction, showing first two zones.

circular, the energy depending only on the magnitude of the momentum, not on its direction. From the resemblance of the curves to circles, we see that the free electron picture is not entirely incorrect. The comparison is better shown in Fig. 3, in which we plot energy as a function of the magnitude of k, for the 110 direction, or the 45 degree direction of Fig. 2. The free electron distribution would correspond to a parabolic curve, the kinetic energy being proportional to the square of the momentum. As we see, the actual curve agrees rather closely with the free electron parabola, which is drawn with the correct constants. In fact, for the lower half of the bottom zone, which alone is filled with electrons in the normal state of the metal, the agreement is practically perfect. This is an unexpected and significant result of the present calculations. It has been expected that the true curve would be represented by a parabola in its lower part, but it was generally supposed that the curvature of the parabola would be less than for free electrons. As a matter of fact, if we draw

similar curves for a distance of separation decidedly greater than the normal distance, say twice as great, we do find a decidedly smaller curvature, the gaps becoming much larger in proportion, and the curves for the occupied regions much flatter, so that these regions are narrower than for the case of the free electron distribution, as pointed out by Wigner and Seitz. But at, or even in the general neighborhood of, the equilibrium distance, the free electron energy is a good approximation, except in the immediate neighborhood of the gaps. Another point may be noticed from Fig. 3. The forbidden energy bands are closely connected with electron diffraction by the crystal; if electrons are thrown at the crystal in such a direction and with such energy that they would lie in a forbidden band within the metal, they are totally reflected, and form the Bragg reflected beams. The Bragg law of reflection, which is experimentally verified for the electrons, is correct only if the forbidden bands come just at the places predicted by the free electron curves. These energies and momenta lie at the intersection of the parbola with the vertical lines at the edges of the zones, in Fig. 3, and it is significant that they lie within the gaps as actually found. Thus our energy distribution would lead to Bragg reflections, not just at one definite angle, but through a range of angle, resulting in a broadening, but the angle predicted by the elementary law would lie within the actual broadened beam of directions.

The wave functions themselves show interesting form. In Fig. 4, we plot the wave function from the lowest zone, normal distance of separation, energy -0.60, corresponding to a long wave-length. The wave is travelling in the 110 direction, and a line is drawn through a set of atoms in the 111 direction (the closest direction to the wave normal in which we can find a closely packed line of atoms). The real part of the wave function is plotted as a function of distance along that line, the nuclei being indicated. In the neighborhood of the nuclei, the function has the character of an atomic function, being like a $3s$ function at the left side of the diagram, a $3p$ at

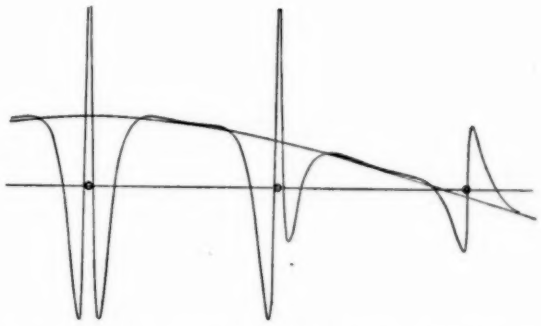

FIG. 4. Electronic wave function, real part, for points on a line in 111 direction.

the right. In the imaginary part of the wave function, the rôle of $3s$ and $3p$ would be interchanged. But now we note that in between nuclei the wave function follows close to a sinusoidal curve, which is drawn for comparison. The accuracy of the agreement is another unexpected result of the present calculation. It has been checked by cutting through the same wave in other directions, and also by considering waves of other wave-lengths. It means that in all that part of the metal when the valence electron is not actually penetrating into the core of an atom, its wave function is much like that of a free electron, just as its energy is approximately that of a free electron. Here again, for distances of separation much larger than the normal distance, we no longer have agreement with the free electron picture. It is worth pointing out that the essentially new results of the present paper, namely the indication of the accuracy of the free electron picture both in energy and in the part of the wave function outside the atom (but not inside), and the detailed investigation of the nature of the energy gaps and zones (which can be carried much further than we have indicated) both depend on the possibility of actually solving the wave equation for an electron in a periodic field without important approximations. We could hardly expect them to follow with anything like the same certainty from a perturbation method which would be inaccurate at the actual internuclear separation.

The Absorption Spectrum of the Iodine Atom

J. H. McLeod, *Research Laboratory of Physics, Harvard University*

(Received April 9, 1934)

The absorption spectrum of atomic iodine has been investigated in the spectral range λ2100 to 1400Å. The iodine was dissociated by heating to 1000°C. A hydrogen discharge tube or an iodine discharge tube was used as the source of illumination. The former source revealed clearly that λ1830 and 1783Å are absorption lines. When light from a discharge in iodine was passed through the heated iodine the following lines were found to be weakened by absorption, λ1830, 1783, 1642, 1618, 1583, 1515, 1507 and 1422Å.

IODINE is one of the few remaining elements whose atomic arc spectrum is not as yet well analyzed. Turner[1] measured the wave-length of the arc lines in the Schumann region and later[2] identified the fundamental multiplet which arises from electronic transitions to the fundamental $^2P_{1/2,\ 3/2}$ energy level. In a later paper Turner[3] also described experiments on the absorption of iodine emission lines when the light was passed through a column of iodine gas partially dissociated by radiation from a quartz mercury arc. Evans[4] and Deb[5] have analyzed some of the lines appearing in the visible and infrared portions of the spectrum.

With a view to getting more information about the spectrum of iodine two experiments were carried out to further investigate the absorption spectrum of iodine in the Schumann spectral region.

In the first experiment the continuous radiation from a hydrogen discharge tube was used as a source. Fig. 1 shows the general arrangement of the apparatus. The hydrogen discharge tube at H emitted ultraviolet light. The fluorite lenses L_1 and L_2 directed the light through the quartz absorption cell and on to the slit of the spectrograph.

The absorption cell was 15 cm in length and had very thin windows of quartz. The temperature of the absorption cell could be raised to 1000°C by means of the electric resistance furnace.

Iodine at a partial pressure of approximately 0.3 mm was admitted to the absorption cell from a side tube kept at 26°C. At a temperature of 1000°C practically all of the iodine was in the atomic form.[6] Pure argon at a pressure of about 55 cm was mixed with the iodine. The purpose of the argon was to broaden the absorption lines of iodine to such a width that they would be recorded as lines on the plate, even with a spectrograph of low resolving power.

Two spectrographs were used. The first was a small Hilger quartz instrument from which all the oxygen was displaced by flowing through it a stream of tank nitrogen. Fig. 2a is a positive print of a spectrogram taken with this instrument. The resonance line at λ1830Å is seen to be clearly absorbed by the iodine gas. Attempts were made to observe in absorption other lines in this region namely λ1844, 1876 and 2062Å. No trace of absorption at these wave-lengths was observed. This result agrees with Turner's

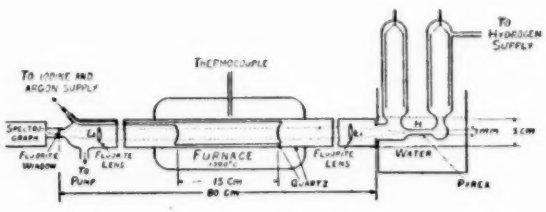

FIG. 1. General arrangement of absorption tube.

[1] Turner, Phys. Rev. **27**, 397 (1926).
[2] Turner, Phys. Rev. **31**, 983 (1928).
[3] Turner, Phys. Rev. **41**, 627 (1932).
[4] Evans, Proc. Roy. Soc. **A133**, 417 (1931).
[5] Deb, Proc. Roy. Soc. **A139**, 380 (1933).

[6] Starck and Bodenstein, Zeits. f. Elektrochemie **16**, 965 (1910).

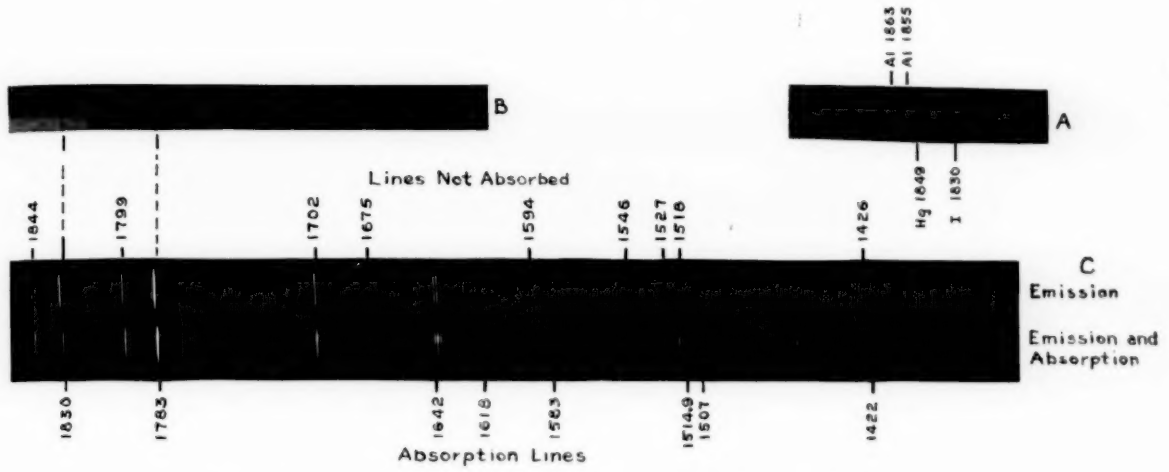

FIG. 2. Spectrograms showing lines which appear in emission and absorption.

analysis since he allotted the lines mentioned to transitions to the upper or metastable $^2P_{1/2}$ member of the doublet P low level. The temperature of 1000°C was too low to elevate a sufficient number of atoms into the metastable level which is 7600 cm^{-1} higher up in energy value.

For investigations of shorter wave-lengths a vacuum grating spectrograph was employed. The grating had 30,000 lines per inch and a radius of curvature of one meter. Fig. 2b is a reproduction of the absorption spectrum observed with the grating spectrograph. The lines at λ1830 and 1783Å are seen to be absorbed. The iodine was at a pressure of about 0.3 mm and the argon at a pressure of 30 cm.

It will be noted that the hydrogen continuous spectrum did not extend much below λ1783. This was because the quartz windows absorbed shorter wave-lengths when the quartz was heated to 1000°C. When the furnace had cooled off, the upper spectrum of Fig. 2b was made by running the hydrogen discharge tube for a short time. The quartz windows then transmitted to below 1630 and the hydrogen lines in the region 1630–1650 were recorded. The position of these lines and the known dispersion of the spectrograph served to identify with certainty the two absorption lines. A trace of the mercury absorption line at λ1849 appeared on the original plate and served as an additional check on the wave-length of the absorption lines.

For the investigation of the absorption spectrum below λ1783 a different method was necessary. Obviously all quartz in the path of the light had to be eliminated. Below λ1650 the continuous spectrum of hydrogen is very weak and to make matters worse a many-line spectrum begins. The hydrogen discharge tube was therefore unsuited for the work.

Fig. 3 shows the arrangement of the new apparatus. It consisted essentially of two tubes, an emission tube to emit the spectrum of iodine and an absorption tube to reabsorb any absorption lines. The emission tube was of Pyrex glass about 8 mm internal diameter. It contained iodine at about 0.04 mm pressure and argon at about 5 mm pressure. A current of 100–140 m.a. a.c. produced a brilliant arc spectrum of atomic iodine. The absorption tube was of quartz and the central portion was surrounded by a furnace to dissociate the iodine molecules. No focussing lenses were used, instead the high reflecting power of quartz and glass for rays at nearly grazing incidence was depended on to produce sufficient light at the slit of the spectrograph in spite of the distance of half a meter between the discharge tube and the slit.

Care was taken to prevent the iodine from coming into contact with wax or stopcock grease. The Kittlack wax used to fasten the fluorite window over the slit was coated with paraffin. Other joints were designed to present a minimum of area of wax to the action of the

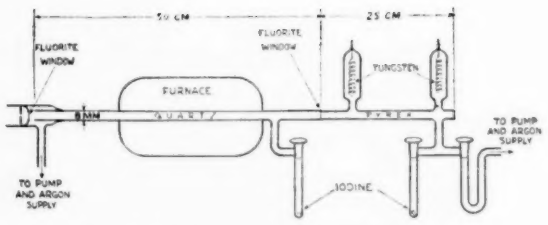

FIG. 3. Arrangement of new apparatus.

iodine. Access of iodine to stopcock grease was reduced to a minimum by having all stopcocks connecting directly with the emission or absorption tube of a "dry" type. They were the right-angle type and had grease only around the outer end. A circular groove ground around the plug of the stopcock prevented the grease from working down to the main portion of the stopcock. The cocks were perfectly tight to the outside atmosphere but of course were not leakproof from one side to the other. However, when closed, they served admirably to prevent the heavy iodine molecules from diffusing through with any great rapidity. Other stopcocks, fully greased, were placed between the "dry" cocks and the pump as shown in the diagram.

The absorption tube contained a mixture of about 0.3 mm iodine and 20 cm of argon. The temperature of the furnace was raised to about 900° and an exposure of 35 hours gave a spectrum extending to about λ1400Å.

Another exposure was then made with the furnace cold. The gas pressures in the absorption tube were suitably reduced so as to have approximately the same number of atoms of argon and *molecules* of iodine in the path of the light as there were when the furnace was hot. In this way a spectrum was photographed under conditions that were similar to the first one except that there were no iodine atoms in the light path.

Fig. 2c shows a pair of spectrograms taken as described above. It will be noticed that some lines are relatively weaker in the spectrogram taken with absorbing atoms in the path. They are undoubtedly absorption lines. A careful examination of the plates showed that the lines λ1830.4, 1782.9, 1642.5, 1617.9 and 1514.9 are absorbed. In addition there is good evidence that the lines λ1582.8, 1507.3, and 1421.6 are absorption lines.

In this spectral region the following lines are long wave-length members of doublets having the frequency difference 7600 cm^{-1}; λ1782.9, 1642.5, 1617.9, 1582.8, 1507.3, 1486.1, 1459.0, 1458.2 and 1421.6. Since 7600 cm^{-1} is the frequency difference of the inverted low levels $^2P_{1/2}$ and $^2P_{3/2}$ of the iodine atom it would be expected that the long wave-length members of lines having this frequency difference would be absorbed. It is seen that this is so except for the lines λ1486.1, 1459.0 and 1458.2. It may be that more accurate measurements of wave-lengths will show that the lines λ1486.1, 1459.0 and 1458.2 are not associated with the frequency difference of the two low levels. On the other hand it may be that uncertainties associated with very long exposures in the extreme ultraviolet were such as to mask slight absorptions for these lines.

The line λ1514.9 was absorbed but is not associated with the frequency difference 7600 cm^{-1}. This would indicate that it must be due, in emission, to a transition from an upper state having $j=5/2$ to the lowest state $^2P_{3/2}$.

The experiment indicated that the following lines were not absorbed, λ1844.5, 1799.2, 1702.3, 1675.4, 1593.8, 1545.9, 1526.6, 1518.3 and 1425.7. This would suggest that the lines are due to transitions to the upper or $^2P_{1/2}$ low metastable energy level of atomic iodine. It follows that each should be the short wave-length member of a doublet, $\Delta\nu=7600$ cm^{-1}. This is the case except for λ1526.6.

Other lines in the region were too weak or presented conflicting evidence so could not be safely classified either as absorbed or non-absorbed lines.

A new measurement of the arc and spark wave-lengths of atomic iodine in the Schumann spectral region is now in progress.

It is with great pleasure that I take this opportunity to thank Professor O. Oldenberg for his interest and numerous suggestions during the course of this research.

A New Band System of Tin Oxide

F. W. Loomis and T. F. Watson, *University of Illinois*

(Received April 4, 1934)

A new band system of SnO with origin at 36,803 cm^{-1} has been observed in an arc at reduced pressures. The lower state of this system is identical with that of the known A and B systems. The upper state is new and has a vibrational frequency, $\omega_e = 497.8$ cm^{-1}. The complexity of the isotope effect prevents rotational analysis.

IN the course of an investigation conducted with another object, a new band system of tin monoxide has been observed in the region from 2400 to 3100A. Some 100 bands of SnO in the region 3070 to 4800A have previously been observed in various flame and arc sources at or near atmospheric pressure and have been assigned by Mahanti[1] and Connelly[2] to one fairly extended band system (A) and two somewhat dubious ones (B and C).

The light source in the present investigation was a tin arc operated in oxygen at reduced pressures. With this source the intensities of all bands were considerably enhanced, and in particular the new ones were developed to the point where they could be photographed in 40 hours in the second order of a 30,000 line/inch grating. The electrodes were of hollow copper containing metallic tin, the upper electrode being so constructed that molten tin dropped through a small hole and kept a supply of fresh tin on the lower electrode. The optimum pressure for the production of the new bands seemed to be about 2 to 6 cm of mercury. The bands were photographed with a Hilger E-2 quartz spectrograph, a 3-meter quartz prism spectrograph and in the first and second orders of a 30,000 line per inch 21-foot grating in a Paschen mounting.

Because of the complex isotopic structure of tin, it is hard to measure the heads accurately, particularly those remote from the origin of the system. The frequencies of most of the measured band heads, including all the strong ones, can be expressed within the accuracy of measurement by the formula

$$\nu = 36{,}803 + \{497.8(v'+1/2) - 2.56(v'+1/2)^2\} - \{821.9(v''+1/2) - 3.6(v''+1/2)^2\}. \quad (1)$$

In this equation the term in v'' is identical with those of Mahanti's and Connelly's A and B systems, which indicates that the lower level in all three systems is the same.

Table I gives the frequencies and roughly estimated intensities of all measured bands of the new system, together with quantum numbers and differences between the observed frequencies and those calculated from Eq. (1) for bands which have been assigned. In Table II the intensities are entered as a function of v' and v'', showing that the locus of maximum intensity is a wide open Franck-Condon curve such as is to be expected from the great difference between the vibrational spacings in Eq. (1).

Tin, according to Aston,[3] consists of eleven isotopes, whose atomic weights and relative abundances (given in parentheses in percents) are as follows:

112 (1.07) 114 (0.74) 115 (0.44) 116 (14.19) 117 (9.81) 118 (21.48) 119 (11.02) 120 (27.04) 121 (2.96) 122 (5.03) 124 (6.19)

Hence each line in the spectrum should be split by the isotope effect into eleven lines, of which about five should be prominent. The isotopic displacement is approximately equal to $(\rho-1)(\nu_v+2\nu_r)$, in the usual notation, and the

[1] Mahanti, Zeits. f. Physik **68**, 114 (1931).
[2] Connelly, Proc. Phys. Soc. **45**, 780 (1933).
[3] Aston, *Mass Spectra and Isotopes*, p. 237 (1933).

TABLE I. *Frequencies and intensities of the new band system.*

Intensity	v'	v''	Frequency	Observed − Computed Frequency	Intensity	v'	v''	Frequency	Observed − Computed Frequency	Intensity	v'	v''	Frequency	Observed − Computed Frequency
0	13	1	41827	−5	1	4	2	36964	+5	4	6	6	34743	+3
0	10	0	41334	−4	2			36838		6	1	3	34707	−4
0	13	2	41022	−3	7	2	1	36795	−12	3	4	5	34582	+2
1	9	0	40889	−2	0	0	0	36648	+8	1	7	7	34425	−6
2	8	0	40439	0	1	5	3	36628	−3	8	0	3	34216	−2
0	11	2	40160	−3	0	10	6	36551	−6	5	3	5	34108	+6
0	9	1	40071	−5	6	3	2	36484	+2	1	6	7	33966	−3
2	7	0	39993	+11	0	13	8	36331	0	6	1	4	33915	−3
3	6	0	39525	+5	4	1	1	36315	−3	1	9	9	33823	−5
0	11	3	39353	−4	3			36215		2			33720	
0	7	1	39159	−9	1	4	3	36164	+5	4	2	5	33619	−1
3	5	0	39052	−1	6	2	2	35994	−5	0	11	10	33517	+3
1			38868		3			35868		2	5	7	33507	+5
0	8	2	38809	−8	3	0	1	35832	+6	8	0	4	33430	+5
1			38788		1	3	3	35683	+2	2	3	6	33332	+8
1	6	1	38703	−3	1	8	6	35652	−7	1			33182	
4	4	0	38585	+4	0	13	9	35581	+7	2	1	5	33144	+11
5	5	1	38241	+2	2			35562		0			33102	
5	3	0	38108	+4	8	1	2	35516	+4	0	10	10	33068	0
2			38068		2			35300		0	7	9	32908	−1
0	8	3	38011	−6	2			35258		2	4	7	33032	+4
6	4	1	37768	+2	0	12	9	35144	+2	6	2	6	32846	+5
6	2	0	37610	−12	1	5	5	35045	−7	0	5	8	32744	+7
6	3	1	37291	+2	4	0	2	35022	+3	3	0	5	32637	−2
0	1	0	37142	+8	2			34947		0	6	9	32442	−5
2	6	3	37106	+8	1		4	34890	+2	1	1	6	32360	+6
0	11	6	37001	+2										

bands are degraded sharply to the red, that is, ν_r is essentially negative. Hence the isotope effect should be zero where $\nu_v = -2\nu_r$, i.e., at points halfway between the origin of the band system and the origin of any band which lies to the short-wave side of the system origin. Although the complexity of the isotope effect in tin renders the rotational analysis practically impossible, the effect can be seen to be qualitatively in accord with these considerations. For instance, near 2680A, which is halfway between the system origin and the origin of the (4,1) band, the band lines are fairly sharp and single, and branches can be followed for some distance. In bands a little further from the origin the lines become diffuse; further on they are split into about five lines; and further still the isotope splitting becomes so large that it overlaps the successive rotational lines and the whole spectrum becomes hopelessly complex. Since the isotope splitting vanishes in the expected region, and where observable is of the right order of magnitude, it can be taken as confirmation of the general vibrational arrangement of the system, and of the assumed carrier. This is also true of the *A* system.

TABLE II. *Intensities as functions of v' and v''.*

v' \ v''	0	1	2	3	4	5	6	7	8	9	10
0	0	3	4	8	8	3					
1	0	4	8	6	6	2	1				
2	6	7	6	–	–	4	6				
3	5	6	6	1	1	5	2				
4	4	6	1	1		3		2	0		
5	3	5		1	1			2		0	
6	3	1		2			4	1		0	
7	2	0						1			
8	2		0	0			1				
9	1	0								1	
10	0										0
11			0	0			0				0
12										0	
13		0	0							0	

Temperatures Indicated by Intensity Distributions in Band Spectra

O. S. DUFFENDACK, R. W. REVANS* AND A. S. ROY,* *University of Michigan*

(Received April 7, 1934)

It is generally supposed that the intensity of any particular line in a band spectrum may be calculated from the Maxwell-Boltzmann law, assuming the gas to be in temperature equilibrium. From the results of this experimental work, it appears that under some conditions of excitation other factors than the temperature of the gas govern the intensity distribution. Measurements on the negative bands of N_2^+ excited in low voltage arcs in the pure gas show that at 1100°K and 2800°K the distribution of intensities among the rotational lines is exactly the same, whilst the admixture of helium with nitrogen alters the distribution completely and gives a much lower indicated temperature. Similar results are found with the first negative bands of CO^+. The differences are accounted for by the conversion of translational energy of the electrons into rotational energy of the molecules when the bands are excited by electron impacts in the pure gas. When the bands are excited by impacts of the second kind in gas mixtures, no change in rotational energy occurs and thus the indicated temperature is much lower. The distribution of intensity among the vibrational states of the molecules has been examined for the complete system of negative bands of N_2^+. While almost all of the energy is concentrated in the low vibration states when the bands are excited by electron impacts, the energy is spread out towards the higher vibration states when the excitation is by collisions of the second kind with metastable helium atoms.

INTENSITY DISTRIBUTION AMONG THE ROTATIONAL LINES

A NUMBER of investigations have been made on the relation between the distribution of intensity among the rotational lines of a band and the temperature of the gas in which the molecules are excited. The general conclusion has almost universally been that the temperature of the gas is correctly revealed by the distribution of intensity among the rotational lines. Thus in 1922, Birge[1] came to this conclusion for various absorption and emission bands and applied this method in estimating the temperature of the sun. More recently Ornstein[2] and his pupils have estimated the temperatures of various types of electric arcs by similar methods, and Vegard[3] drew some conclusions relative to the temperature of the upper regions of the atmosphere from observations on the distribution of intensity in the negative bands of nitrogen.

While the weight of evidence points to the correctness of the assumption that temperatures can be ascertained by this means, certain cases have been noted of distributions of intensity among the rotational and vibrational states of molecules other than that expected from the temperature of the gas. In cases of thermal excitation, there is no doubt that the distribution will accord with that expected, but in other types of excitation, it is not so obvious that the distribution will accord with that predicted from the tempeature of the gas. One such case is that of the distribution of intensity among the vibration states in the B band system of BO excited by active nitrogen as reported in 1931 by Elliott.[4] Very recently Johnson and Turner[5] found from studies of the distribution of intensity in the helium bands that, while the intensity distribution was Maxwellian, the indicated temperature was much higher than the temperature of the gas. Duffendack and Smith[6] in 1929 reported a significant difference in the appearance of the first negative bands of CO^+ when excited in low voltage arcs in the pure gas and in a mixture of 10 percent CO and 90 percent He. The present investigation is an outgrowth of this observation and it will be shown that in

* Commonwealth Fellow.

[1] Birge, Astrophysical J. **55**, 273 (1922).

[2] Ornstein and v. Wijk: Zeits. f. Physik **49**, 315 (1928); Proc. Amst. Acad. **33**, 44 (1930). v. Wijk, Zeits. f. Physik **59**, 313 (1930).

[3] Vegard, Ter. Mag. and Atmos. Elec. p. 389, Sept., 1932.

[4] Elliott, Zeits. f. Physik **67**, 75 (1931).

[5] Johnson and Turner, Proc. Roy. Soc. **A142**, 574 (1933).

[6] Duffendack and Smith, Phys. Rev. **34**, 77 (1929).

some instances the temperature indicated by the intensity distribution is not related to the temperature of the gas.

If the molecules of a gas are in thermal equilibrium at a temperature of T°K, then the number of molecules that possess an amount of energy E is proportional to the Boltzmann factor, $\exp(-E/kT)$, where k is the Boltzmann constant. If this energy E consists partly of energy of electronic excitation E_e, partly of atomic vibration E_v, and partly of molecular rotation E_r, this temperature factor may be written

$$\exp[-(E_e+E_v+E_r)/kT].$$

For molecules of the same gas and the same electronic and vibrational energies, i.e., for molecules whose transitions give rise to a particular band, E_e and E_v are constant, and so the temperature factor becomes $\exp(-E_r/kT)$. The intensity of an emission line in a band may thus be written

$$I=Ci\exp(-E_r/kT),$$

where i is an intensity factor proportional to the probability of the transition and to the statistical weight $2j+1$ of the initial level, where j is the rotational quantum number. The factor C is a constant, or very nearly a constant, for a given band and must be calculated for the particular state in question. In the case of the negative bands of nitrogen, the intensities of the rotation lines, after inserting the appropriate intensity factor, reduces to

$$I_j=Cj\exp(-j(j+1)h^2/8\pi^2IkT).$$

If, then, we plot the values of $\ln I_j/j$ against $j(j+1)$, the slope of the line is given by $-B/kT$, where $B=h/8\pi^2I$.

The value of the parameter T may also be obtained from the quantum number of the line of maximum intensity, for

$$T=j_m(j_m+1)h^2/4\pi^2Ik,$$

where j_m is the rotational quantum number of the line of maximum intensity in the band. Both methods were used to determine the temperature parameter in this investigation.

Apparatus

A low voltage arc excited in a Pyrex bulb 12 cm in diameter was the source of radiation in most of the experiments. The space between the filament and the anode was about 15 mm. The anode was a disk of nickel 15 mm in diameter, and the gas was at a pressure of 2 mm of Hg. At 100 m.a. current, the discharge confined itself to a bright glow between the anode and filament. At higher currents, the gases, especially CO, cleaned up very rapidly. The filament was either of six turns of 12 mil tungsten wire, run white hot, or an oxide coated strip of nickel. To start the discharge with the oxide coated filament, it was necessary to employ sufficient current to heat one spot bright red, but once the discharge started, the glow remained bright and steady without extraneous heating of the filament. It was just possible to see the dull red glow of the oxide coating and so the temperature of the filament could hardly have been more than 1000°K.

The spectrographs employed were a Hilger E-1 with a quartz prism, used in the third region for the ultraviolet bands of CO^+, and the 21 ft. grating of the department for the negative bands of nitrogen. The photographic plate used was the Eastman Polychrome, the contrast of which is well known from its extensive use in this laboratory. In the first experiments, the temperature parameters were determined from the position in the band of the line of maximum intensity and the relative intensities of the lines were not measured. If a Maxwellian distribution exists, this method gives the correct temperature parameter. In order to avoid making this assumption, the relative intensities of the lines were measured[7] in the later work and the temperatures determined both from the position of the line of maximum intensity and from the slope of the $\ln(I_j/j)$ *vs.* $j(j+1)$ plot. Excellent agreement was had between the values obtained from the two methods.

Experimental Procedure

The discharge tube was baked out thoroughly and the metal parts thoroughly degassed in order to remove all traces of CO especially as this

[7] Thomson and Duffendack, J.O.S.A. **23**, 101 (1933).

affects the distribution of intensity in the negative bands of nitrogen. The tube was then filled with nitrogen, or nitrogen and helium, to a total pressure of 2 mm. The discharge current was kept at 100 m.a., and some part of the discharge placed to form an image on the slit of the spectrograph. Four positions in the glow were photographed. In the first case, the end-on image of the filament was thrown on the slit, and, in the case of the tungsten filament, the temperature of the gas inside the helix was about 2600°C. The other parts of the discharge investigated were at 5 mm, 10 mm and 15 mm from the filament. In the last case, the image of the cold anode was thrown close to the slit, and the layer of gas next to that was photographed. The object of this experiment was to photograph gas at various temperatures and determine the effect on the temperature parameter in the intensity formula.

The time of exposure necessary to obtain a mean plate blackening, the same in all cases, increased enormously in the four successive positions. The intensity probably fell off exponentially with the distance from the filament. The results show that it was not stray light from the intense glow around the filament which was forming the photographic image. Were that the case, the variation of exposure time would not be expected to be so marked. The actual times necessary were from one minute at the filament to four hours at the anode. This point was further tested by welding small nickel shields to the filament leads, so placed that no light from regions near the filament could fall upon the condensing lens.

Photographs of the negative bands of nitrogen at 3914A and 4278A were taken in pure nitrogen and in mixtures of nitrogen with helium, carbon monoxide, argon and neon, respectively, each containing various percentages of nitrogen. Photographs of the first negative bands of CO^+ were taken in mixtures with nitrogen, helium and argon. The negative bands of oxygen were also examined in the pure gas and in mixtures with helium. Both for O_2 and for CO, the first negative bands lie in the ultraviolet, and, although the experimental procedure is more difficult and less weight is to be placed on the observations, they do confirm the conclusions arrived at for nitrogen.

In addition to the low voltage arc two other sources were used: an electrodeless discharge, and the glow discharge excited by a sixty cycle neon sign transformer giving a potential difference of 14,000 volts on open circuit. The lengths of exposure needed for the 21 foot grating with these sources were forty hours and eight hours, respectively.

In order to determine whether there was any relation between the electron temperature in the plasma of the low voltage arc and the temperature parameter of the intensity distribution, measurements were made on the electron temperatures by the usual Langmuir probe method. The collector consisted of a molybdenum wire 0.2 mm in diameter and was mounted about 2 mm from the filament. The currents collected gave very nice straight-line semi-logarithmic plots indicating two groups of electrons. The primary group had the temperature corresponding to the accelerating potential of the electrons from the filament. The large group of plasma electrons in a 100 m.a. arc at 50 volts had temperatures of about 20,000°K and the results were the same for pure nitrogen and for mixtures of 10 percent nitrogen and 90 percent helium. The electron temperatures were enormously greater than the temperatures indicated by the intensity distribution in the bands and had no relation to them.

Results

Typical microphotometer traces are shown in Fig. 1 (a) and (b). The upper is a trace of the N_2^+ band at 3914A taken in the pure gas. The source was a 100 m.a. low voltage arc at 200 volts. The gas pressure was 2 mm and the light was taken from a point 5 mm from the tungsten filament. The lower trace is of the same band taken under the same conditions of arc current and voltage, gas pressure and position in the discharge, but this time the nitrogen formed but 5 percent of the total gas mixture, the balance being helium. The high peak next to the line corresponding to $j=21$ in the R branch is the helium line at 3888A. It is readily seen that the intensity distribution is entirely different and

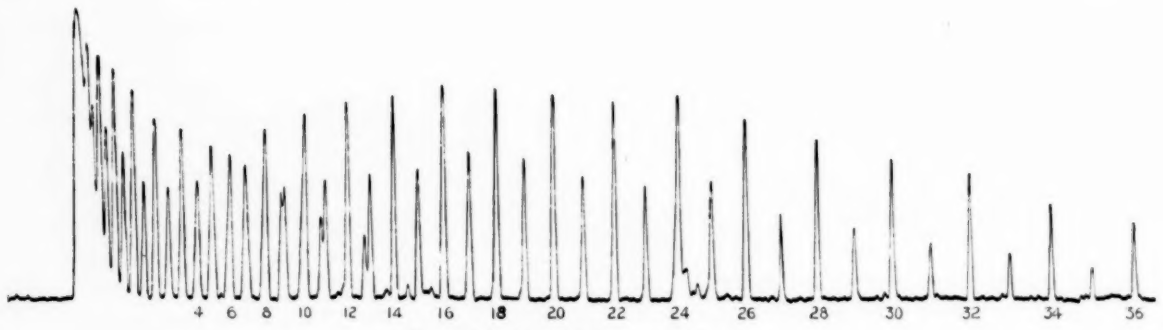

FIG. 1(a). 3914 N_2 in pure nitrogen.

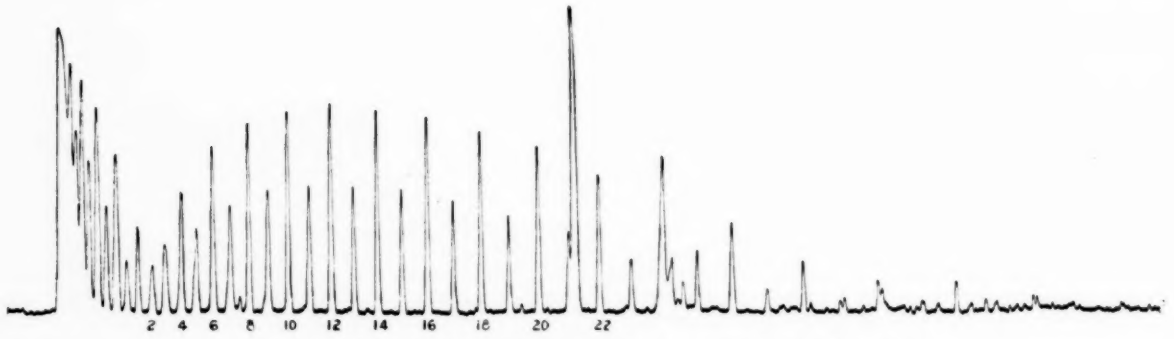

FIG. 1(b). 3914 N_2 in helium; 0.1 mm nitrogen, 1.9 mm helium.

that in the excitation with helium a lower value of the parameter T must be taken. The temperatures indicated by the intensity distributions are 1425°K for the pure gas and 500°K for the mixture. This procedure was repeated for various percentages of nitrogen in helium, and the variation of T with the nitrogen content of the mixture is shown in Fig. 2.

Traces identical with those of Fig. 1 were obtained when the much cooler oxide coated filament was used and show that the intensity distribution among the lines of the bands is independent of the temperature of the filament. Furthermore the indicated temperatures in a given arc were the same for all positions in the arc between the filament and the anode, and therefore the temperature parameter is also independent of the temperature of the gas. Except for a small change in the indicated temperature with a change in the arc voltage, to be discussed later, the parameter T depends only on the composition of the gas. The results are the same in the case of the first negative bands of CO^+ in the pure gas and in mixtures with helium. Microphotometer traces of some of these bands are shown in Fig. 3.

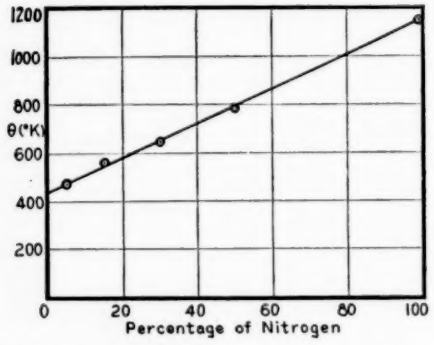

FIG. 2. Showing the relation between θ and the percentage of N_2 in the nitrogen—helium mixture. This relation is independent of the filament temperature.

In the spectra of the same bands excited in the electrodeless discharge and in the glow discharge produced by the neon sign transformer, the indicated temperatures were much lower. The values obtained from the positions of the lines of maximum intensity were 330°K and 430°K, respectively, both of which must have been close to the true temperatures of the gas in the discharges. Furthermore, in these cases when

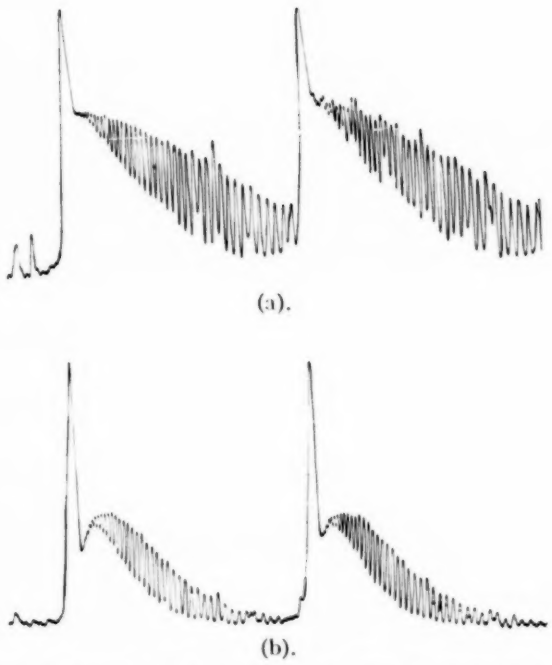

(a).

(b).

FIG. 3. Negative bands of CO^+ excited (a) by electron impacts (b) by metastable helium atoms.

the current density was small, the intensity distribution was the same in the helium mixture as in the pure gases.

DISTRIBUTION OF INTENSITY AMONG THE VIBRATIONAL STATES OF NITROGEN

Ornstein and Brinkman[8] have shown that, in the case of the electric arc, the vibrational energy distribution in the violet cyanogen band system obeys the Maxwell-Boltzmann law and that the temperature derived from this distribution is the same as that derived from the distribution of intensity among the rotational lines of one of the bands. This is very probably always true whenever the excitation is almost completely due to thermal action but may not be true for other modes of excitation.

The complete system of the negative bands of N_2^+ has been examined when excited in the low voltage arc by means of electron impacts in the pure gas and also when excited by collisions of the second kind with metastable helium atoms in mixtures of helium and nitrogen. In Fig. 4, a section of one of the plates is reproduced. The spectrum (a) was excited by electron impacts in the pure gas and (b) was excited by impacts of the second kind with metastable helium atoms. For (a), a low voltage arc of 62 milliamperes at 100 volts was maintained in pure nitrogen at 0.3 mm pressure, and for (b) the arc had the same current and voltage in a mixture of 90 percent helium and 10 percent nitrogen at a total pressure of 2 mm. Tables I and II give a list of the bands observed in each case together with an estimate of the photographic densities of the bands. From the tables it is seen that we get the usual parabolic distribution of intensity among the vibrational states. But when the bands are excited by electron impacts, the intensity is concentrated largely among the bands of low vibration, while,

[8] Ornstein and Brinkman Kon. Akad. van Wet. te Amster. **34**, 33 (1931).

TABLE I. *Densities of negative bands excited by electron impacts.*

v′ \ v″	0	1	2	3	4	5
0	3914 40	4278 18	4709 9			
1	3582 10	3884 8	4237 10	4652 4		
2	3308 ——	3564 2*	3858 ——	4199 3	4600 2	
3	3078 †	3299 ——	3549 1*	3835 ——	4166 1	4516 1

* Partially obscured by other bands.
† Not in region of spectrum photographed.

TABLE II. *Densities of negative bands excited by metastable atoms of helium.*

v′ \ v″	0	1	2	3	4	5	6	7	8	9
0	3914 20	4278 15	4709 9							
1	3582 12	3884 10	4237 12	4652 8						
2	3308 5*	3564 10	3858 6	4199 10	4600 7					
3	3078 †	3299 4	3549 10	3835 2*	4166 6	4554 5				
4	2885 †	3076 †	3293 5	3538 6*	3818 2*	4141 4	4516 4			
5					3533 3*			4486 3		
6									4467 2	
7										4459 1

* Partially obscured by other bands.
† Not in region of spectrum photographed.

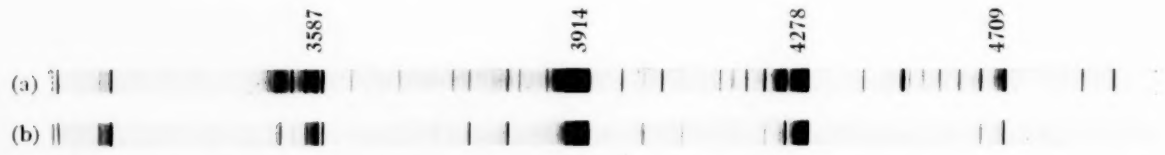

FIG. 4. Low voltage arc. (a) 10 percent N_2, 90 percent He at total pressure of 2 mm; (b) N_2 at 0.2 mm pressure.

on the other hand, when the bands are excited by collisions of the second kind, the intensity is spread out toward the higher vibration quantum states. Smyth and Arnott[9] found a similar distribution when these bands were excited by canal rays.

If thermal equilibrium exists, the intensity of a particular band is given by

$$I_{v'}=AP_{v'v''}\exp(-E_{v'}/kT),$$

where $E_{v'}$ is the vibrational energy in the initial state and $P_{v'v''}$ is the transition probability for a transition from v' to v''. From this formula, it is obvious that the temperature indicated by the intensity distribution in (a) where the excitation was by electron impacts is much lower than that in (b) where the excitation was by collisions of the second kind. This result is in direct contrast with that obtained from the distribution of intensity among the rotational lines of individual bands excited in the same two sources. The intensity distribution among the vibrational states in the second positive band system of nitrogen was found to be the same in pure nitrogen and in mixtures of nitrogen with helium, although the bands are much weaker in the latter case. This agreement of intensity distribution in the positive band system was to be expected as these bands are not excited by collisions of the second kind with metastable helium atoms and are excited by electron impacts in both the pure gas and in the mixture with helium.

DISCUSSION

It is obvious from the results that, under the conditions of excitation prevailing in these experiments, the effective parameter, T, has little to do with the temperature. In the case of excitation by impacts of the second kind, the parameter for the rotational distribution has a value which is probably close to the real temperature while the parameter for the vibrational distribution is far from it. The close agreement between the value of the parameter for the rotational distribution and the temperature of the gas can be accounted for in the following manner. In such an impact, the exchange of momentum is not different from that in ordinary kinetic theory impacts between gas molecules and the quantum number of the rotational state will not change by more than one unit as a general rule. In fact, the action radius of the metastable helium atom for this impact may be so great that there will be no mechanical reaction at all. In any case, the rotational distribution of the gas molecules will not be greatly disturbed, and so the parameter, T, will have a value close to the temperature of the gas.

On the other hand, the vibrational distribution may be expected to be considerably altered by impacts of the second kind. The force between the nitrogen atoms in an impact of the second kind with metastable helium atoms, for example, will be affected by the field of the metastable atom. As a consequence, the distance between the atoms of the molecule may change markedly during the time the molecules are in proximity of each other and the resulting ion be left in a higher vibrational state. Thus the temperature parameter for the vibrational states may be higher than that for the rotational states of the same molecules and have a value higher than the temperature of the gas.

That the high indicated temperature for the vibrational distribution is a consequence of the impacts of the second kind and is not due to the mere presence of another gas is shown by the fact that the positive bands of nitrogen and of carbon monoxide when excited in mixtures with helium have the same vibrational distribution as well as the same rotational distribution as when they are excited in the pure gas. It was also observed that the negative bands of N_2^+ are

[9] Smyth and Arnott, Phys. Rev. **36**, 1023 (1930).

strongly excited in a mixture of 10 percent N_2 with 90 percent CO, and the rotational and vibrational distributions are quite like those of the same bands excited by metastable helium atoms. The negative bands of CO^+ are, however, only weakly excited in a similar mixture with nitrogen as the preponderant gas. In this case the rotational and vibrational distributions are quite like those of the same bands excited in a low voltage arc in the pure gas. Thus it would seem that the first negative bands of N_2^+ are excited by impacts of the second kind by excited CO^+ ions whereas the negative bands of CO^+ cannot be excited by impacts of the second kind with excited N_2^+ ions. As the energy level of the initial state of the negative band system of N_2^+ is 19.6 volts while that of the initial state of the first negative system of CO^+ is 19.8 volts, these results are to be expected. The kinetic energy of the ions in the discharge was too low to make up the deficit in energy in the latter case.

The distribution of intensity among the vibrational states when the bands were excited by electron impacts in a low voltage arc in the pure gas is the usual one which has been accounted for by the Franck-Condon theory. The temperature parameter of this distribution was not determined, but it is probably close to the temperature of the gas.

The higher temperature indicated by the rotational distribution under these same conditions should be explained. It is obvious from the experiments that the value of the parameter has nothing to do with the temperature and varies for pure gases very slowly and only with the accelerating potential of the electrons. Several possible explanations have been considered, such as the possibility of the gradual raising of the rotational states of the molecules by successive electron impacts previous to the exciting impact and the action on neutral molecules of the impacts of positive ions moving through the gas. Neither of these seemed adequate and they were rejected in favor of the following proposal based upon the direct effect of an electron impact at the time of the ionization and excitation of the molecule.

The electrons will be scattered by the impacts with the gas molecules and the angular momenta after impact with respect to the centroid of the molecule will be different from the angular momenta before impact. One might apply the principle of the conservation of angular momentum if he knew enough about the scattering of electrons under these conditions, but very little is known about this type of scattering. In general, inelastic scattering is at smaller angles than elastic scattering and is nearly all forward so that very small changes in the angular momentum of the molecule would be expected. However, when the molecule is ionized simultaneously so that the ejected electron must be taken into consideration, one can say nothing about a probable change in the angular momentum of the molecule. For this case, Mott and Massey[10] state that the intensity of the scattered electron beam will be greater than for elastic scattering for angles near zero and ninety degrees and less at intermediate angles.

Let us consider the case of excitation by electrons of energy distributed about a mean value of 100 electron-volts. The range of velocities in this distribution will be very small compared with the average velocity, so that the number of electrons will be a sharp-peaked function of the velocity. If, on impact, a small fraction of the electron energy is transformed into energy of rotation of the molecule one will get a new rotational distribution of the molecules about an angular velocity increased by a few quantum units. Before impact, this distribution was Maxwellian and could be characterized by a certain temperature, the gas temperature. The nature of the distribution would be altered very little and so the new distribution could also be characterized by a temperature which would be higher than gas temperature. This is what the experiments seem to show. The position of the line of maximum intensity in the N_2^+ 3914 band was at $j_m=12$ for a low voltage arc at 25 volts, at $j_m \backsimeq 13{\cdot}5$ for an arc at 100 volts and at $j_m \backsimeq 15{\cdot}5$ for a 200 volt arc. The temperatures corresponding to these positions are 855°K, 1078°K, and 1425°K, whereas the gas temperature was probably about 550°K. Thus it is seen that the shift of the position of the maximum is very small and increases slowly with the voltage of the exciting electrons. Hence

[10] Mott and Massey, *Atomic Collisions*, p. 174.

only a small fraction of the energy of the electrons need be transformed into increased energy of rotation of the molecule in order to account for the results. For 100 volt electrons the shift would require that approximately 0.009 electron-volt energy be transformed or only 0.009 percent of the kinetic energy of the electron before impact.

In this connection, mention should be made of the observations of Lindh[11] who investigated the intensity distribution in the 3914 band excited by electrons projected into a field free enclosure. He found that the distribution was Maxwellian and that the indicated temperatures were 551°K and 596°K for electrons accelerated by 150 volts and 175 volts, respectively. These temperatures, while lower than those indicated for the low voltage arcs in pure gases, show that increasing the voltage increases the temperature parameter. The difference in the experimental conditions undoubtedly accounts for the difference in the values of the indicated temperatures in the experiments of Lindh and those of the present investigation.

In conclusion, the authors wish to express their appreciation for the suggestions of Professor G. E. Uhlenbeck and Dr. L. A. Young during discussions of this problem with them.

[11] Lindh, Zeits. f. Physik **67**, 67 (1931).

The Numerical Solution of Schrödinger's Equation

G. E. KIMBALL AND G. H. SHORTLEY,* *Massachusetts Institute of Technology*

(Received February 26, 1934)

Schrödinger's equation may be approximated to any desired accuracy by a difference equation over a lattice covering the region of integration. The solutions of this difference equation minimize a certain quadratic form (analogous to the energy integral $\int\psi^*H\psi$) subject to certain normalization and, for the higher states, orthogonality conditions. A practical numerical method is developed for the solution of this variation problem. By altering the values of a rough solution at each lattice point in turn by a simple improvement formula, the value of the quadratic form is continually decreased until the desired minimum is reached. Illustrations of the method are given for one-dimensional problems. Practical details are given for handling two-dimensional lattices, in particular for the solution of the problem of one electron in an axially symmetric field.

INTRODUCTION

FOR only the simplest problems of quantum mechanics can Schrödinger's equation be solved exactly. Numerical solutions of any problem in which the variables are separable can be found by applying the ordinary methods of numerical integration to the separated equations, but for those problems in which the variables cannot be separated no direct method of solution has been given. Problems of this type have hitherto always been treated by the use of analytical approximations such as perturbation theory and the Ritz variation method.

Methods have been developed for the numerical solution of non-separable differential equations, subject to given boundary conditions, which do not involve the determination of eigenvalues.[1] These methods all depend on replacing the continuum over which the differential equation is to be integrated by a discrete set of lattice points and the differential equation itself by a difference equation which is equivalent to a set of nonhomogeneous linear algebraic equations.

It has been shown[2] that a differential equation of the eigenvalue type may similarly be replaced by a difference equation which is equivalent to a set of *homogeneous* linear algebraic equations containing a parameter. The values of this parameter for which the homogeneous equations have non-trivial solutions approach the eigenvalues and the corresponding solutions approach the eigenfunctions of the differential equation as the lattice spacing decreases to zero. The determination of these solutions has been reduced[2] to the problem of minimizing a certain quadratic form (which is analogous to the energy integral $\int\psi^*H\psi$) subject to certain normalization and, for the higher states, orthogonality conditions. We here develop a practical numerical method of solving this variation problem. By altering the values of a rough solution at each lattice point in turn according to formula (12), the value of the quadratic form is continually decreased until the desired minimum is reached. In this respect the method is similar to the procedure[1] for the solution of Laplace's difference equation in n-dimensions by successively replacing the values of a rough solution by the arithmetic means of the $2n$ neighboring values. While we shall discuss the procedure in particular for Schrödinger's equation in coordinate systems in which the Laplacian is a simple sum of second derivatives, the method is readily extended to other eigenvalue equations and other types of coordinate system.

GENERAL THEORY

Having chosen a suitable lattice, not necessarily uniform, composed say of N points (boundary points at which $\psi=0$ not included), we consider from now on only the values ψ_1, ψ_2,

* National Research Fellows.

[1] L. F. Richardson, Trans. Roy. Soc. **A210**, 307 (1911), Math. Gazette **12**, 415 (1925); Phillips and Wiener, J. Math. and Phys. **2**, 105 (1923); Courant, Zeits. f. Ang. Math. u. Mech. **6**, 322 (1926); Courant, Friedrichs and Lewy, Math. Ann. **100**, 32 (1928).

[2] R. G. D. Richardson, Trans. Am. Math. Soc. **18**, 489 (1917); Courant, Friedrichs and Lewy, Math. Ann. **100**, 32 (1928).

$\cdots \psi_N$ of ψ at the lattice points. The solutions of Schrödinger's equation

$$-k^{-2}\nabla^2\psi + V\psi = E\psi \tag{1}$$

are then approximated by the solutions of a set

$$\Sigma_{(j)} b_{ij}\psi_j = E\psi_i \tag{2}$$

of linear homogeneous algebraic equations. For example, if i is a point in an n-dimensional cubic lattice with spacing h, and a, b, c, $\cdots$ the $2n$ adjacent points, the i^{th} equation of (2) has the form

$$-h^{-2}k^{-2}[\psi_a + \psi_b + \cdots - (2n + h^2k^2V_i)\psi_i] = E\psi_i. \tag{3}$$

To each point is given a weight c_i equal (with certain exceptions which we shall discuss later) to the volume of the "unit cell" of the lattice at i, so that the integral $\int \phi\psi$ over the given region is approximated by the sum $\Sigma c_i\phi_i\psi_i$. The lowest solution of (2) is then that function ϕ which minimizes the ratio

$$E_\phi = [\Sigma_{(ij)} c_i b_{ij}\phi_i\phi_j]/[\Sigma_{(i)} c_i\phi_i^2], \tag{4}$$

and the corresponding E_ϕ is the lowest eigenvalue. This is true only if the quadratic form in the numerator of (4) is symmetric, i.e., if

$$c_i b_{ij} = c_j b_{ji}. \tag{5}$$

We shall now give a method of determining numerically the lowest state of (2). Let us choose any function as a rough approximation to the solution and then change each point in turn in such a way as to lower E at each step. The condition for the vanishing of $\partial E_\phi/\partial\phi_p$ suggests that E will be lowered by replacing ϕ_p by

$$\phi_p' = -[\Sigma_{(j)}' b_{pj}\phi_j]/[b_{pp} - E_\phi], \tag{6}$$

where Σ' denotes summation over all values of j except $j=p$. This amounts to satisfying the p^{th} equation of the set (2). We shall now show that this change actually lowers E if the lattice is not too coarse.

Let $\Delta\phi_p = \phi_p' - \phi_p$. Then

$$E_{\phi'} - E_\phi = -(b_{pp} - E_\phi)\left[\frac{c_p(\Delta\phi_p)^2}{\Sigma c_i\phi_i^2} - \frac{2c_p^2\phi_p(\Delta\phi_p)^3}{(\Sigma c_i\phi_i^2)^2} + \cdots\right]. \tag{7}$$

If the number of lattice points is large, $c_p(\Delta\phi_p)^2/\Sigma c_i\phi_i^2$ is small compared to unity. In this case we need consider only the first term of (7), and E will be decreased by the change in ϕ_p if $b_{pp} - E_\phi$ is positive. But $b_{pp} - E_\phi$ may certainly be made positive by using a sufficiently fine lattice since b_{pp} is a constant plus a positive term of order $1/h^2k^2$, where h is the lattice spacing, while E_ϕ approaches a limit as $h \to 0$.

Therefore, if we take a lattice sufficiently fine to make $b_{pp} - E_\phi$ positive for all points for our initial rough approximation, we may continuously decrease E by using (6) as an improvement formula point by point on our function. As E converges to the true lowest eigenvalue, the function must converge to the true lowest eigenstate, for only for an eigenfunction can $\Delta\phi$ and hence ΔE approach zero.

It is not necessary to recalculate E_ϕ after each improvement by formula (6); it may be shown that if the change in ϕ is small compared to ϕ itself, the whole lattice may profitably be run over using a single value of E_ϕ.

We shall now develop a similar method for the calculation of the states of higher energy. Suppose that we know the μ states $\psi^1, \psi^2, \cdots, \psi^\mu$ of lowest energy, and seek the $(\mu+1)^{\text{st}}$ state $\psi^{\mu+1}$. Let the states ψ be normalized so that

$$\Sigma \psi_i{}^\alpha \psi_i{}^\beta = \delta_{\alpha\beta}, \tag{8}$$

$$\Sigma b_{ij}\psi_j{}^\beta = E^\beta \psi_i{}^\beta. \tag{9}$$

Then $\psi^{\mu+1}$ is that state orthogonal to $\psi^1, \cdots, \psi^\mu$ which gives the lowest value of E in (4).

For any function ϕ, let us use the notation

$$\Sigma c_i\phi_i\psi_i{}^\alpha = M^\alpha, \tag{10}$$

and to avoid confusion with sums over the lattice points $1 \cdots N$, let the repetition of the index α in a term denote summation over $\alpha = 1, \cdots, \mu$. Then the function

$$\chi = \phi - M^\alpha\psi^\alpha \tag{11}$$

is orthogonal to $\psi^1, \cdots, \psi^\mu$ and may, if it does not vanish identically, be considered as a rough approximation to $\psi^{\mu+1}$. Since the energy $E_\chi = \tilde{E}_\phi$ is calculated for a state orthogonal to $\psi^1, \cdots, \psi^\mu$, it must be greater than the energy $E^{\mu+1}$ (or equal if χ is proportional to $\psi^{\mu+1}$).

If we can find a function ϕ' such that $\tilde{E}_{\phi'} < \tilde{E}_\phi$, we can consider χ' a better approximation than χ to $\psi^{\mu+1}$. Hence let us seek an improvement

formula which reduces $\bar{E}_\phi$. Setting $\partial\bar{E}_\phi/\partial\phi_p=0$ suggests that we use

$$\phi_p'=-\frac{\Sigma' b_{pi}\phi_i-M^\alpha\psi_p{}^\alpha(\bar{E}_\phi-E^\alpha)}{b_{pp}-\bar{E}_\phi} \qquad (12)$$

That this gives a definite improvement for a sufficiently fine lattice is shown by the calculation of the change of $\bar{E}$ when ϕ is replaced by $\phi'\equiv\phi_1, \phi_2, \cdots, \phi_p', \cdots, \phi_N$.

It may be shown that one obtains exactly the same change in $\bar{E}$ whether the formula (12) is applied to ϕ_p or the corresponding formula with $M^\alpha=0$ is applied to χ_p:

$$\chi_p'=-[\Sigma' b_{pi}\chi_i]/[b_{pp}-E_\chi]. \qquad (13)$$

This improvement formula has the advantage of simplicity over (12), and may be used on an "orthogonalized" ϕ. χ' is of course no longer orthogonal and must be reorthogonalized if (13) is to be used again. Only if $\bar{E}_\phi$ is the true eigenvalue, will (13) reproduce the function χ. If $\phi=\psi^{\mu+1}+d^\alpha\psi^\alpha$, $\bar{E}_\phi$ will equal $E^{\mu+1}$, and alteration by (12) will simply reproduce ϕ. Hence the process will converge to a combination of this type, which must be orthogonalized to obtain $\psi^{\mu+1}$. Just as in the case of the ground state, we can in general profitably go over the whole lattice with the same values of $\bar{E}_\phi$ and M^α.

At a boundary point where ψ is to vanish, ϕ is held permanently at zero, this zero value being used in the improvement of adjacent points. At a boundary point where $\partial\psi/\partial n$ is to vanish, we hold $\partial\phi/\partial n$ to zero by effectively maintaining equal values of ϕ on the two sides of the boundary, i.e., we calculate at such a boundary point as if the missing points outside the region had the same values as the corresponding points within the region.

Application to One-Dimensional Problems

We can best illustrate this method of integration by considering a specific and well-known example, the s states of the hydrogen atom. These states satisfy the equation

$$-(\partial^2\psi/\partial r^2)-2\psi/r=E\psi \qquad (14)$$

with energy -1 for the $1s$, -0.25 for the $2s$, $\cdots$. The range of r is from 0 to ∞, with boundary conditions $\psi=0$. Let us take our lattice points as in Fig. 1, with, starting from $r=0$, four intervals of 0.4, four intervals of 0.8, and then intervals of 1.6 to $r=\infty$.

At those points whose neighbors are both at the same distance h, $c_i=h$, $b_{i,i-1}=b_{i,i+1}=-1/h^2$, $b_{ii}=V_i+2/h^2$. The only exceptional points are those for which the interval on one side is h and on the other side $2h$. In order to approximate to $\partial^2\phi/\partial r^2$ at such a point we take the parabola through the point and its two neighbors and find its second derivative. Thus $c_i=\frac{3}{2}h$, $b_{i,i-1}$

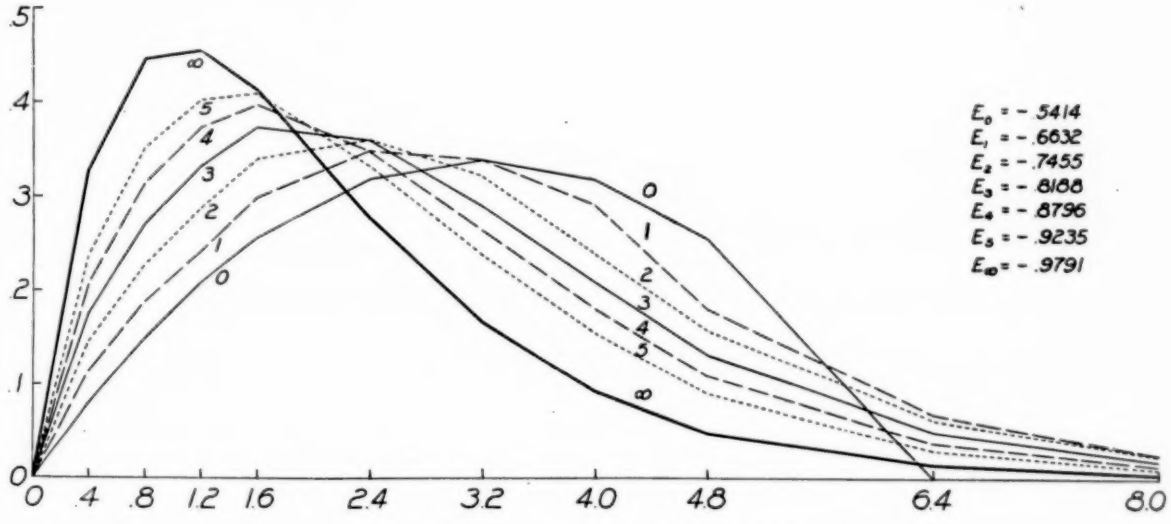

FIG. 1. The improvement of the $1s$ state of hydrogen.

$=-2/3h^2$, $b_{i,i+1}=-1/3h^2$, $b_{ii}=V_i+1/h^2$, if $i-1$ is at a distance h and $i+1$ at a distance $2h$ from i.

The improvement formula (6) or (13) becomes for our two types of point, respectively,

$$\begin{aligned}\phi_p'&=[\phi_{p-1}+\phi_{p+1}]/[2+h^2(V_p-E_\phi)];\\ \phi_p'&=[\tfrac{2}{3}\phi_{p-1}+\tfrac{1}{3}\phi_{p+1}]/[1+h^2(V-E_\phi)].\end{aligned}\tag{15}$$

With a table of the denominators in these formulas at hand the improvement of ϕ can be carried out extremely rapidly. In actual practice it is never necessary to recalculate E_ϕ until the whole set of points has been improved, while in the latter stages the function may be safely improved a large number of times with the same E_ϕ, since E_ϕ converges to its final value much more quickly than ϕ itself.

The process of improvement is illustrated in Fig. 1. Starting from the parabolic arch marked 0, five successive improvements from left to right gave the curves marked 1, 2, 3, 4, 5, the energy being recalculated after each complete improvement. These energies are shown in Fig. 1. The final result is shown as the curve marked ∞ and the final energy as E_∞. Each of these curves has been normalized to the same value (0.4) before plotting.

The convergence of the eigenfunction and eigenvalue to that of the differential equation as the lattice spacing is decreased is illustrated in Fig. 2, where the final eigenvalues and functions are shown for the lattice of Fig. 1 and for lattices of half, double, and quadruple this spacing. The circles represent the final function for lattice spacing starting at 0.2, and this function differs from the continuous solution, re^{-r}, by less than one-half percent, i.e., less than the accuracy of the plot, at any point.

Fig. 3 shows the rapidity of improvement in the calculation of the $2s$ state. The parabola of Fig. 1 was used again as a starting function. When orthogonalized to the ground state, this gave the curve marked 0. Since $M=0$ for this curve, the improvement formula (13) was used, the improvement being carried through from left to right without altering E or M. The result was then orthogonalized and plotted as curve 1. This process was repeated four times. The fourth approximation here is considerably closer to the final curve than it was in Fig. 1 because the initial curve had a more correct shape.

Practically, the computation of ψ_∞ for any of these lattices is much more rapid than these plots would indicate because with such a process of improvement, one is permitted to do anything he pleases to the function. The improvement of the function can be made at the rate of several points per minute, and is much simpler than the calculation of the energy, so that in practice one can profitably use the same energy several times, or at least as long as regions of the curve are sinking in absolute value.

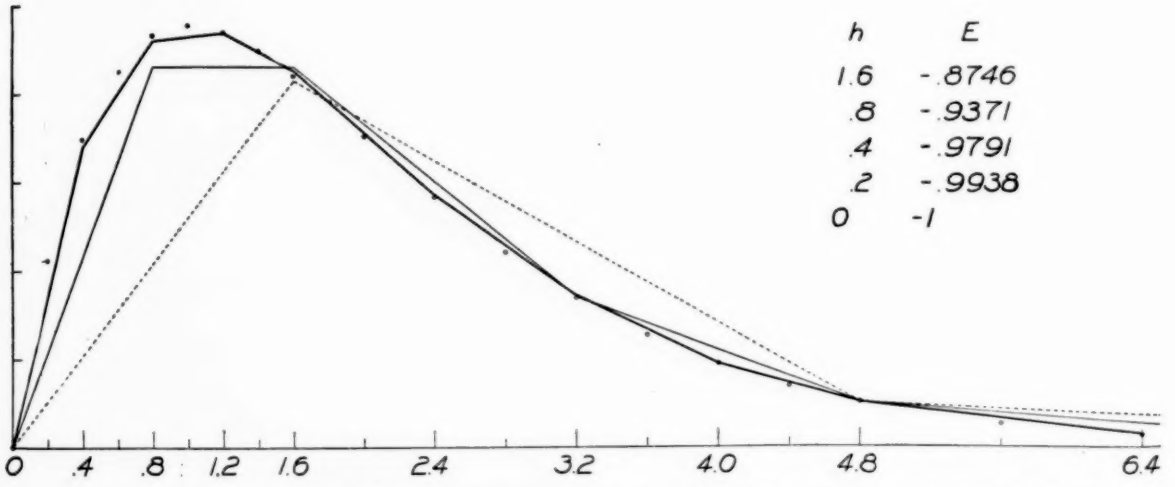

FIG. 2. Convergence of the solution of the difference equation to that of the differential equation as the lattice spacing is decreased for the $1s$ state of hydrogen. The energy is tabulated as a function of the finest interval. To the accuracy of the plot (about one-half percent), the circles represent both the solution of the difference equation for the 0.2 lattice and the solution of the differential equation.

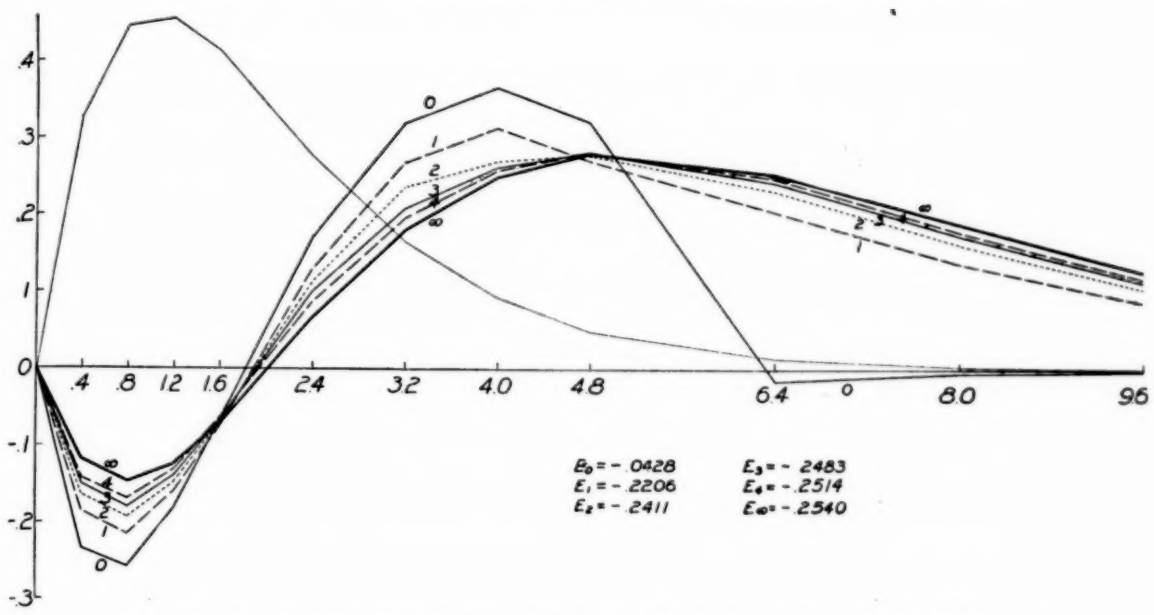

FIG. 3. The improvement of the 2*s* state of hydrogen. The 1*s* state is shown by the light curve.

However, really rapid convergence is obtained by using the formula twice to find out how the function is moving at each point and then altering the function by hand several times the amount of its last motion. Since the improvement formula quickly eliminates sharp irregularities, this process of "hand tooling" enables one to reach the final value of the function very quickly. All computation is facilitated by the fact that errors, unless of a size to be immediately obvious, are unimportant and soon corrected so that no calculation need be checked.

APPLICATION TO TWO-DIMENSIONAL PROBLEMS

In two-dimensional problems even more use may be made of the device of increasing the lattice spacing in regions where ψ is flat in order to reduce the number of points. Thus the number of lattice points can be made a fraction of the product of the numbers along the two rectangular axes. We must then consider the coefficients to be used for points in the region where the lattice constant changes. For the square lattice shown in Fig. 4, Table I gives a representative set of b's and c's; these satisfy the condition (5) and are such that the two quadratic forms occurring in (4) approach the corresponding integrals of a given continuous function ϕ as the number of points is successively quadrupled by halving all intervals. If the left-hand column of points in Fig. 4 are along a boundary where $\partial\psi/\partial n$ is to vanish, we take $c_r=\frac{1}{2}h$, $b_{ru}=b_{rs}=-1/h^2k^2$, $b_{rl}=-2/h^2k^2$, $b_{rr}=V_r+4/h^2k^2$.

TABLE I. *This table gives* c_ν, $h^2k^2(b_{\nu\nu}-V_\nu)$, *and* $-h^2k^2b_{\nu\mu}(\nu\neq\mu)$ *for a representative set of points in Fig. 4.*

c_ν	ν	μ: *a*	*b*	*c*	*d*	*e*	*f*	*g*	*i*	*j*	*k*	*l*	*m*	*n*	*o*	*p*	*q*
1	*d*	1		1	4	1				1							
9/4	*g*		3/5				1/5	2	2/5				1/5				
3/2	*i*			3/5				1	3	1			1/5	1/5			
3/2	*j*				2/5				1	3	1			1/5			
4	*m*							3/5	1/5			1/4	1	1/4		1/4	
4	*n*								1/20	1/5	1/20		1/4	1	1/4		1/4

The corresponding improvement formulas obtained from (6) are seen to be little more complicated than for one dimension. The amount of labor involved in an improvement or a calculation of energy in any number of dimensions is essentially proportional to the *number* of lattice points used. Practically, we have found it convenient in two dimensions to draw on heavy paper a square to represent each lattice point of color to indicate the type of formula used. In this square are placed permanent entries of V_i, $(4+h^2k^2V_i)$ or the corresponding form for the color in question, and the weights to be used in summing $h^2k^2\phi_i\Sigma b_{ij}\phi_j$ and

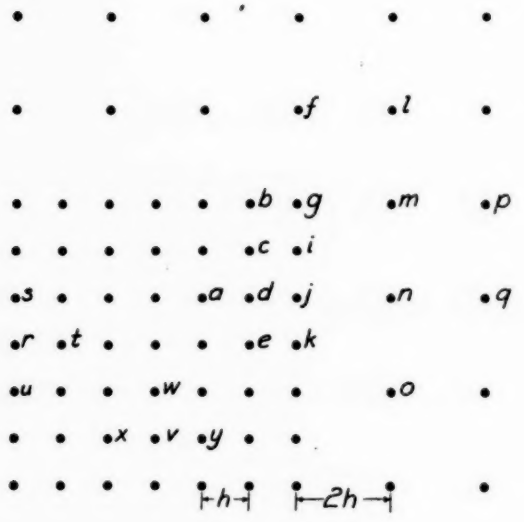

FIG. 4.

ϕ_i^2 when determining the energy. In pencil is entered $4+h^2k^2(V_i-E)$ or the corresponding form, and the last four or five ϕ_i's so that the changes may be watched. Older ϕ_i's are erased as space is needed for new ones. With experience in hand-tooling, it is feasible in this way to solve a lattice of several hundred points in a couple of weeks. Smaller lattices giving more approximate values of the energy and the function may be solved in much less time, since halving the lattice constant quarters the work. Two computers are required, one to read and the other to operate the machine.

The axially symmetric one-electron problem

Schrödinger's equation in atomic units for the motion of one electron in an axially symmetric field is reduced, in cylindrical coordinates r, z, φ to the equation

$$-\frac{\partial^2 S}{\partial r^2}-\frac{\partial^2 S}{\partial z^2}+\left(V-\frac{1}{4r^2}+\frac{\lambda^2}{r^2}\right)S=ES$$

by the transformation

$$\psi=[S(r,z)/r^{\frac{1}{2}}]e^{i\lambda\varphi}.$$

This two-dimensional equation may be handled by the methods outlined if we replace V by the effective potential $(V-1/4r^2+\lambda^2/r^2)$ and use the boundary condition $S=0$ when $r=0$. If we make a power series expansion near the axis $r=0$ we find that S starts as $r^{\lambda+\frac{1}{2}}$ so that our parabolic approximation will be valid near $r=0$ for all λ except $\lambda=0$.

For $\lambda=0$, if the bottom row of lattice points in Fig. 4 is along the line $r=0$, the second derivative at the point v can be approximated by putting a curve of the form $\alpha+\beta r^2$ through $S_v/h^{\frac{1}{2}}$ and $S_w/(2h)^{\frac{1}{2}}$. This gives $b_{vw}=-2^{\frac{1}{2}}/3h^2$, $b_{vv}=V_v+10/3h^2$, and $c_v=3/2^{\frac{1}{2}}$.

If the potential V is both axially symmetric and an even function of z, S will either be an even or odd function of z, and the two types of functions may be obtained separately by using the boundary conditions $\partial S/\partial z=0$ and $S=0$, respectively, when $z=0$. If V has a first-order pole along the axis $r=0$ the necessity of differentiating along a radius passing through the pole is best avoided by using a lattice such that no lattice line passes through the pole.

We have checked the practicability of these formulas by a calculation of the ground state of the hydrogen molecule ion on a coarse lattice, with results in satisfactory agreement with the known values. We are proceeding with the application of this method to the calculation of eigenfunctions for other diatomic molecules.

The Perfection of Quartz and Other Crystals and Its Relation to Surface Treatment

R. M. BOZORTH AND F. E. HAWORTH, *Bell Telephone Laboratories, New York*

(Received April 9, 1934)

The perfection of various crystals has been determined by using an x-ray double crystal spectrometer. The materials examined were quartz, Rochelle salt, fluorite, tourmaline, pyrites, barite, rocksalt, gypsum, and the metallic crystals aluminum, iron, nickel, tungsten, and permalloy (65 percent nickel). The results indicate that quartz is a "perfect" crystal and that specimens of Rochelle salt, fluorite and possibly tourmaline and pyrites, might be found which could be so classed. The others tested are definitely in the "imperfect" class, the widths of the rocking curves at half-maximum lying between 100 and 1500 seconds of arc. The effect of surface treatment on perfection, as determined by x-rays, was examined for quartz by grinding with carborundum of two different sizes and by etching for different lengths of time. The surface of the permalloy crystal was also investigated by etching to different depths. As a result of the tests here reported, etched quartz crystals are suggested as suitable for use in the double crystal spectrometer on account of their high resolving power which is about twice that of calcite.

INTRODUCTION

IT was found in the course of some earlier work that x-ray reflections from single crystals of quartz were unusually sharp, and it seemed of interest to determine more accurately the perfection of these crystals by the use of a double crystal spectrometer. Since other kinds of crystals were available in sufficient size, and since the perfection of very few crystals have been reported in the literature, a variety of other specimens was also examined. In addition to some well-known minerals, specimens of several metallic crystals were measured, including a single crystal of an alloy. These metal crystals were of particular interest because electron diffraction experiments had been made on some of these same specimens by L. H. Germer.[1]

It soon appeared that the treatment of the surface, known to be important in the case of the non-metallic crystals, was especially important for the softer metallic crystals. Accordingly, experiments were made on the treatment of the surface of one of the metallic crystals as well as on several specimens of quartz.

METHOD OF MEASUREMENT

The crystals were measured on a double crystal spectrometer, usually in the $(1, -1)$ position. The first crystal (crystal A) was set to reflect with maximum intensity the $K\alpha$-radiation from moybdenum. The second crystal (crystal B) was mounted on a holder with one axis in the plane of the crystal surface and perpendicular to the x-ray beam. This holder also turns about a second axis perpendicular to the first and also lying in the plane of the crystal surface. Motion around the latter axis, for azimuthal adjustment, could be read directly to 6 seconds on a tangent screw head. Motion about the former axis, important for the final rocking curves, was read directly on the head of a screw pressing on a lever arm. The screw head was 25 cm in circumference, one complete revolution of the head causing a rotation of B through 100 seconds. The distance between the two crystals was 15 cm. The position of the axis of crystal B was adjusted, with the crystal surface always parallel to the beam reflected from crystal A, until the intensity of the beam was cut to one-half.

The intensity of the twice reflected beam was measured by an ionization chamber containing methyl bromide, in connection with an amplifier and a Moll galvanometer. The current from the ionization chamber passed through a resistance of 10^{11} ohms connected between the grid and filament of the "electrometer tube" of the amplifier, so that the deflection of the galvanometer was proportional to the x-ray intensity. The galvanometer had a full period of less than a

[1] L. H. Germer, Phys. Rev. **44**, 1012 (1933).

second and readings were made in three or four seconds after movement of the crystal.

Crystal *B* was adjusted in azimuth until the rocking curve was narrowest. Actually this position was found by making an azimuthal adjustment and noting the deflection of the galvanometer at the peak of the rocking curve. A curve was plotted showing the relation between azimuthal settings and these maximum galvanometer deflections, and the final azimuthal setting made for which this curve was a maximum.

No absolute measurements were made of reflection angle or intensity of reflection.

Materials

The single crystals examined were as follows:

Quartz

(1a) Brazilian quartz, cut and ground with 100 mesh carborundum parallel to a (11·0) plane (perpendicular to a natural prism face), within 10 minutes of arc.

(1b) Same as (a) except a different specimen.

(2) Quartz similar to (1) but in addition etched 40 hours at 30°C in 48 percent hydrofluoric acid solution, to give a smooth surface free from surface irregularities and strains due to cutting and grinding. Two specimens.

(3) Quartz similar to (1) but ground with 600 mesh carborundum.

(4) Quartz similar to (1), except cut and ground with 100 mesh carborundum parallel to a (10·0) plane (the natural prism face).

(5) Quartz similar to (4), but etched 100 hours. Two specimens.

(6) Quartz similar to (4), but given successive etches ranging from 20 seconds to 20 hours, measurement being made between etches.

(7) Quartz similar to (4), except ground with 600 mesh carborundum.

(8) Quartz similar to (7), but given successive etches ranging from 20 seconds to 20 hours.

Other non-metallic crystals

(9) Rochelle salt, cut and ground parallel to a (100) plane, and lightly etched with water.

(10) Rocksalt, cleaved parallel to a (100) plane.

(11) Calcite, cleaved parallel to a (100) plane.

(12) Gypsum, cleaved parallel to a (010) plane.

(13) Fluorite, cleaved parallel to a (111) plane.

(14) Fluorite, natural (100) face.

(15) Barite, natural (001) face.

(16) Iron pyrites, natural (210) face.

(17) Same as (16), but etched in hot concentrated nitric acid.

(18) Tourmaline,[2] ground and polished parallel to a (10·0) plane.

Metallic crystals

(19) Iron, grown and annealed in hydrogen, surface inclined slightly to a (100) plane.

(20) Iron, ground and polished parallel to a (100) plane to within 15 minutes of arc, and then etched in dilute acid.

(21) Nickel, ground and polished parallel to a (111) plane, and etched in dilute acid.

(22) Aluminum, ground and polished parallel to a (100) plane, and etched in dilute acid.

(23) Tungsten, ground and polished parallel to a (110) plane, and etched in alkaline potassium ferricyanide.

(24) Permalloy, 65 percent nickel, ground and polished parallel to a (100) plane, and annealed in hydrogen at 1400°C for two hours.

(25) Same as (24), but given successive etches totaling 60 minutes, in a mixture of concentrated hydrochloric and nitric acids.

Results with Etched Quartz Crystals, and Comparison with Theory

The rocking curve widths at half-maximum, for several pairs of crystals, are shown in Table I.[2a]

According to Darwin's theory[3] of reflection from a perfect crystal, total reflection of x-rays polarized so that the electric vector is parallel to the plane of incidence occurs over an angular range

$$\Delta\theta = 2nFZ^{-1}\lambda^2e^2(\text{ctn } 2\theta)/(\pi mc^2) \qquad (1)$$

where n is the number of extranuclear electrons per cm^3, Z the number of extranuclear electrons in the unit of structure on the basis of which the structure factor F is calculated, and the other symbols have their usual significance. For two crystals in the parallel position, S. K. Allison[4] has shown that following Darwin's theory the width of the rocking curve at half-maximum is

$$W = 1.40\Delta\theta \qquad (2)$$

---

[2] The hexagonal unit cell of this specimen was determined from three reflection photographs from faces mutually perpendicular: $c = 7.05$A, $a = 15.78$A. See also C. Kulaszewski, Abh. d. Sachs. Akad. d. Wiss. (M.-P. Kl. 3) **38**, 81 (1921).

[2a] Rocking curves for the natural faces of quartz and some other crystals have been taken by Sakisaka, Jap. J. Physics **4**, 171 (1927) and **12**, 189 (1930), the narrowest for quartz being 14″ wide at half-maximum. The effect of grinding the surface was also investigated, but no etching experiments were reported. More recently, Richtmyer, Barnes and Manning, Phys. Rev. **44**, 311 (1933) have determined the effect of etching the surfaces of calcite crystals and have found considerable narrowing of the rocking curves for small angles of reflection.

[3] C. G. Darwin, Phil. Mag. (6) **27**, 675 (1914).

[4] S. K. Allison, Phys. Rev. **41**, 1 (1932).

when absorption by the crystal is neglected, and that when absorption is allowed for by Prins'[5] method, the relation is usually not much changed. When the incident rays are unpolarized the width of the region of total reflection is unchanged, but there is some change in the amount of reflection at angles for which the reflection is not perfect. The width of the rocking curve for unpolarized incident rays may then be expected to lie between the two limits corresponding to polarizations parallel and perpendicular to the plane of incidence. Substituting in Eq. (2) the mean of these two values of $\Delta\theta$, the width of the rocking curve at half-maximum is given by

$$W = 0.45nFZ^{-1}\lambda^2 e^2 \operatorname{ctn}\theta/(mc^2) \qquad (3)$$

an equation which should be correct within a few percent when the values of θ are as small as they are in the experiments described here.

The width given by Eq. (3) is about three-fourths of that calculated by earlier methods, according to which the theoretical effective width of the once-reflected ray, 4/3 of the $\Delta\theta$ of Eq. (1), was multiplied by $2^{\frac{1}{2}}$ to obtain W.

The width calculated by this equation can be compared with that experimentally determined for the etched quartz crystals (2). The structure factor, however, is not accurately known so we calculate FZ^{-1} from Eq. (3) using the observed value of W, and obtain the result

$$FZ^{-1} = 0.36.$$

This may be compared with the value of FZ^{-1} calculated for the case in which the centers of all of the atoms lie on (11·0) planes and the atoms have the scattering powers[6] appropriate for the value of $\sin\theta/\lambda$ of our experiment. The FZ^{-1} so obtained is 0.72, just twice that calculated from the rocking curve. A powder photograph of quartz indicates that the structure factor for this plane has neither an exceptionally large nor exceptionally small value. The structure factor calculated from the structure proposed by Gibbs[7] is small, but little significance can be attached to this because the parameters are not sufficiently well determined. A similar calculation was made for the second order reflection from (11·0), for which $W = 1.7$ seconds. Using Eq. (3) we obtain $FZ^{-1} = 0.41$, whereas the maximum value for a silicon and two oxygen atoms[6] at this angle and wave-length is 0.44. The corresponding figures for reflections from (10·0) ($W = 11$ seconds) are 0.9 and 0.87. Thus the results of the application of Eq. (3) show that quartz is a perfect crystal as nearly as can be determined with our present knowledge of the structure factors.

A determination of percent reflection was made for first order reflection from (11·0). When the (11·0) planes of the two crystals (2) were parallel, the intensity of the beam reflected from crystal B was 40 percent of that reflected from crystal A. This is lower than the 80 percent reflection predicted by Darwin's theory[4] and may be compared with the 60 percent observed[4] for calcite for this wave-length and with the 35 percent observed for calcite for a wave-length of 0.2A.

The use of quartz crystals cut parallel to the (11·0) planes has some advantage over calcite in a double crystal spectrometer. The rocking curve width is half that for calcite and the reflection angle is slightly greater, the resolving power of quartz being consequently 2.5 times that of calcite in the first order. With a beam of x-rays of given intensity incident upon the first crystal and with the crystals exactly parallel, the intensity of the twice reflected beam is less for quartz than for calcite, largely on account of the greater resolving power of the quartz.

Quartz with Ground Surfaces

As shown in Table I, quartz finished with 100 mesh carborundum gives a rocking curve 36 seconds wide at half-maximum. Since the rocking curves for etched crystals are much narrower, it was important to know how much of the ground surface had to be etched away before the narrower rocking curve could be obtained. To test this point, crystals (6) (ground with 100 carborundum) and crystal (8) (600 carborundum) were prepared, and their rocking curves measured after various times of etch in 48 percent hydrofluoric acid at 30°C. In these experiments crystal A of the spectrometer,

[5] J. A. Prins, Zeits. f. Physik **63**, 477 (1930).
[6] L. Pauling and J. Sherman, Zeits. f. Krist. **81**, 1 (1932).
[7] R. E. Gibbs, Proc. Roy. Soc. London **A110**, 443 (1926).

specimen (5), was one that had been etched a long time, and crystal *B* was the one under test. The results are shown in Fig. 1. From other experiments it is known that the thickness of quartz etched away from each surface under these conditions is about 0.005 mm/hr.[8] for specimen (6) and 0.001 mm/hr. for (8), so that the rocking curve width has decreased to one-half of its original width when a layer less than 200A in thickness (as measured) has been removed from the surface of the crystal. It is rather surprising that the imperfections due to grinding are confined to such a thin layer.

Crystals with ground surfaces were also used in another series of experiments. In each instance both crystals of the spectrometer were cut to (10·0) planes and used in the parallel position, but the surfaces were treated differently. The combinations used and the results obtained are shown in Table I. Besides showing that the angular distortion of the surface is greater after grinding with coarser carborundum, a result to be expected, the data indicate also that the width of the rocking curve for a combination of two "imperfect" surfaces is more nearly equal to the *sum* than to the root mean square of the rocking curve widths of each surface when paired with a perfect crystal. This latter result is in approximate accord with the suggestion of Hoyt[9] that the form of the rocking curve is best expressed by the equation

$$y=a(1+b^2x^2)^{-1},$$

and is definitely contradictory to the assumption frequently made that the curve follows the Gaussian error function. The predicted width of the rocking curve for the two ground crystals (1a) and (1b) used in combination is 77 seconds by Hoyt's formula,[10] 88 seconds by experiment and only 59 seconds by the Gaussian error formula. In crystals (4) and (7) the corresponding values are 59, 61 and 44 seconds, respectively.

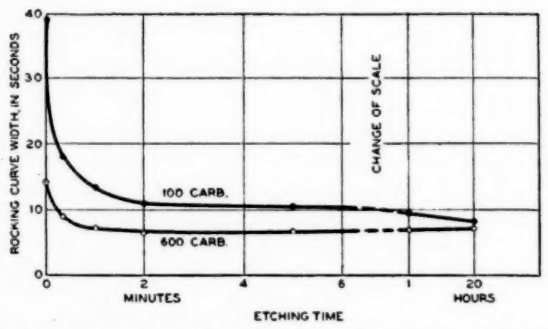

FIG. 1. Effect of etching on the rocking curve width at half-maximum, for (10·0) surfaces of quartz originally ground with 100 or 600 carborundum. Reflections are in the second order.

TABLE I. *Rocking curve widths at half-maximum.*

No. of Quartz Specimen Crystal *A*	Crystal *B*	Surface of crystal *B*	Order $n_A, -n_B$	θ	*W* sec.
(Reflection from (11·0) planes)					
(2)	(2)	Etched	1	8° 20′	2.6
(2)	(2)	"	2	16° 51′	1.7
(2)	(1a)	Ground[a]	1	8° 20′	28[b]
(2)	(1b)	"	1	8° 20′	52
(1a)	(1b)	"	1	8° 20′	88
(2)	(3)	Ground[c]	1	8° 20′	13
(Reflection from (10·0) planes)					
(5)	(5)	Etched	1	4° 48′	11
(5)	(5)	"	2	9° 38′	3.8
(5)	(4)	Ground[a]	2	9° 38′	36[d]
(5)	(7)	Ground[c]	2	9° 38′	24[e]
(4)	(7)	"	2	9° 38′	61

[a] Ground with 100 mesh carborundum.
[b] Several specimens similarly prepared gave rocking curve widths (at half-maximum) from 28 to 52 seconds.
[c] Ground with 600 mesh carborundum.
[d] Several specimens similarly prepared gave rocking curve widths (at half-maximum) from 29 to 59 seconds.
[e] Several specimens similarly prepared gave rocking curve widths (at half-maximum) from 13 to 49 seconds.

[8] As measured between a plane surface and one 2 mm in diameter, both optically perfect.

OTHER NON-METALLIC CRYSTALS

The widths of the rocking curves of the other non-metallic crystals are shown in Table II. In most of these experiments the first crystal of the spectrometer was the etched quartz specimen (2), one of the pair for which the rocking curve width was 2.6 seconds. In other experiments, when preliminary work indicated a wide rocking curve, the ground crystal (3) was used as crystal *A* to increase the intensity of the reflected x-ray beam. Since the Bragg angles θ are never the same for the first and second crystals of the spectrometer, in order to obtain the angular deviation due to the second crystal alone a correction to the observed widths of Table II may

[9] A. Hoyt, Phys. Rev. **40**, 477 (1932).
[10] As worked out by S. W. Barnes and L. D. Palmer, Phys. Rev. **43**, 1050 (1933).

be applied according to the usual equation[11]

$$W^2 = W_A^2 + W_B^2 + D^2 W_\lambda^2.$$

In our case[12] this reduces to

$$W^2 = W_A^2 + W_B^2 + 8400(\tan\theta_A - \tan\theta_B)^2$$

where W_A and W_B refer to the widths in seconds at half-maximum of the functions (now assumed Gaussian) representing reflection from crystal A and from crystal B, and θ_A and θ_B are the Bragg angles for these reflections. In almost all cases listed in Table II, however, this correction is negligible, the greatest correction being for Rochelle salt where it amounts to 1.4 seconds or about 25 percent.

TABLE II. *Widths of rocking curves.*

Crystal B	hkl	θ_B	W sec.
(Crystal A = quartz (2), (11·0), etched, $\theta_A = 8°\ 20'$)			
Rochelle salt (9)	100	6° 53′	5.2
Rocksalt (10)	100	7° 15′	400
Calcite (11)	100	6° 43′	7.8
Fluorite (13)	111	6° 28′	17
Fluorite (14)	100	14° 52′	66
Barite (15)	001	11° 29′	250
Tourmaline (18)	10·0	13° 29′	27
Pyrites (16)	210	8° 27′	44
(Crystal A = quartz (3), (11·0) ground 600 mesh, $\theta_A = 8°\ 20'$)			
Pyrites (17)	210	8° 27′	56
Gypsum (12)	010	2° 41′	42

The materials listed in Table II show great variations in perfection, the rocking curve widths varying by a factor of almost 300. Rocksalt has been known for many years to be decidedly imperfect, and some quantitative measurements have been reported for this material,[13] for barite,[14] and for Rochelle salt.[14] The results for Rochelle salt reported previously are qualitatively confirmed here. Assuming for the moment that this crystal was perfect, we calculated the structure factor from Eq. (3) and found FZ^{-1} to be 0.88. Since this is much too high to be consistent with the scattering powers of these atoms in planes of this spacing, even if arranged in the most favorable way, we may conclude that this specimen of Rochelle salt is not a perfect crystal. On the other hand, the small width indicates that perfect crystals might be grown. The data for some of the other substances, such as fluorite and tourmaline, indicate that perfect specimens of these may also exist.

METALLIC CRYSTALS

The results on the single crystals of Al, Fe, Ni and W, given in Table III, show that they are unquestionably "imperfect" crystals. The most complete experiments were performed on a single crystal of permalloy, containing approximately 65 percent Ni and 35 percent Fe. This crystal was made in the following way: Eight hundred grams of technically pure iron and nickel were heated to 1400°C in an alundum boat in an atmosphere of carefully purified moist hydrogen and maintained at that temperature for 16 hours. The material was then melted and after about two hours was allowed to cool through the melting point at the rate of 10°C/hr. It was then cooled to room temperature in two hours. About half of the piece so prepared was a single crystal from which a slab about 6 mm thick was cut parallel to a (100) plane, using a revolving metal disk fed with 100 mesh wet carborundum. This surface, about 2 cm² in area, was finally polished with No. 0000 emery paper and

TABLE III. *Rocking curve widths for metallic single crystals.*

Crystal B	hkl	θ_B	W sec.
(Crystal A = quartz (3), (11·0) ground 600 mesh, $\theta_A = 8°\ 20'$)			
Iron (20)	100	14° 28′	840[a]
Nickel (21)	111	10° 8′	1500
Aluminum (22)	100	10° 8′	1500
Tungsten (23)	110	9° 9′	360
(Crystal A = quartz (1), (11·0) ground 100 mesh, $\theta = 8°\ 20'$)			
Permalloy (24)	100	11° 27′	660
Permalloy (25)	100	11° 27′	132

[a] Using two crystals of iron similar to iron (19), a rocking curve was obtained for which W was 480 seconds.

[11] M. Schwarzchild, Phys. Rev. **32**, 162 (1928); see also S. K. Allison and J. H. Williams, Phys. Rev. **35**, 1476 (1930) for discussion.

[12] With $W_\lambda = 0.29$ X.U., the wave-length width of the $K\alpha_1$ line according to S. K. Allison, Phys. Rev. **44**, 63 (1933).

[13] W. L. Bragg, R. W. James and C. H. Bosanquet, Phil. Mag. (6) **42**, 1 (1921); B. Davis and W. M. Stempel, Phys. Rev. **19**, 504 (1922); P. Kirkpatrick and P. A. Ross, Phys. Rev. **43**, 596 (1933); W. L. Bragg, C. G. Darwin and R. W. James, Phil. Mag. (7) **1**, 897 (1926), discuss the perfection of fluorite, barite and calcite as determined by the integrated intensity of reflection.

[14] Kirkpatrick and Ross, reference 13.

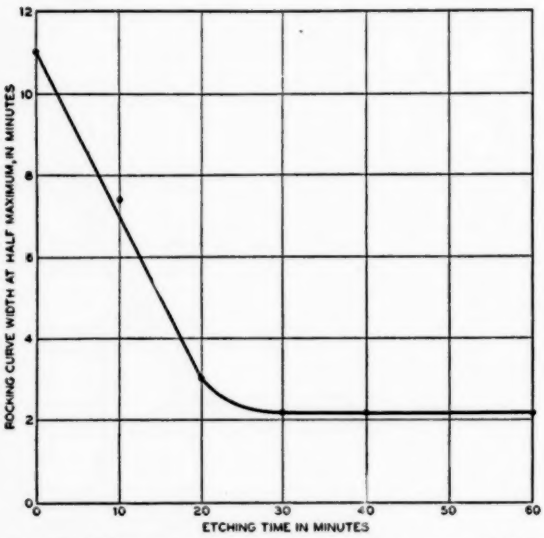

FIG. 2. Effect of etching on the rocking curve width at half-maximum, for first order reflection from the (100) surface of a single crystal of permalloy containing 65 percent nickel. The first crystal was quartz (11·0), first order reflection from a ground surface.

the slab annealed for two hours at 1400°C in hydrogen. The rocking curve for this surface was 11 minutes wide at half-maximum, as shown in Table II. The specimen was then etched repeatedly in strong acid (equal parts conc. HCl and conc. HNO_3), rocking curves being taken between etchings. The time for each etch was 10 minutes, about 0.1 mm being removed during this time. Fig. 2 shows that the width decreases as the surface is etched and it is not until about 0.3 mm has been etched away that the narrowest rocking curve is obtained. The final width, 2.2 minutes, is apparently characteristic of the interior of this crystal. These results indicate that the atomic planes of metallic single crystals are easily disturbed, and in this sense are in accord with many other observations which have been made since the technique for growing metallic single crystals has been developed. The results also indicate that metallic crystals are imperfect, even when prepared from pure materials under the best conditions so far known.

The single crystals of iron (20), nickel (21), and tungsten (23) were the same specimens as those used by Germer[1] in his experiments on electron diffraction. His measurements showed that some of the crystal planes were inclined as much as 1 degree to the average position of the planes. By combining the x-ray with the electron diffraction data, it may be concluded, as already pointed out by Germer, that parts of the surface of these crystals are inclined considerably more than are the internal mosaic blocks to the mean position of the planes. The results obtained with the crystal of permalloy emphasize the conclusion that the misalignment observed by Germer is the direct result of the method of preparation of the surfaces which he examined.

ACKNOWLEDGMENTS

We wish to express our indebtedness to Mr. P. P. Cioffi for the preparation of the single crystal of permalloy, to Dr. L. H. Germer for the loan of most of the other metallic crystals, to Professor Bergen Davis for the minerals (except quartz and tourmaline), and to the Brush Laboratories for the Rochelle salt crystal.

X-Ray Wave-Lengths from Crystals and Ruled Gratings

ARTHUR EDWARD RUARK, *Department of Physics, University of Pittsburgh*

(Received March 19, 1934)

Energies of photoelectrons ejected by x-rays from thin foils have been measured by Kretschmar and by Robinson and his colleagues, using the magnetic spectrograph. Their values are compared with those computed from wave-lengths of the incident rays and x-ray terms of the atoms in the foils, using (a) wave-lengths measured with crystals, based on the actual calcite spacing rather than the conventional one; (b) ruled grating wave-lengths, which are higher by 0.25 percent. Using Birge's value of e, 4.7668 $\times 10^{-10}$ e.s.u., Bearden's value for the calcite spacing becomes $(3027.91 \pm 1.0)10^{-11}$ cm. To get photoelectron energies from crystal wave-lengths, accurate x-ray terms are worked out by a new plan, which avoids uncertainties involved in using absorption-edge wave-lengths. Term differences are obtained from x-ray line spectra, and are added to the value of some low term obtained from optical spectra. Birge's values of universal constants are employed in getting photoelectron energies. These energy values average 0.36 percent higher than those computed from crystal wave-lengths, or 0.61 percent higher than those from ruled-grating wave-lengths. This fact supports, but does not conclusively prove, the correctness of crystal wave-lengths based on the actual calcite grating space.

1. Magnitude of the Discrepancy Between Crystal and Ruled-Grating Wave-Lengths

THE work of Bearden, Cork and his colleagues[1] and other investigators shows that x-ray wave-lengths measured with ruled gratings are consistently higher than those obtained with crystals. Bearden found that the discrepancy P is 0.22 percent in the region 1.4 to 2.3A; Cork found 0.29 percent for two L series lines at about 5A. Data of Howe,[2] Purdom and Cork, and Witmer and Cork cover the range from 3.7 to 25A. Their values indicate that P lies between 0.3 and 0.5 percent over this whole region. Siegbahn and Magnusson[3] found $P=0.17$ percent for oxygen $K\alpha$ (23.6A).

It has been customary to express ruled-grating wave-lengths in terms of the unit 10^{-11} cm, while crystal wave-lengths are based on the conventional grating space of calcite, 3029.45 X.U., which is employed in Siegbahn's treatise and by nearly all x-ray spectroscopists. Here we need crystal wave-lengths based on the actual calcite grating space, so I have recomputed Bearden's[4] value, using Birge's latest values of the universal constants involved, as quoted below. The result is $(3027.91 \pm 1.0)10^{-11}$ cm at 20°C. In view of the above-mentioned spread of the data of Cork and his colleagues, it is not worth while to recompute them; but employment of this grating space raises Bearden's P-values to 0.25 percent. For the purposes of this paper we may take the value of P to be 0.25 percent up to 3A, and at least 0.25 percent for greater wave-lengths. [It must be emphasized that the calcite spacing is so accurately known and so nearly constant from one good crystal to another that we cannot remove the difficulty by changing its value. Further, Bearden[5] estimates the experimental error of his ruled-grating measurements as 0.01 percent.]

It is probable that the question of which scale is correct can be decided by grating work in the region of very soft x-rays, where higher orders of the K and L series lines of light elements can be compared with optical standards. However, x-ray line widths are great in that region, and so far we have no conclusive evidence from such studies. Meanwhile, two arguments favoring the correctness of the crystal wave-lengths have been presented. (1) Bearden[6] showed that wave-lengths from measurements of the dispersion of x-rays in crystal quartz are in close agreement

[1] For bibliography, see Bearden, Phys. Rev. **39**, 1 (1932) and Purdom and Cork, Phys. Rev. **44**, 974 (1933).
[2] C. E. Howe, Phys. Rev. **35**, 717 (1930).
[3] Siegbahn and Magnusson, Zeits. f. Physik **87**, 291 (1934).
[4] Bearden, Phys. Rev. **38**, 2089 (1931).
[5] Bearden, Phys. Rev. **37**, 1224 (1931).
[6] Bearden, Phys. Rev. **39**, 1 (1932).

with crystal values; (2) Birge[7] pointed out that certain universal constants calculated from ruled-grating wave-lengths do not agree with mean values obtained from experiments which do not involve x-ray measurements, while there is much better agreement if crystal wave-lengths are employed.

The purpose of this paper is to present a third line of evidence which supports the crystal values. It consists in comparing the energies of photoelectrons ejected from thin films by monochromatic x-rays with the values to be expected from the wave-lengths of the incident rays and the energy levels of atoms in the films. The data employed are those of Kretschmar and of Robinson, Andrews and Irons.[8] The discussion in both papers requires reconsideration for two reasons. Improved values of the universal constants are available; and, more important in its effect on the interpretation of the data, we shall use a method for getting x-ray energy levels which yields more accurate values than that employed by Siegbahn in calculating the tables in his treatise. The improvement of these energy levels is the chief point of novelty. Robinson[9] used his older data to compute x-ray terms, and considered whether they should be compared with those obtained from crystals or from ruled-gratings. Here the viewpoint is converse. We obtain accurate term values from x-ray and optical spectra, using the crystal scale, and show that they agree better with the photoelectric results than those computed from the ruled-grating scale.

2. A Method for Obtaining X-Ray Terms

As Siegbahn[10] says, the determination of x-ray absorption edges is usually afflicted with greater errors than the measurement of lines. This is shown by double crystal spectrometer measurements. Ross[11] finds that in passing from Zr (40) to I (53) the width of the main K-absorption edge increases from 13 to 38 volts while Allison[12] shows that in passing from Zr (40) to Ag (47) the width of $K\alpha_2$ runs from 6.9 to 11.3 volts, $K\alpha_1$ being slightly narrower. This difference in widths, and the presence of fine structure on the short wave-length side of the main absorption edge are not, however, the only considerations. So far, there is no theory to indicate what point in the absorption edge should be taken as corresponding to ejection of an electron to a position of rest at infinity. Indeed, Sandström[13] showed that in some cases, and presumably in all, the middle of an absorption edge corresponds to the energy required to raise an electron to the first unfilled shell at the periphery of the atom. For example, in the elements preceding gold the $O_{IV,\,V}$ level is incomplete. For these elements the line L_{III}–$O_{IV,\,V}$ ($L\beta_5$) agrees well with the middle of the L_{III} absorption edge, but for elements from gold to uranium the $O_{IV,\,V}$ shell is complete and the L_{III} edge lies at shorter wave-lengths than the $L\beta_5$ line. Furthermore, we cannot expect that the value of the term difference L_IL_{II} (for example), obtained from line combinations, will agree with the measured difference of the L_I and L_{II} absorption limits. This is due to the fact[14] that the azimuthal selection principle holds true for edges as well as for lines, so that electrons ejected from the L_I and L_{II} shells by frequencies corresponding to the L_I and L_{II} edges, respectively, should land on different peripheral levels of the atom.

For these reasons it is often desirable not to use tables of term-values, but rather to work with tables of *term differences obtained from lines*, like those prepared by Idei[15] for heavy elements. To obtain more accurate term values, we add such term differences to values of small x-ray terms obtained from optical spectra. The method will be made clear by applying it to gold. In the isolated gold atom, the configuration of the outer electrons is $5d^{10}6s$. The O terms with azimuthal number $l=2$ are the energies required to remove a $5d$ electron, leaving the ion in the condition $5d^96s$. These energies can be obtained, theoretically, in two ways:

(1) From observation of the sequences $5d^96s\,ms$,

[7] Birge, Phys. Rev. **40**, 228 (1932).
[8] Kretschmar, Phys. Rev. **43**, 417 (1933); Robinson, Andrews and Irons, Proc. Roy. Soc. **A143**, 48 (1933).
[9] Robinson, Phil. Mag. **14**, 605 (1932).
[10] Siegbahn, *Spektroskopie der Röntgenstrahlen*, 2nd Ed., p. 336.
[11] Ross, Phys. Rev. **44**, 977 (1933).
[12] Allison, Phys. Rev. **44**, 63 (1933).
[13] Sandström, Zeits. f. Physik **66**, 784 (1930).
[14] Siegbahn, Zeits. f. Physik **67**, 567 (1931).
[15] Idei, Sci. Rep. Tohoku Imp. Univ. **19**, 559 (1930); also Siegbahn's treatise, p. 352.

or $5d^9 6s\, mp$, etc. (where $m=6$, 7, etc.), and computations of their limits.[16] The lowest term of the $5d^9 6s\, ms$ sequence is known, but unfortunately higher terms are not identified with certainty so we must attack the problem in another way.

(2) The energy required to remove a $5d$ electron is the same as that required for the process: removal of the $6s$ electron followed by excitation of the ion from $5d^{10}$ to $5d^9 6s$. From the work of McLennan and McLay and of Sawyer and Thompson[17] we find that the ν/R value corresponding to removal of the $6s$ electron is 0.68, and that the ion has the following low terms, its normal state being taken as the origin:

		ν/R
$5d^{10}$:	$^1S_0$	0
$5d^9 6s$:	$^3D_3$	0.137
"	$^3D_2$	0.161
"	$^3D_1$	0.253
"	$^1D_2$	0.270

Thus there are four terms which take the place of the two terms $O_{IV,\,V}$ of the customary x-ray energy diagram. If the $6s$ electron were removed from the ion, the triplet D terms with $j=3$ and 2 would approach the O_{IV} term of the *ion* as a limit and the other two would approach O_V. However, we do not need to consider this matter in detail because in the L and M spectra of gold the terms $O_{IV,\,V}$ are not resolved. We may use the mean of the four D terms, weighted according to their statistical weights. This is 0.19, so $O_{IV,\,V}=0.68+0.19$ or 0.87 ν/R units. The uncertainty is negligible compared with that involved in getting $O_{IV,\,V}$ from lines and absorption edges. Having $O_{IV,\,V}$, we obtain the x-ray terms of the isolated gold atom from Idei's table of level differences, using 3029.45 X.U. for the grating space of calcite. Table I gives results, with those for other elements discussed in this paper, obtained by similar methods.

[16] These sequences form a part of the I^b spectrum of neutral gold. The existence of such spectra was first pointed out by Mohler and Ruark, J. O. S. A. **7**, 819 (1923) in the case of thallium. Beutler (Zeits. f. Physik **86**, 495 (1933) and later papers) has made extensive studies of absorption lines in I^b spectra, which are very useful in calculating x-ray terms by the methods here set forth.

[17] McLennan and McLay, Trans. Roy. Soc. (Canada) **22**, 103 (1928); Sawyer and Thompson, Phys. Rev. **38**, 2294 (1931).

TABLE I. *ν/R values for x-ray terms of Cu, Ag, Pt and Au.* (Based on the conventional calcite grating space 3029.45 X.U.)

	Cu 29	Ag 47	Pt 78	Au 79
L_I	—	279.29	1022.69	1057.98
L_{II}	70.73	260.21	978.12	1012.25
L_{III}	69.26	247.51	852.32	878.56
M_I	9.26	53.58	243.39	253.08
M_{II}	—	43.28	223.46	232.68
M_{III}	—	41.02	195.33	202.79
M_{IV}	0.78	28.24	162.74	169.45
M_V		27.62	156.85	163.13
N_I	—	7.59	53.70	56.68
N_{II}	—	3.13	45.40	48.14
N_{III}	—		38.69	40.77
N_{IV}	—	0.94	24.86	26.68
N_V	—		23.66	25.30
N_{VI}	—	—	6.04	7.09
N_{VII}	—	—	5.75	6.72
O_I	—	—	8.06	8.53
$O_{II,\,III}$	—	—	4.62	4.95
$O_{IV,\,V}$	—	—	0.72	0.87

It is necessary to estimate the accuracy of the data in Table I. We must consider how much the terms Cu $M_{IV,\,V}$, Ag $N_{IV,\,V}$, and Au and Pt $O_{IV,\,V}$ are changed when atoms of these elements enter the solid phase. Data which would provide a direct answer are not in existence, so we must estimate the change from other evidence. It is reasonable to assume that (1) the deeper a term lies in the atom, the less it will be affected by change of phase, so that the energy change of an absorption edge will be mainly due to shift of the upper level; (2) the alteration of a small x-ray term of a metal atom, due to solidification, should be less than that due to chemical combination. This judgment is based on the fact that, in general, heats of vaporization of metals are low compared with heats of formation of salts.

Hanawalt[18] measured absorption edges for elements in the vapor phase and in other states of aggregation. Two of these, zinc and mercury, have monatomic vapors. The following list shows $\Delta\nu/R$, the shift of an absorption edge of the solid or liquid relative to that of the vapor:

Zn, solid, K,	-0.11,
Hg, liquid, L_{III},	$+0.18$.

Shifts observed in passing from one compound of an element to another are usually larger; according to the extensive work of Lindh,

[18] Hanawalt, Phys. Rev. **37**, 715 (1931).

Stelling and others,[19] they can be as high as 1.5 ν/R units, but broadly speaking, values larger than 0.5 ν/R units are associated with large change of valence. Further information may be obtained from Valasek's[20] work on the wave-length of $K\beta_1$ from sulfur and its compounds. The maximum shift of this line in passing from one compound to another was 0.11 ν/R units.

It seems fair to take 0.4 ν/R units as the maximum possible error in the data of Table I, due to our use of small terms of the isolated atoms. The error in level differences may sometimes be 0.4, though evidence from internal consistency of the wave-length data indicates it is usually smaller, and the maximum overall error is therefore 0.8 of a unit. This value is small compared with the widths of absorption edges (that of tungsten L_{III} is 2.5 ν/R units) and considering the uncertainties in the interpretation of edges, we may justly claim that the values in Table I are more accurate than those based on absorption measurements. The values for the silver L-limits agree well with those of van Dyke and Lindsay,[21] but not with those given in Siegbahn's book.

3. Analysis of the Data of Kretschmar and of Robinson, Andrews and Irons

Kretschmar, using the magnetic spectrograph, measured the energy of photoelectrons ejected from thin films by Mo $K\alpha$-rays, in order to obtain e/m. If e is expressed in electromagnetic units, the equation used becomes

$$\frac{e}{m}=\frac{2Rc(h/e)[\nu/R-(\nu/R)_A]}{(Hr)^2-R^2(h/e)^2[\nu/R-(\nu/R)_A]^2}. \quad (1)$$

R is the Rydberg constant for infinite mass; ν is the wave number of the incident x-rays; $(\nu/R)_A$ refers to an absorption limit of the atoms in the film; and H and r are the magnetic field employed, and the radius of curvature for a photoelectron moving in that field. Kretschmar made the ingenious suggestion that if the value of h/e obtained from the limit of the continuous x-ray spectrum is used, the resulting value of e/m is independent of the grating space assumed, because the effect of the grating space on h/e is balanced by its effect on the wave-lengths. A value of e/m computed in this way throws no light on the question as to which wave-length scale is correct. However, the ν/R value for a photoelectron may be written as

$$\frac{\nu^*}{R}=\frac{e}{h}\frac{c}{R(e/m)}\left[\left\{1+\left(\frac{eHr}{mc}\right)^2\right\}^{\frac{1}{2}}-1\right]. \quad (2)$$

If one employs in this equation the best values of e/m and e/h obtainable from experiments which do not involve x-rays, then Kretschmar's determinations of Hr yield values of ν^*/R which can be compared with $(\nu/R)-(\nu/R)_A$, as obtained from crystal spectra and from ruled-grating spectra.

Birge[7] has given values of e/m and h/e obtained from data which do not make use of x-rays. These are based on a least squares solution in section h of his paper. However, the values of e/m employed in this solution are higher than those indicated by recent data, which he would no doubt include if the computation were repeated now. Therefore, it seems best to use the most recent values of universal constants which he has published,[22] using data from all sources. These are:

$$e=(4.7668\pm0.0038)10^{-10}\text{ e.s.u.},$$
$$e/m=(1.7592\pm0.0011)10^{7}\text{ e.m.u./gram},$$
$$e/h=(2.4303\pm0.0029)10^{6}\text{ e.m.u./erg sec.},$$
$$c=(2.99796\pm0.00004)10^{10}\text{ cm/sec.},$$
$$R=109{,}737.42\pm0.06\text{ cm}^{-1}.$$

The ν/R values for the x-ray lines employed, on the basis $d_{\text{calcite}}=3027.91$ X.U., are as follows:

Mo $K\alpha_1$	1288.06	Cu $K\alpha_1$	593.04
Cu $K\alpha_2$	591.56	Cu $K\beta$	656.24

Detailed comparisons of photoelectric energies with those computed from crystal spectra are too voluminous to record here. Table II gives typical data and Table III presents a summary of the results.

Altogether, thirty-seven values were studied, and the measured energy of the photoelectrons is higher than the computed value in all cases

[19] Siegbahn, 2nd ed., p. 278 ff. See also Barnes, Phys. Rev. **44**, 141 (1933).
[20] Valasek, Phys. Rev. **43**, 612 (1933).
[21] van Dyke and Lindsay, Phys. Rev. **30**, 562 (1927).
[22] Birge, Phys. Rev. **42**, 736 (1932).

TABLE II. *Typical data on photoelectrons from gold.* (Robinson, Andrews and Irons.) Incident radiation, Cu $K\alpha_1$.

Absorption level	$(\nu/R)_A$ ($d=3027.91$ X.U.)	$(\nu/R)-(\nu/R)_A$ (Crystal values)	Observed ν^*/R for ejected electrons	Percent discrepancy
M_I	253.21	339.83	341.9	0.62
M_V	163.21	429.83	432.5	0.62
N_I	56.71	536.33	539.7	0.63
$N_{IV,\ V}$	25.77	567.27	570.6	0.58

TABLE III. *Discrepancy between photoelectric and crystal values of* $(\nu/R)-(\nu/R)_A$.

	Kretschmar, using Mo $K\alpha_1$	Robinson, using Cu $K\alpha_2$, $K\alpha_1$ and $K\beta$
Gold	0.23%	0.61%
Silver	0.24	0.45
Copper	0.18	−0.04
Platinum	0.24	
Weighted mean:	0.23	0.50

except two. These are Robinson's electron lines Cu $K\alpha_2$ − Ag L_I and Cu $K\alpha_1$ − Cu L_{III}, for which the percentage discrepancy is −0.04. Thus the photoelectric values of $(\nu/R)-(\nu/R)_A$ are about 0.36 percent higher than the crystal values (average of the two mean values in Table III). The discrepancy would be 0.61 percent if we employed the higher wave-lengths from ruled grating.

CONCLUSIONS

The photoelectric measurements support the crystal scale rather than the ruled grating scale. They do not quite suffice to *prove* that the former is correct because of the possibility of errors in measurements of the energies of photoelectrons, and because some of the universal constants may be wrong by amounts greater than the probable errors now assigned to them. As to the first point, retardation of electrons in the film from which they are ejected would lower their energy, while the values recorded here are higher than the ones from crystal wave-lengths. As to the second point, use of a lower value of e/m, such as the value $1.757\ 10^7$ e.m.u./gram obtained in the recent spectroscopic work of Kinsler and Houston and of Gibbs and Williams[23] would reduce the photoelectron energies by 0.12 percent, so agreement with crystal values would be improved. The possibility of reconciling the photoelectric energies with the ruled-grating scale appears, however, quite remote.

I am indebted to Professor R. T. Birge for information concerning universal constants, and to Dr. Victor Hicks for helpful discussions. March 8, 1934.

Note added in proof: A letter from Dr. Robinson informs me that as a result of recalibration of his apparatus it appears that his Hr values may be 1 part in 1200 to 1 part in 1500 too high. This correction is such as to reduce the discrepancy between observed photoelectric energies and those computed from crystal spectra.

[23] Kinsler and Houston, Phys. Rev. **45**, 104 (1934); Gibbs and Williams, Phys. Rev. **44**, 1029 (1933).

Scattering of X-Rays by Cold-Worked and by Annealed Beryllium*

JAMES E. BOYD, *Sloane Physics Laboratory, Yale University*

(Received April 13, 1934)

The intensities of reflection of Mo $K\alpha$-radiation by important crystallographic planes in powdered beryllium have been measured by an ionization method under the following conditions: (I) cold-worked particles of average diameter about $3\times(10)^{-3}$ cm; (II) the same after $\frac{1}{2}$ hr. at 800°C; (III) cold-worked particles of average diameter about $(10)^{-2}$ cm; (IV) the same after 1 hr. at 950°C. In (II) and especially in (IV) cold-working strains should have been relieved. The atomic structure factors derived from these data show no appreciable change with annealing and further show that Be crystals are rather imperfect. The mass absorption coefficient is found to be 0.26 in good agreement with a value computed according to Compton's empirical formula.

INTRODUCTION

THE atomic structure factor for x-ray scattering, generally plotted against $\sin\theta/\lambda$ in so-called F-curves, is closely dependent upon the charge distribution in the atom.[1,2] It has been suggested[3] that the charge distribution in the atoms of a cold-worked metal differs from that in the same atoms in annealed crystals, and if so a change in the F-curve is to be expected when a cold-worked metal is annealed.

Because of its low atomic number beryllium was chosen for test. Since the atomic number Z is 4, a given change in the position of one electron should have a large proportional effect. The outermost electrons contribute little to the F-values in the accessible range of $\sin\theta/\lambda$, so that changes in their distribution would be much harder to detect than a change in the position of a K electron.

The crystal structure of beryllium is hexagonal close-packed.[4] In a powder the (101) planes give the strongest reflection. Therefore, measurement of this reflection should furnish the best opportunity for detecting any small change because of cold-work since errors in the background here have a smaller proportional effect. The (101) planes are unevenly spaced so that their crystallographic structure factor S is $\sqrt{3}/2$ instead of 1.

If extinction is negligible, F^2 can be computed from the scattered intensity[5] for the case of transmission of x-rays through a plate of powdered crystals, the normal to which is equally inclined to the incident and emergent beams. F is usually defined by the equation

$$F=Z\int_{-D/2}^{D/2}p(z)\cos\left[(4\pi z\sin\theta)/\lambda\right]dz, \quad (1)$$

Z being the atomic number and $p(z)dz$ the probability that an electron will be between z and $z+dz$ from the lattice plane.

If the initial or final distributions of charge differ, the effect on F-values will be different for planes with different indices. It is therefore advisable to get F-values for several planes, even though the precision of the results for some of them may be low. Calculation shows that F for (101) may vary between 2.0 and 0.8 for extreme assumptions regarding the positions of the two L electrons. The probable range in F is much narrower.

PREPARATION OF SPECIMENS

A 5-gram lot of 99.5 percent Be, produced electrolytically by Siemens and Halske, was obtained in pea-sized lumps from the Metal and

* Part of a dissertation presented to the faculty of the Graduate School of Yale University in candidacy for the degree of Doctor of Philosophy.

[1] W. Ehrenberg and K. Schäfer, Phys. Zeits. **33**, 97 (1932).

[2] E. O. Wollan, Rev. Mod. Phys. **4**, 205 (1932).

[3] W. Geiss and J. A. M. van Liempt, Zeits. f. anorg. Chemie **133**, 107 (1924); **143**, 259 (1925), have supposed that the normal state of the metal atom is changed by cold-work. This led to the investigation here described. Since its beginning W. A. Wood, Phil. Mag. [7] **13**, 355 (1932), has independently proposed a test of this kind.

[4] L. W. McKeehan, Proc. Nat. Acad. Sci. **8**, 270 (1922).

[5] A. H. Compton, *X-Rays and Electrons*, Chapter V.

Thermit Corporation. The hardness and brittleness of the metal make plastic deformation difficult, but microscopic examination showed that small particles are flattened by crushing and grinding so that such processes produce some degree of cold-work. Two samples were prepared. A hardened steel crusher and an agate mortar were used to obtain particles of average size about 3×10^{-3} cm (I), the cold-work being done under toluene because of the reputed affinity of Be for oxygen. The surface of the mortar was scratched by the grinding, so to avoid this source of contamination a second cold-worked sample (III) was prepared with the crusher alone. Since larger particles were so obtained the use of toluene to prevent oxidation was dispensed with. The average size of the particles of (III) was about 10^{-2} cm. The crystal powders were packed lightly in flat brass containers, the windows in which were covered with thin cellophane.

In order to obtain Be crystals free from cold-work the powders were subjected to an annealing process in hydrogen at atmospheric pressure. Sample (I) was heated at 800°C for ½ hr., sample (III) at 950°C for 1 hr. The melting point of Be is 1280°C, so fine powders should have been well annealed by such treatments. After annealing (I) and (III) were designated (II) and (IV), respectively.

Apparatus and Measurements

Molybdenum x-rays from a G.E. water-cooled tube were filtered through ZrO_2 to give a fairly homogeneous beam. The primary intensity was controlled by a rheostat[6] in the filament circuit. Ionization currents (in CH_3Br) were measured with a quadrant electrometer at 1000 to 5000 divisions per volt.

Fig. 1 is a curve for sample (III), showing the strongest reflections. The lower curve is for the NaCl (220) reflection which was used to standardize the measurements, the F-values for NaCl (220) being well known.[2] The standard curve is low because of the thickness of the specimen used, but is convenient for comparison with the majority of the Be peaks.

Effective absorption coefficients μ' were found by placing each of the Be samples in the primary beam while measuring the intensity of NaCl (220). By taking the integrated area of the peak above background this measurement is limited, as is desirable, to the Mo $K\alpha$ wave-lengths.

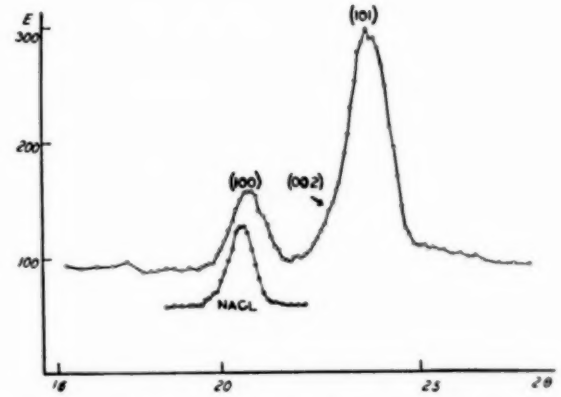

FIG. 1. Principal peaks for Be and NaCl standard. X-ray intensities in divisions per sec.$\times10^2$ are plotted along the ordinate, scattering angle in degrees along the abscissa.

Results

Absolute values of F can be found if the known value of F for NaCl (220) is used to eliminate measurement of the x-ray power input which is difficult with such a sensitive instrument as the electrometer. Then

$$F^2=(C/S^2\chi(\theta))(\rho/\rho')e^{\mu' h \sec\theta}R, \qquad (2)$$

where C is a constant for all reflections, $\chi(\theta)$ a function of the angle of scattering only, h is the thickness of the plate of powder, ρ' is the apparent density, ρ the density of the particles, R the ratio of the intensity of the Be reflection to the standard NaCl reflection and S the crystallographic structure factor.

The value found for ρ by weighing in air and in toluene was 1.85 g cm^{-3}. This value of ρ agrees with most others,[7] but differs from that given by Jaeger and Rosenbohm[8] (1.90 g cm^{-3}), who used metal from the same supplier.

Values of F for the four samples are given in Table I. The values for (002) reflections are of low precision because of poor resolution and

[6] P. Kirkpatrick, J.O.S.A. and R.S.I. **7**, 195 (1923).

[7] Siemens-Konzern (Beryllium), Chem. Catalog Co. (1932).

[8] F. M. Jaeger and E. Rosenbohm, Proc. Roy. Acad. Amst. **35**, 1055 (1932).

TABLE I. *Values of F for the four samples.*

Plane	$(\sin\theta)/\lambda$	F_1	F_2	F_3	F_4
100	0.254	2.3	2.0	2.3	2.1
002	.277	1.4	1.4	1.3	1.3
101	.289	2.08	2.11	2.05	2.03
102	.376	1.6	1.5	1.7	
110	.438	1.62	1.75	1.69	
103	.486	1.3	1.4	1.3	
112 201	.517	1.41	1.44	1.39	

uncertainty of background. Relative values of F (101) for the cold-worked and annealed samples indicate that the cold-work to the degree here attained had no appreciable effect upon charge distribution in the atom.

One can only conclude, from the fact that a 2 percent change in F, which could have just been detected, was not actually observed in the case of the (101) reflection, that the average effect of cold-work of this limited sort is small. If large local changes in F exist they must be limited to a small fraction of the total volume. It is conceivable that Be is self-annealing at the temperature of experiment[9] though this would be anomalous in view of its melting temperature.

The effect of change in particle size from 3×10^{-3} to 10^{-2} cm was very small. This is evidence that Be is a rather imperfect crystal since the sizes were near those which are minimum for primary extinction in the notably imperfect crystal NaCl.[10]

The average values for F for all samples agree fairly well with theoretical values given in a paper by James and Brindley.[11]

The data also furnish values for μ/ρ which are computed from the experimentally measured μ'/ρ' by correcting[12] for known impurities, in this case 0.4 percent iron. The same result $\mu/\rho=0.26$ was so obtained from samples (III) and (IV). This agrees well with $\mu/\rho=0.28$ as given by Compton's empirical formula.[13]

In conclusion the author wishes to express his thanks to Professor L. W. McKeehan, who suggested the problem and gave much helpful advice, and to Professor C. D. Cooksey for his constant interest and assistance in designing the apparatus.

[9] L. Thomassen and J. E. Wilson, Phys. Rev. **43**, 763 (1933), found Al to show line-broadening when worked at −75°C, but not when worked at room temperature.

[10] R. J. Havighurst, Phys. Rev. **28**, 882 (1926).

[11] R. W. James and G. W. Brindley, Phil. Mag. **12**, 81 (1931).

[12] R. J. Havighurst, Proc. Nat. Acad. Sci. **12**, 477 (1926).

[13] Reference 5, p. 189.

Critical Remarks on a Paper by G. Lemaitre and M. S. Vallarta on Cosmic Radiation

CARL STÖRMER, *Oslo, Norway*

(Received November 16, 1933)

1. INTRODUCTION

IN a recent paper Lemaitre and Vallarta[1] have discussed the latitude effect in cosmic rays discovered by Clay and Berlage[2] and confirmed by Compton's extensive measurements.[3] LV make use of my mathematical theory of the motion of an electrical particle in the field of a magnetic doublet. Their paper is very difficult to understand even for those who are familiar with the subject, due partly to real errors and partly to misprints. I think therefore it serves a useful purpose to give a detailed criticism of the paper, and to put it into historical perspective as far as the theory of electronic motions in the field of a magnetic doublet is concerned. In a later paper I hope to show how far my earlier researches in this field may be taken over in the theory of cosmic rays.

2. ON THE FUNDAMENTAL PRINCIPLES USED BY LEMAITRE AND VALLARTA

As to the fundamental principles enumerated in Section II of their paper LV say: "If now we assume that the intensity distribution of cosmic radiation at infinity is homogeneous and isotropic, the intensity in all allowed directions at any point in the earth's magnetic field is, by Liouville's theorem the same." This statement is given without further proof as if it were a direct consequence of Liouville's theorem. It has been pointed out by W. Swann[4] that Liouville's theorem cannot be applied in the manner of LV because they neglected the fact that the canonical momenta entering Liouville's theorem contain the magnetic vector potential; but Swann says that in a modified form Liouville's theorem can still be applied to an infinitely small tube of orbits. But this correction does not give the full story. The essential difficulty met with in the application of Liouville's theorem to this problem in the manner of LV is that the question, which directions are allowed and which are forbidden, is not decided by Eq. (14) and by the LV studies of asymptotic orbits only, but requires a detailed study of the shape of all the orbits from infinity, as function of their initial conditions.

If one remembers the immensely great variety of complicated orbits which may occur,[5] spiral orbits and nearly periodic ones and so on, one is warned to be very cautious in drawing general conclusions which are not well founded.

They say further: "Thus the question of calculating the intensity at any point at the earth's surface reduces to that of finding out in which directions particles coming from infinity can reach that point. There are as we shall see, three possibilities, either all directions are forbidden, or all directions are allowed, or only certain directions are allowed and the rest forbidden." The occurrence of forbidden directions was pointed out in my paper[6] many years ago. It was deduced from a formula found in 1904,[7] which is the same formula (14) given by LV. As is well known, the allowed and forbidden directions have also played an important part in the application to the aurora borealis.

3. THE EQUATION OF MOTION

The first error in LV comes from the sign of the earth's magnetic field. In fact the magnetic

[1] G. Lemaitre and M. S. Vallarta, Phys. Rev. **43**, 87 (1933). In the following we shall refer to this paper or to the authors as LV simply.

[2] J. Clay and H. P. Berlage, Proc. Roy. Acad. (Amsterdam) **30**, 1115 (1927); **31**, 1091 (1928); **33**, 711 (1930) and Naturwiss. **20**, 687 (1932).

[3] A. H. Compton, Phys. Rev. **41**, 111, 681 (1932) and a paper presented at the Chicago Meeting of the American Physical Society, November 25, 1932.

[4] W. F. G. Swann, Phys. Rev. **44**, 224 (1933).

[5] Carl Störmer, Vid. Selsk. Skr. Christiania (Oslo) 1913; Zeits. f. Astrophysik **1**, 237 (1930) and *How the horseshoe-formed auroral curtains can be explained by the corpuscular theory*, Terr. Magn. and Atm. Elec. **37**, 375 (1932).

[6] Carl Störmer, Vid. Selsk. Skr. (1904).

[7] Reference 6, formula VI.

pole in the northern hemisphere is not a north pole, but a south pole, which gives for H_r and H_z the *opposite* sign of that in their paper. This has the consequence that the equations of motions (1), (2) and (3) come out with wrong signs for the second members.

Another less important thing is the fact that LV consider the axis of the earth's magnetic field to coincide with the axis through the *magnetic poles of the earth*. It is well known, however, and beautifully illustrated by the distribution of aurorae, that in the first approximation due to Gauss's series for the magnetical potential, the magnetic axis cuts the earth's surface in the neighborhood of Smith's Sound in northwestern Greenland, halfway between the magnetic and geographical poles.

As to the deduction of the equations of motion, which is not given in LV's paper, it can be done by general principles or by specializing the general equations I have published in a paper in 1912.[8]

As the Eq. (4) is deduced from the equations of motion the same wrong sign comes out here. As to the splitting up of the motion and the Eq. (5) references to my papers are given.

In the Eq. (7) there is a misprint. In fact the factor 1/2 on the left side has to be dropped. This equation is not different however from the equation VIII,7 which I published in 1907,[9]

$$r_1^4\left[\tfrac{1}{2}d^2(r_1^2)/ds_1^2-1\right]=\cos^2\lambda-\alpha^2 r_1$$

where r_1 and the arc of the trajectory s_1 are measured with

$$c_1=(M|e|/mv)^{\frac{1}{2}}\text{ centimeters}$$

($|e|$ the absolute value of e)

as unit of length and where α^2 is a constant of integration. In fact if we introduce here $r=c_1 r_1$, $t=c_1 s_1/v$ we get

$$\frac{d(r\dot{r})}{dt}-v^2=\frac{e^2M^2}{m^2}\frac{1}{r^4}\left(-\frac{\alpha^2}{c_1}r+\cos^2\lambda\right)$$

and if we call with LV 2γ the constant $-\alpha^2/c_1$ their Eq. (7) with correct first member comes out.

It is to be pointed out that the constant 2γ used by LV is not the same as the constant 2γ used in my papers.

The next step, the deduction of the Eq. (8) and the resulting Eqs. (9) and (10) is an original contribution of value in LV's paper. In Eq. (9) there is, however, a new misprint: the sign for the integral in the numerator has to be changed. Furthermore the constant of integration C in the Eq. (10) is not necessarily identical with the constant C in Eq. (9); that depends on the limits adopted for the indefinite integrals.

4. The Normalized Coordinates and Formula (14)

The introduction of what LV call normalized coordinates is the same transformation I used in my paper from 1907 and what they call x is thus the length of the radius vector measured with the unit of length c_1 introduced in the foregoing section.

On account of the wrong sign for the magnetic components the *formula (14) in LV's paper is also wrong*. The sign must be chosen in such a manner that + corresponds to positive and − to negative charges. The constant γ_1 in their formula is identical with the constant γ_1 in my papers (equal to $-\gamma$ where γ is the constant I have introduced).[10]

It is useful to compare the corrected LV formula with my formula of 1907.[10]

My formula is

$$\sin\theta=-2\gamma_1/R+R/r^3$$

and if we introduce $R=r\cos\lambda$:

$$\sin\theta=-2\gamma_1/r\cos\lambda+\cos\lambda/r^2.$$

The corrected LV formula is for negative particles

$$-\sin\theta=-2\gamma_1/x\cos\lambda+\cos\lambda/x^2,$$

which coincide with my formula if we remark that x is the same as r and the positive direction of θ is the opposite one (Figs. 1 and 2).

5. Remarks on Section IV

This section is very difficult to understand even for readers who are familiar with my papers

[8] Carl Störmer, Vid. Skr. Christiania 1912, Eqs. (V).

[9] Carl Störmer, Archives des sciences phys. et natur. **24** (1907).

[10] Reference 9, formula (3).

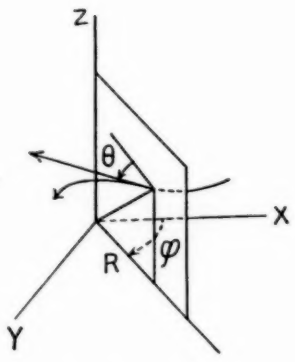

FIG. 1. Positive directions of θ and φ in my papers.

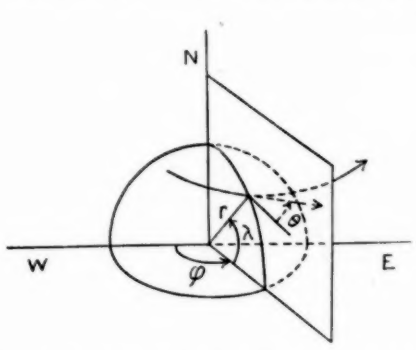

FIG. 2. Positive directions of θ and φ in LV.

on the subject. There is a great lack of precision and the exposition is very obscure.

The first part, the discussion of the regions of the earth's surface into which no particles can enter, is a repetition of a discussion which I have already given in my paper from 1907. A formula for the limiting value λ_1 is also given explicitly in my paper on the problems of the aurora.[11]

Further they say: "For latitudes greater than λ_1 and values $x_0<1$ there are trajectories coming from infinity but they have a limit and this limiting trajectory must be asymptotic to a periodic orbit." It can scarcely be maintained that this sentence conveys a definite meaning. It looks as if the authors mean that an asymptotic trajectory forms a limit between the trajectories reaching the earth and those not doing it. This, however, is not the case. Such questions were discussed by me in a paper published in 1911,[12] where I have found the conditions which they suggest. I content myself with that reference, hoping to come back to the question in a later communication.[13]

Then comes a reference to my paper on periodic orbits where the following explanation is given: "A good approximation to the mean value of x for a periodic orbit can be found directly from (9) in agreement with the numerical computations of Störmer. By neglecting the integral and using a mean value for λ, the constant C in the denominator of Eq. (9) must be so chosen that this denominator has a double root."

We will try to explain what they mean: They first presuppose that the Eq. (11) is brought to a reduced form by introducing normalized coordinates and the value γ_1. We have $r=c_1x$, $\gamma=-\gamma_1/c_1$, which gives

$$\frac{x^2d\lambda^2}{dx^2}=\frac{-\dfrac{4\gamma_1^2}{\cos^2\lambda}-\dfrac{\cos^2\lambda}{x^2}+C_1-2\displaystyle\int\frac{\cos^2\lambda}{x^3}dx}{x^2+\dfrac{4\gamma_1}{x}-C_1+2\displaystyle\int\frac{\cos^2\lambda}{x^3}dx},$$

where $C_1=Cc_1^2$, C_1 is called C in their paper.

If we now, as they propose, neglect, that is, drop, the integral, the denominator will be $x^2+4\gamma_1/x-C_1$.

But this cannot be their meaning, for the condition of a double root here gives a condition different from their Eq. (17).

If we however use a *constant* mean value of $\cos^2\lambda$ given by the Eqs. (15) and (16) we get:

$$2\int(\cos^2\lambda/x^3)dx=-\cos^2\lambda/x$$

and

$$\frac{x^2d\lambda^2}{dx^2}=\frac{C_1-4\gamma_1^2/\cos^2\lambda}{x^2+4\gamma_1/x-C_1-\cos^2\lambda/x^2}$$

and the condition for a double root x_p in the denominator is now

$$x_p-2\gamma_1/x_p^2+\cos^2\lambda/x_p^3=0,$$

which reduces to the Eq. (17) if we use the Eqs. (15) and (16).

In this connection it may be pointed out that a more natural way to this and to more general results is given in my paper of 1931.[13] It is sufficient to specialize the results in the third part of my

[11] Carl Störmer, *Ergebnisse der kosmischen Physik*, Akad. Verlagsbuch. 1931, p. 56.

[12] Carl Störmer, Archiv f. Math. og Naturv. **31**, No. 11, (1911).

[13] Carl Störmer, Zeits. f. Astrophysik **3**, 31 (1931).

paper[14] which gives the approximate system:

$$(dx/d\sigma)^2 = x^4 - C_1x^2 + 4\gamma^2{}_1x - \alpha^2,$$
$$(d\lambda/d\sigma)^2 = C_1 - 4\gamma_1{}^2/\cos^2\lambda,$$

where α^2 is just such a mean value of $\cos^2\lambda$ and where σ is related to the arc s_1 of the trajectory by the equation $ds_1 = x^2 d\sigma$.

This system has great advantages for the study of the asymptotic trajectories and of the periodic orbits to which they approach. We will come back to this question in a later paper.[15]

As to the Eq. (16) in LV it is already given in my general paper from 1907 §6, as formula for $\cos\psi'$ for $k_1 = 1$.

The formula (18) seems to be wrong. The correct formula should be

$$C_1 = 2x_p{}^2 + 2\gamma_1 x_p{}^{-1}.$$

As to the value of γ_1 for which the periodic orbits disappear their estimate $\gamma_1 = 0.783$ is very good. See my paper.[15]

[14] Carl Störmer, Zeits. f. Astrophysik **4**, 290 (1932).

[15] Carl Störmer, *On the Trajectories of Electric Particles in the Field of a Magnetic Dipole with Applications to the Theory of Cosmic Radiation*, first and second communication, Publications from Oslo University Observatory No. 10 and No. 12. Oslo, 1934.

On the next page LV say: "We have carried out the numerical integration of Eq. (10) for $\gamma_1 = 0.911$ corresponding to $\lambda_m = 20°$, beginning at $\log x = -0.04$ and $\lambda = 14.14°$ and decreasing values of λ. From the results of this integration we have made estimates of the inclination with the radius vector of the asymptotic family of trajectories passing through points of coordinates $x = 0.5$, 0.6, 0.7, 0.8, and 0.9 both for $\lambda = 0$ (equator) and 10°. For each pair of values x_0 and λ we know three points of the cone, i.e., the value of θ_1 for $\gamma_1 = 1$ for which the angle $\eta = 0$, for $\gamma_1 = 0.911$ for which we have estimated values of η as described above, and θ_3 for $\gamma_1 = 0.783$, for which $\eta = 90°$."

Here the exposition is so obscure that it is very difficult to guess their meaning. It would be a delusion to believe it possible from the numerical integration of a few orbits to be able to make any trustworthy estimates in the way attempted by LV.

It seems, on the whole that the numerical results on the intensity distribution of cosmic radiation given by LV must be illusory.

LETTERS TO THE EDITOR

Prompt publication of brief reports of important discoveries in physics may be secured by addressing them to this department. Closing dates for this department are, for the first issue of the month, the twentieth of the preceding month; for the second issue, the fifth of the month. The Board of Editors does not hold itself responsible for the opinions expressed by the correspondents.

Directions of Discontinuous Changes of Magnetization in a Rotating Monocrystal of Silicon Iron

We have continued, by a more powerful method, the study[1] of Barkhausen effects in a monocrystal specimen wherein $\mathbf{H}_a$, the applied magnetic field intensity, changes in direction but not in magnitude. Instead of using a two-element galvanometer (G. E. oscillograph) to record the impulses in the two search coils (with axes at right angles) surrounding the disk specimen, we use a cathode-ray oscillograph. With each pair of deflector plates fed through a suitable amplifier by one of the search coils we obtain an excursion of the luminous spot on the screen in a direction which corresponds to the direction of any sudden change in magnetization, $\Delta\mathbf{I}$, occurring in the specimen. A photographic record is made covering selected short intervals during the slow and uniform rotation of $\mathbf{H}_a$ in the plane of the disk. Fig. 1 shows how the directions of large changes, $\Delta\mathbf{I}$, are related to the momentary direction of $d\mathbf{H}_a/dt$ and to the directions in the disk (four in number) which correspond most nearly to axes of the form $<100>$. By large changes we mean those which give a trace on the photograph (at one-fourth size) at least two millimeters in length, i.e., long enough to make the azimuth of the trace determinate. Many traces too short for individual measurement occur somewhere near the angles at which long traces are observed.

The specimen, for which we are indebted to Dr. W. E. Ruder of the General Electric Company's Research Laboratories, is a disk of 3 percent silicon iron, 1.33 cm in diameter and 0.023 cm thick, cut from the rectangular piece furnished us. The orientation and perfection of the crystal were tested by taking Laue photographs both before and after annealing (2.5 hr. at 870°C). A slight improvement in the symmetry of the Laue spots resulted from this treatment, and there was no indication in the final state of any residual strain. Neither the orientation of the axes nor the angular distribution of $\Delta\mathbf{I}$ were noticeably altered by annealing.

Evidence for the heterogeneity of magnetization at this value of $\mathbf{H}_a$ is furnished by the fact that $\Delta\mathbf{I}$ varies over a considerable range of angles about the momentary value of $d\mathbf{H}_a/dt$. This means that many changes $\Delta\mathbf{I}$ take place in which the magnetic potential energy density seems to increase, i.e., $\mathbf{H}\cdot\Delta\mathbf{I}<0$. The reasonable view is that the local direction of $\mathbf{H}$ in the parts affected differs so much from the direction of $\mathbf{H}_a$ that the anomaly is apparent rather than real. The same difficulty arises on the descending branch of any ordinary hysteresis loop for $\mathbf{H}_a>0$.

The largest excursions of the spot frequently show changes in the direction of $\Delta\mathbf{I}$ during the time of tracing, so that narrow loops or zigzags are traced. This seems to mean that a major discontinuity can traverse regions in which the change in the direction of magnetization is widely different from that in regions where a discontinuity is likely to grow to observable size.

Fig. 1 shows that practically all of the large changes are explicable as due to simple reversals along one of the directions of easy magnetization, here of the form $<100>$. At lower $\mathbf{H}_a$ this preference is not nearly so marked. At

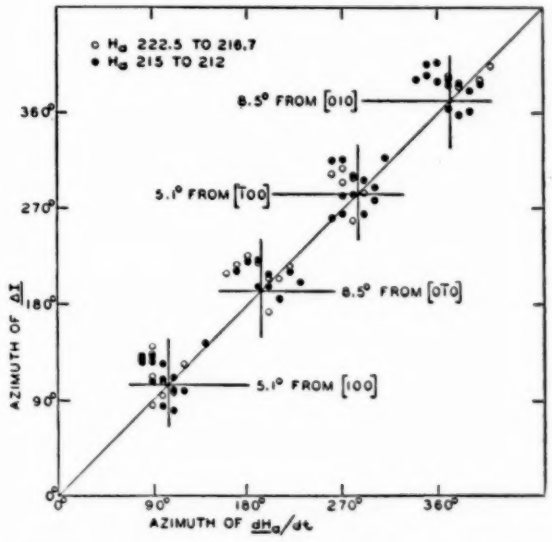

FIG. 1. Angular distribution of $\Delta\mathbf{I}$. The abscissa is the momentary direction of $d\mathbf{H}_a/dt$, the ordinate is the direction of $\Delta\mathbf{I}$, both referred to an arbitrary zero line on the specimen. The 45° line represents the locus of $\Delta\mathbf{I}$ if always parallel to $d\mathbf{H}_a/dt$. Points above the line have $\mathbf{H}_a\cdot\Delta\mathbf{I}$ negative, points below it have $\mathbf{H}_a\cdot\Delta\mathbf{I}$ positive. If only reversals along directions of form $<100>$ are possible the points should lie at the intersections of horizontal and vertical lines so marked. The values of $\mathbf{H}_a$ are indicated. One rotation required 250 seconds.

[1] F. J. Beck, Jr., and L. W. McKeehan, Phys. Rev. **41**, 385; **42**, 714–720 (1932).

the same time the number of large changes becomes less. The probable error in the measured azimuth of a single ΔI may be set at $\pm 5°$. This was estimated by picking up the ΔI from a small rod of the same silicon iron rotated about a transverse axis in the same field and search coils. We know that each ΔI in such a specimen must lie very close to its axis of figure. The angular resolving power in the earlier work[1] was not so high as that now attained and we suggest that the results then obtained were inconclusive mainly for this reason.

The work of Sixtus and Tonks[2] affords an explanation for the effect here observed. We suppose that Barkhausen discontinuities are propagated through a considerable volume only if they result in substantial and favorable changes of **H** in front of an advancing boundary. Since reversal of magnetization in any domain best meets this condition discontinuities which arise and proceed in this way have the best chance to grow to a size here observable. We have already pointed out that the largest Barkhausen discontinuities here observed may transcend this condition in their later stages.

L. W. McKeehan
R. F. Clash, Jr.

Sloane Physics Laboratory,
Yale University,
May 1, 1934.

[2] K. J. Sixtus and L. Tonks, Phys. Rev. **35**, 1441 (1930); **37**, 930–958 (1931); **39**, 357–358; **42**, 419–435 (1932); L. Tonks and K. J. Sixtus, Phys. Rev. **41**, 539–540 (1932); **43**, 70–80, 931–940 (1933).

The Heat of Dissociation of N_2

The observation[1] of the long sought intercombination band system $A^3\Sigma \rightarrow X^1\Sigma$ in N_2 has made possible a new determination[2] of the energy of dissociation of N_2. This value $D(N_2) = 7.4$ v seems at first glance to be in disagreement with either my[3] electron impact measurements or those of Tate, Smith and Vaughan.[4] This however is not the case. My results were that it requires 8.62 ± 0.02 v to form $N^+ + N$ from N_2^+. The question involved is the determination of the state of excitation of the N^+ and N formed by electron impact. Possible interpretations are listed below, where I.P. represents the energy necessary to form N_2^+ from N_2. The data in the last column are the result of using for I.P. the accurate value 15.65 ± 0.02 v obtained by Tate, Smith and Vaughan[4]

$N^+ + N$	$D(N_2^+)$	$D(N_2)$	$D(N_2)$
^3P $^4S^0$	8.62 v	I.P.—5.86 v	9.79 v
^1D $^4S^0$	6.73	I.P.—7.75	7.90
^3P $^2D^0$	6.25	I.P.—8.23	7.42
^3P $^2P^0$	5.06	I.P.—9.42	6.23
^1S $^4S^0$	4.59	I.P.—9.89	5.76

As already discussed[3] $D(N_2) = 9.79$ v is certainly too great. The last two values, 6.23 v and 5.76 v seem unreasonably low and the decision rests between 7.90 v and 7.42 v. In my paper 7.90 v was chosen because it was in agreement with Birge's[5] extrapolation of the vibration levels of the A' state of N_2^+ obtaining $D(A') = 3.67$ v and $D(N_2^+) = 6.82 \pm 0.1$ v. If the extrapolation of $D(A')$ is too high and can be lowered to 3.1 v, $D(N_2^+)$ becomes 6.25 v and $D(N_2) = 7.42$ v in agreement with Kaplan and with our third possibility listed in the table. However if Birge's estimate of $D(A')$ and Kaplan's value of $D(N_2)$ are both correct, the value of I.P.[4] for N_2 must be incorrect. My results are in agreement with either alternative and cannot discriminate between the two possibilities.

W. Wallace Lozier

Palmer Physical Laboratory,
Princeton, New Jersey,
May 2, 1934.

[1] L. Vegard, Zeits. f. Physik **75**, 43 (1932).
[2] J. Kaplan, Washington Meeting Am. Phys. Soc. 1934, Paper 92. The conclusions presented at the Meeting were different from those contained in the Abstract.
[3] W. Wallace Lozier, Phys. Rev. **44**, 575 (1933).
[4] J. T. Tate, P. T. Smith and A. L. Vaughan, Phys. Rev. **43**, 1054A (1933).
[5] R. T. Birge, *Molecular Spectra and Molecular Structure*, Faraday Society, p. 713 (1929).

A Stable Hydrogen Isotope of Mass Three

The unexpected announcement at the Physical Society meeting last week by Bleakney and his colleagues from Princeton that they had now found evidence that their deuterium samples contain hydrogen atoms of mass three to the extent of a few parts per million, makes it desirable that we place on record the evidence which had led us to announce a similar conclusion in an abstract (on another subject) submitted for the same program.[1] Using the Allison magneto-optic method, Latimer and Young[2] last autumn announced the detection of a mass-three hydrogen isotope in a sample of heavy water, however, without being able to give a quantitative estimate.

The method we used depends on the simple fact, theoretically predicted and already verified by the comparison of proton and deuton ranges in air, that the rate of loss of energy by any high speed hydrogen nucleus of a given velocity projected into a gas (ion-pairs per millimeter path) is approximately the same irrespective of its mass, whereas

[1] Abstract No. 35, Bull. Am. Phys. Soc., April 10, 1934 (Program of the Washington Meeting). The qualifying phrase "but not proof" was inserted in the abstract, not by reason of any uncertainty in our observations or concerning the reality of the effect, but because we feel that adequate scientific proof of the existence of a new isotope cannot be obtained by any one method. We had not found time to verify our result by collision experiments and we wished to forestall the type of emphatic overstatement so usual in press and magazine reports of scientific news.
[2] W. M. Latimer and H. A. Young, Phys. Rev. **44**, 690 (1933).

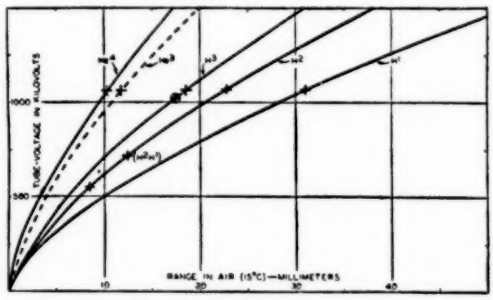

FIG. 1.

the kinetic energy is proportional to its mass. Thus, for the same *initial velocity* the range of a deuton is twice that of a proton, and the range of a mass-three hydrogen nucleus must be expected to be three times that of the proton. Because the focussed beam of million-volt ions from our tube is parallel and highly homogeneous in velocity, and because of the degree of purity of its magnetic resolution, range-measurements on the mass-three spot provided a simple and exceedingly sensitive test for the presence of hydrogen nuclei of mass three, projected without collision from the ion-source at the top of the high-voltage tube.

The range-curve for protons of various energies is marked H^1 in Fig. 1. The range-curve for deutons calculated as above indicated is marked H^2, and has been verified in this and other laboratories during the past two years. The predicted range-curve for hydrogen nuclei of mass three is similarly calculated and marked H^3. Thus with the mass-three spot resolved on to the range-measuring window, we would expect to find protons of energy corresponding to one-third the tube voltage (from H^1 H^1 H^1 and from H^2 H^1), deutons corresponding to two-thirds the tube voltage (from H^2 H^1) and full-voltage H^3 and He^3 nuclei if these exist in the ion-source. Of these possibilities, the H^3 nuclei will have a range considerably in excess of the others (6 millimeters excess at 1100 kilovolts; see crosses, Fig. 1).

Observations last December on the first deuterium introduced into our tube, a sample of heavy water kindly given us a year ago by the late Dr. Washburn, showed the presence of particles having the range expected for full-speed H^3 nuclei.

Arrangements were immediately made to increase the currents in our tube to improve the observations, with the result that our focussing and magnetic resolution were temporarily impaired, and these particles were obscured by a background. Other observations bearing on the stability of the deuton claimed our time and attention until March. Then a repetition of these range measurements with a highly-concentrated H^2 sample, using two copper-foil windows and two mica windows, practically eliminated any possibility that the weak group of range 5 to 6 millimeters beyond the expected deuton value (for 1100 kv H^2 H^1) as found with the mass-three spot might be due to a thin spot in a window, or to soft x-rays or other short "range" spurious effect from the window itself. Disintegration processes known to be occurring in the window (H^2 on H^2) were shown by other measurements to be of far too small a magnitude to affect the electrometer.

With our tube operating at 1100 kilovolts we observed the expected protons from the mass-one spot as a strong purple glow extending out from the window to within a millimeter or two of the expected distance, and measurements with a movable flat ionization-chamber about 2 millimeters deep, connected to an electrometer, showed that the protons have a range of 31 to 32 millimeters. With the mass-two spot similar observations showed the expected 23-millimeter deutons. From neither of these spots was any faint longer-range group in evidence. The mass-three spot showed the expected 12.5-millimeter deutons as a bright purple glow extending about 2 millimeters beyond the window, but in addition a faint purple glow (visible only to the dark-adapted eye) extended beyond this group a distance of 5 or 6 millimeters. The electrometer measurements also showed the presence of a group of maximum range approximately 17.5 millimeters (circle, Fig. 1), as would be predicted for full-speed H^3 nuclei. Assuming the correctness of this identification, from the ionization measured by the electrometer and the current measurements on the various spots we calculated that stable hydrogen atoms of mass three comprised of the order of one part in a million of the particular 98 percent deuterium sample in use during March.

The H^3 nuclei indicated by these observations could not have originated in the high-voltage part of the tube, but must have come directly and without collision from the arc-space of the ion-source, in order to have the spot-position and the range observed. Furthermore, any H^3 formed in the main tube could hardly diffuse back into the ion-source against the pressure-gradient in the probe-canal (1.6 millimeters in diameter and 48 millimeters long). The deuterium flowing through the arc-space was exposed to the 60-volt arc-discharge and the 2000-volt probe-voltage for only a brief time, consequently very few, if any, disintegrations yielding H^3 could be expected in the ion-source itself. Thus the conclusion was reached that the observed proportion of H^3 nuclei must have been present in the dueterium sample as stable H^3 atoms.

We expected shortly to undertake the measurement of the collisions of these particles with protons in a low-pressure cloud-chamber as a final check on their identity; however, the approximate numerical agreement of the Princeton estimate with our own, in which radically different technique and samples from separate sources are used appears to us a satisfactory proof of the existence of H^3 atoms in concentrated deuterium samples.

We are grateful to Professors Urey, Zanetti and La Mer for the deuterium samples used in most of our experiments and to Dr. Brickwedde for whose initial use part of the deuterium was specially prepared.

M. A. TUVE
L. R. HAFSTAD
O. DAHL

Department of Terrestrial Magmetism,
Carnegie Institution of Washington,
Washington, D. C.,
May 3, 1934.

The Magnetic Moment of the Neutron

In spite of our knowledge of electrons, positrons and possibly other light particles one can try to establish a preliminary theory of the nucleus by using heavy particles only. The scheme "nucleus = α-particles + neutrons + one or no proton" first suggested by D. Iwanenko[1] accounts indeed for a number of facts concerning the presence and absence of isotopes and their mass defects.[2] The same scheme gives an independent way for calculating, from the observed magnetic moments of higher nuclei, the magnetic moment of the proton.[3] Although the resulting value of about 2 nuclear magnetons deviates from Stern's value 2.5±10 percent from Rabi's value 3.2±10 percent, this does not necessarily mean a failure of our scheme of the nucleus. For in spite of the excellent experimental observations of hyperfine structure and of molecular ray deflections a number of rather crude theoretical assumptions about the orbits of external electrons are used to infer the values of nuclear magnetic moments from the observations in all three cases. Indeed the accuracy claimed by either one is far beyond the discrepancy of the results. The following method for getting information about the magnetic moment of the neutron from observed values for higher nuclei is likewise dependent on the accuracy of the "observed" g-values of Table I.

TABLE I.

Z	M	j	μ	g	
48	Cd^{111}	1/2	−0.67	−1.33	B
48	Cd^{113}	1/2	−0.67	−1.33	B
80	Hg^{199}	1/2	0.55	+1.10	B
80	Hg^{201}	3/2	−0.62	−0.41	B
82	Pb^{207}	1/2	0.60	+1.20	A

According to our scheme one has four distinct types of nuclei belonging to even and odd charge number Z and mass number M, namely: (1) Z even, M even; (2) Z even, M odd; (3) Z odd, M even; (4) Z odd, M odd. In type 1 the nucleus consists of α-particles and an even number of neutrons. Nuclei of this type, of which the α-particle itself is an outstanding example, prove to have no mechanical moment j and no magnetic moment $\mu = g \cdot j$ at all. The even arrangements of neutrons seem to form closed shells and thus they give us no information about the magnetic properties of their constituents. Type 4 differs from type 1 only by one additional *proton* and was used to determine the above-mentioned value of its magnetic moment. Type 2 differs from the closed shell type 1 only by one additional *neutron*. We suppose then, that this one neutron alone is responsible for the mechanical and the magnetic moment of the whole nucleus. Hyperfine-structure measurements of isotopes of this type have been made in a few instances only. According to Goudsmit's calculations[4] one has the following nuclear data (Table I). The letters A and B mean grades of reliability of these data. Our interpretation starts with the fact, that the orbit of the neutron furnishes no magnetic moment, since the neutron is uncharged. Hence there is no magnetic coupling force between the orbit and the spin of the neutron. Both are completely uncoupled, and the smallest external magnetic field will produce a complete Paschen-Back effect. The spin of the neutron is known to be ½. Hence if l is the quantum number of its orbit, then the total mechanical moment j will be $l+\frac{1}{2}$ or $l-\frac{1}{2}$. If μ_0 is the unknown magnetic moment of the neutron, then there are two cases:

For $j = l+\frac{1}{2}$ one has $g = (0+\mu_0)/(l+\frac{1}{2}) = +\mu_0/j$.

For $j = l-\frac{1}{2}$ one has $g = (0-\mu_0)/(l-\frac{1}{2}) = -\mu_0/j$.

From this g-formula one obtains the following Paschen-Back g-tables carried out for the two cases $\mu_0 = 1$ and $\mu_0 = -0.6$.

TABLE II. $\mu_0 = 1$.

l \ j	1/2	3/2	5/2
0	2		
1	−2	2/3	
2		−2/3	2/5

TABLE III. $\mu_0 = -0.6$.

l \ j	1/2	3/2	5/2
0	−1.2		
1	+1.2	−0.4	
2		+0.4	−0.24

The latter case is taken because $\mu_0 = -0.6$ seems to fit best with the "measured" g-values of Table I. It is quite striking that the three first values of the g-Table III in its upper left hand corner alone check perfectly with the observed data in their j-values and their signs and almost perfectly in their numerical values giving due allowance to Goudsmit's grades of accuracy. Our result is:

In addition to its angular moment of ½, the neutron has a magnetic moment of $\mu_0 = -0.6$ nuclear magnetons approximately. The minus sign means that the neutron is a rotator, in which a negative charge is fixed to a light mass and an equal positive charge is fixed to a heavier mass. This would seem to decide the question whether the neutron is or is not an elementary particle.

In our opinion it is much more reliable to use for the determination of μ_0 elements of type 2 than to use for instance the *deuton*, since the latter belongs to type 3 and represents a much more problematic compound than the isotopes of the other three types. Fortunately this complicated type is stable in only 4 cases that are easily understandable exceptions of a general rule that this type decomposes by β-emission and formation of an α-particle out of 2 neutrons and 2 protons in the remainder of the nucleus.

D. R. INGLIS AND A. LANDÉ

Ohio State University,
May 3, 1934.

[1] D. Iwanenko, Comptes Rendus **195**, 439 (1932).
[2] E. N. Gapon, Zeits. f. Physik **79**, 676 (1932); A. Landé Phys. Rev. **43**, 620 (1933).
[3] A. Landé, Phys. Rev. **44**, 1028 (1933).
[4] S. Goudsmit, Phys. Rev. **43**, 636 (1933).

Mass-Spectrograph Determination of the Relative Abundance of Heavy Hydrogen in a Sample

The method of diffusion through palladium has been employed by Harris, Jost and Pearse[1] to effect the separation of the hydrogen isotopes. The increase of concentration of the heavy hydrogen was determined spectroscopically, and it was reported that under the conditions of the experiment approximately a tenfold enrichment was obtained, with a resulting concentration of about one percent deuterium. The spectroscopic method has been subjected to criticism and it was proposed that a test of the enriched sample be made with the mass-spectrograph. The method of Bleakney[2] was not applicable as the mass-spectrograph employed here[3] is designed to operate at pressures of the order of 0.5 mm in the discharge tube with further aging in a drift space; and under these conditions 95 percent or more of all the ions obtained are triatomic. It seemed however that the triatomic ion of mass 4 ($H^1H^1H^{2+}$) observed by Bainbridge,[4] could be used to determine the concentration of heavy hydrogen where the relative percentage was small.

The triatomic ion in light hydrogen is formed by a reaction between the initial molecular ion and a neutral molecule as follows:

$$H^1H^{1+}+H^1H^1\rightarrow H^1H^1H^{1+}+H^1.$$

In mixtures of heavy and light hydrogen the following reactions should occur:

$$H^1H^{2+}+H^1H^1\rightarrow H^1H^1H^{2+}+H^1, \quad (1)$$

$$H^1H^{1+}+H^1H^2 \begin{cases} \rightarrow H^1H^1H^{2+}+H^1 & \text{(a)} \\ \rightarrow H^1H^1H^{1+}+H^2 & \text{(b)}. \end{cases} \quad (2)$$

If f is the fraction of H^2 atoms relative to the total number of atoms, then $2f$ is the fraction of H^1H^2 molecules relative to the total, if f is small. Consequently, reaction number 1 above should yield an intensity of $H^1H^1H^{2+}$ ions of $2f$ relative to $H^1H^1H^{1+}$, and reaction number 2 should yield a relative intensity of f, making a total of $3f$. This reasoning involves the assumption that reactions 2(a) and 2(b) are equally probable, which may not be entirely justified; but any departure from this assumption should lie within the experimental error. It is also required that the ions should be aged sufficiently and f should be small enough so that there is no measurable number of H^2H^{2+} ions present.

A series of runs on a sample of the enriched hydrogen gave an average of about 1.5 percent of mass 4 ions relative to mass 3. This would indicate a relative concentration of hydrogen atoms of about 0.5 percent. A redetermination of the density of the original water used by Harris, Jost and Pearse was made by Dr. E. S. Gilfillan of the chemistry department and it was found that the concentration of heavy hydrogen was about 0.13 percent. The mass-spectrograph results thus indicate a fourfold enrichment by passage through palladium instead of 8 to 10 fold as previously reported.

The mass-spectrograph employing aged hydrogen ions, as was done in this experiment, furnishes a direct and simple method of determining the relative concentration of heavy hydrogen, providing the assumptions involved are justified. No ions of mass 5 or 6 could be observed owing to the small concentration of heavy hydrogen, but a complete study of the nature of aged ions in various mixtures of the hydrogen isotopes would yield interesting information concerning the atomic processes involved in the formation of the triatomic ions.

OVERTON LUHR
LOUIS HARRIS

George Eastman Research Laboratories,
Massachusetts Institute of Technology,
May 8, 1934.

[1] Harris, Jost and Pearse, Proc. Nat. Acad. Sci. **19**, 991 (1933).
[2] W. Bleakney, Phys. Rev. **44**, 256 (1933).
[3] O. Luhr, Phys. Rev. **44**, 459 (1933).
[4] K. T. Bainbridge, Phys. Rev. **42**, 1 (1932).

The Ultraviolet Absorption of Acetylene and Ethylene

For some time we have been investigating the far ultraviolet absorption of various simple hydrocarbons. We find, in the case of acetylene, a rich absorption spectrum which extends from 1520A to 1050A. The absorption is very strong and most of the bands appear with a pressure of only 0.001 mm of acetylene in the spectrograph, the light path being about 1.5 meters.

They can be conveniently divided into two classes. Class I contains bands possessing P, Q and R branches. They appear as narrow absorption doublets at low pressures. They have a sharp head and are shaded towards the red. The bands of Class II show a single head, and therefore contain only more diffuse P and R branches.

On account of the complexity of the spectrum some difficulty was experienced in analyzing it. Recently it has been enormously clarified by the use of the heavy hydrogen isotope. A comparison of the spectrum of light acetylene with that of heavy acetylene (C_2HD) immediately reveals the fundamental band of each electronic transition by its small isotopic shift which is due only to the change in zero point energy. In this way two Rydberg series were found, each containing more than ten terms. They have roughly the same limit and are given fairly well by the following formulas:

$$\text{I} \qquad \nu_0^n = 92{,}000 - R/(n-0.95)^2,$$

$$\text{II} \qquad \nu_0^n = 92{,}000 - R/(n-1.5)^2$$

$$n = 3, 4, 5, \text{ etc.}$$

The bands of class I fall into the first series and those of class II into the second. The first member of the second

series coincides with the bands investigated by Kistiakowsky at 2300A but this may be accidental as those bands appear at much higher pressures.

All the observed facts go to show that one of the valence electrons between the two carbons is excited and that the two series are due to the different coupling of its orbital momentum with the internuclear axis. Thus the upper levels of class I can be provisionally designated as $P\Pi$ levels and those of Class II as $P\Sigma$ levels.

As many as ten vibrational transitions accompany some of the fundamental electronic transitions. Their analysis is greatly simplified by the magnitudes of the isotopic shifts. It appears that the CC bond is weakened considerably in the upper states whereas the CH bond remains practically unaltered. This is in agreement with the fact that no CH vibration is excited by absorption from the normal state and also that the shift in zero point energy is only about 20 cm^{-1}. All the bands of appreciable intensity are included in our classification.

The band system at 1520A shows strong predissociation. The next system at 1340A is slighly diffuse whereas all the bands at shorter wave-lengths appear to be sharp. If it is assumed that the predissociation is due to interaction with the normal state, then the heat of dissociation of C_2H_2 into CH+CH must be slightly less than 8.1 electron-volts or the energy of the triple CC bond is slightly less than 187 Cal./Mol.

The situation is similar in ethylene. The bands are somewhat more diffuse and only one Rydberg series is observed. Predissociation occurs at 1750A giving the heat of dissociation corresponding to $C_2H_4 \rightarrow CH_2+CH_2 \equiv 7.05$ electron-volts or the strength of the C=C bond $\leq$162 Cal./Mol.

The bond strengths are in good agreement with the best chemical data. It is thus clear that the work is going to be of considerable value in the recently developed chemistry of free radicals.

The early part of the work was done in collaboration with Dr. G. B. Collins.

W. C. PRICE

Department of Physics,
The Johns Hopkins University,
May 1, 1934.

The Orientation of the CO_3 Groups in Ammonium Bicarbonate Crystal

Ammonium bicarbonate, $(NH_4)HCO_3$ crystallizes in the orthorhombic system and its structure has recently been analyzed by x-ray methods by Mooney.[1] He finds that the CO_3 groups in the crystal are all oriented with their planes parallel to $a(100)$, and that the dimensions of the CO_3 groups are practically the same as in the normal carbonates.

Measurements on the magnetic anisotropy of the crystal confirm these conclusions. Denoting by x_a, x_b and x_c the principal gram molecular diamagnetic susceptibilities of the crystal along its a, b and c axes, respectively, it is found that

$$x_b - x_a = 5.0; \qquad x_c - x_a = 4.5$$

in 10^{-6} c.g.s. e.m.u., x_b and x_c are thus nearly equal and greater than x_a by about 4.7×10^{-6}, which is practically the same as the value of the magnetic anisotropy of the CO_3 group in calcite, aragonite, strontianite and witherite, obtained by Krishnan, Guha and Banerjee.[2] This shows that the CO_3 planes in ammonium bicarbonate crystal are oriented parallel to one another in the $a(100)$ plane, and that the magnetic anisotropies of these CO_3 groups, and hence presumably their structure also, are the same as in the normal carbonates quoted above.

In strong contrast to the magnetic behavior of ammonium bicarbonate is that of potassium bicarbonate. The latter crystal (which is monoclinic) exhibits a much feebler anisotropy, which shows that the planes of the different CO_3 groups in the unit cell of this crystal must be considerably inclined to one another.

ASUTOSH MOOKHERJEE

210 Bowbazar street,
Calcutta, India,
April 17, 1934.

[1] Mooney, Phys. Rev. **39**, 861 (1932).
[2] Krishnan, Guha and Banerjee, Phil. Trans. **A231**, 235 (1933).

Two New Phenomena at Very High Pressure

It has long been surmised that there should be another modification of bismuth, denser than the liquid phase, stable only under high pressure, in analogy to the high pressure modifications of ice. Attempts to produce this new phase by the application of pressures up to 20,000 kg/cm² have, however, been unsuccessful. I have recently found that this modification is produced reversibly from the ordinary solid phase at room temperature at about 25,000 kg/cm². The transition is accompanied by a volume decrease of about 9 percent. By extrapolation, the liquid should be about 5 percent more dense than the ordinary solid at the reversible melting point under 25,000 kg/cm², so that we may expect the new solid to be formed from the liquid with a contraction of the order of 4 percent. The next obvious step is to raise the temperature in order to find the location of the triple point between the two solids and the liquid, but this must wait for modifications in the present apparatus.

Hitherto the irreversible transition from white to black phosphorus has not been produced at temperatures below 200°C, where the pressure necessary is about 12,000 kg/cm². I have just made black phosphorus from white at room temperature by the application of about 35,000 kg/cm². In appearance to the eye the mass is indistinguishable from regular black phosphorus, but there was no trace of any red phosphorus on the exterior surfaces;

such has always been found before. However, the transition from white to black is apparently not quite as complete under the new conditions as at higher temperature and lower pressure, for on breaking the freshly formed mass open with a knife there were a few flashes of flame, indicating nuclei of still untransformed white phosphorus. The density is only 2.59 against 2.69 for the regular black phosphorus. It is furthermore to be remarked that at room temperature the transition takes place from that modification of white phosphorus which is stable at atmospheric pressure only below −80°C, instead of from the normal form of white phosphorus stable at room temperature. It is therefore possible that the new black phosphorus is not exactly the same as that known before.

The two experiments described above were instigated by the recent development of a new grade of steel considerably stronger than any steel yet available to me. With this I have reached pressures well over 40,000 kg/cm². A number of interesting questions suggest themselves for rough qualitative examination in this extended pressure range.

P. W. BRIDGMAN

Harvard University,
May 14, 1934.

Beta-Radioactivity of Neodymium

In a previous publication[1] Professor W. M. Latimer and the present author mentioned evidence for the radioactivity of neodymium in connection with a report of work on the alpha-activity of samarium and the possible activity of other rare earths. Since that time, additional evidence for a beta-ray neodymium activity has appeared which seems to be sufficiently interesting and conclusive to justify publication.

A sample of Nd_2O_3 originally prepared by Professor James was carefully purified to remove lead, bismuth, barium, thorium and their radiaoctive homologues, and its activity measured. After having allowed it to stand for seven months the activity was measured again and was found to be the same within fifty percent. In addition, absorption experiments showed 5 mm of air could completely stop the radiation. Magnetic deflection experiments were then completed. It was found possible to bend the hardest of the radiation into circles of 7.5 mm radius, or less, by a field of 500 gauss. Finally, purification of a Nd_2O_3 sample prepared by Professor B. S. Hopkins revealed a residual activity of the same intensity and properties.

These data seem to make the presence of any of the known radioactive series in significant amounts extremely improbable. The possible presence of a rare earth impurity which might emit such a radiation was checked by deflection experiments done on samarium, lanthanum, and praseodymium, none of which showed a deflectable radiation of intensity greater than one-third of that of the neodymium. The intensity of the alpha-radiation from the samarium was about ten times that from the neodymium in the absence of a field.

The apparatus used was essentially a Geiger-Müller counter with a wall of copper screen having five No. 28 wires to the cm. The deflection measurements were made by surrounding the counter with a concentric cylinder having the Nd_2O_3 on its inner surface, 15.0 mm from the counter wall, and with a solenoid wound around it. The charge determination consisted of observing the effect of field reversal when slanting metal vanes were placed between the sample and counter cylinder.

Fig 1. shows the magnetic deflection data. The abscissae are the $H\rho$ values of particles which would just miss the counter under the most favorable conditions of emission and the given field. The maximum $H\rho$ value apparently is

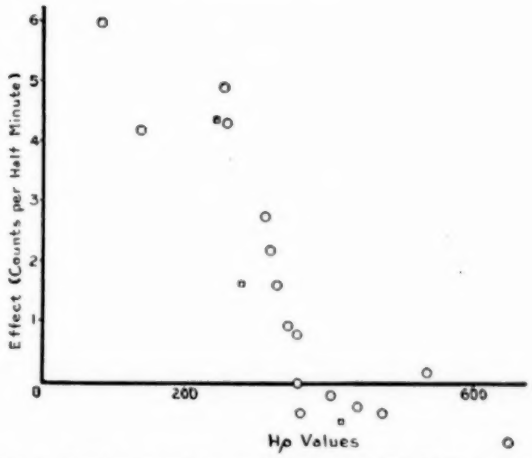

FIG. 1. Circles, James sample; squares, Hopkins sample.

close to 355 which agrees well with the observed range according to the data of Schonland[2] on cathode rays. This means a range of 2.4 mm in air. Table I shows the data from the charge determination experiment. The direction for negative charge was checked by using KCl and by geometrical calculation.

Each of the four values given is the mean of about 900 readings. The runs with sample present and sample absent were made on different days and the absolute values are of little significance. The effect, $+0.90\pm0.22$, of the addition of the sample appears conclusive. The effect indicating low energy positives from the wall in the absence of the sample remains unexplained but definite. The table shows that the

TABLE I.

	Count per half minute with field so		
	negatives pass	positives pass	Effect
Sample present	23.37 ± 0.108	23.07 ± 0.107	$+0.30\pm0.15$
Sample absent	23.38 ± 0.108	23.98 ± 0.11	-0.60 ± 0.15

[1] W. F. Libby and W. M. Latimer, J. Am. Chem. Soc. **55**, 433 (1933).

[2] Schonland, Proc. Roy. Soc. **A104**, 235 (1923); **A108**, 187 (1925).

effects being measured were all small compared to the background count due to cosmic rays, γ-rays, and other effects.

From the $H\rho$ value the range in Nd_2O_3 is calculated to be 3.4×10^{-5} cm. This range, together with the values for the efficiency of the counter obtained from measurement on KCl (3740 ± 200 per mole per half minute) permits the interpretation of the 5.2 ± 0.05 counts per half minute from Nd_2O_3 as giving a half-life of 1.5×10^{12} years.[3]

A fuller account of the work is to be submitted for publication soon. The author wishes to thank Professor Latimer and others for valuable advice and assistance given him during this research.

W. F. LIBBY

Department of Chemistry,
University of California,
Berkeley, California,
April 23, 1934.

[3] The decay constant of K used is that of Mühlhoff, Ann. d. Physik **399**, 205 (1930).

Remark on the Energy Distribution of Neutrons from Fluorine

In a beautiful experiment, Bonner and Mott-Smith[1] obtain the energy distribution of the neutrons ejected by fluorine when bombarded by Po α-particles. Four groups of neutrons are observed. Their velocities and energies as measured by their recoil protons are reproduced in Table I together with the results of Chadwick and Constable[2] on the disintegration of F by α-particles with proton emission. Chadwick and Constable showed that each of the pairs of

TABLE. 1

	Protons from F				Neutrons from F			
Group	Range of H (cm)	K.E. of H (10^6 e.v.)	Vel. of α (10^9 cm/sec.)	K.E. of α (10^6 e.v.)	Group	Range of recoil H	Vel. of neutron	K.E. of neutron
I (l)	56	6.75	1.59	5.25	(a)	10.5	2.20	2.54
(s)	47	6.05			(b)	7.8	2.01	2.11
II (l)	40	5.54	1.39	4.0	(c)	4.9	1.74	1.59
(s)	30.5	4.86			(d)	2.8	1.45	1.10
III (l)	33.5	4.99	1.28	3.4				
(s)	25	4.28						

protons, consisting of one long and one short group, arises from α-particles entering the nucleus through one level; that the shorter group (s) and the longer group (l) correspond to disintegration resulting in a Ne nucleus in an excited and the normal state, respectively. This is strongly supported by the consistency of the values of the energies of disintegration Q

$$Q=(1/2m_N)[m_H(m_N+m_H)v^2_H - M(m_N-M)V^2-2MVm_Hv_H] \quad (1)$$

for protons ejected in the direction of the α-particle and hence having the maximum velocity. m_H, v_H, M, V are the mass and velocity of the proton and α-particle, respectively, m_N the mass of the resulting nucleus. For all the three pairs of proton groups, $Q_1=0.99\times10^6$ e.v. and $Q_0=1.67\times10^6$ e.v., where Q_0, Q_1 correspond to disintegration with resulting nucleus in the normal and the excited state, respectively. This is rendered clear by Fig. 1.

To account for the four neutron groups observed, it is most natural to assume that they arise from disintegration of F by α-particles entering the nucleus through the same energy levels as in the case of proton emission. We may also assume that the resulting nucleus is capable of existing in an excited state. The disintegration scheme must be

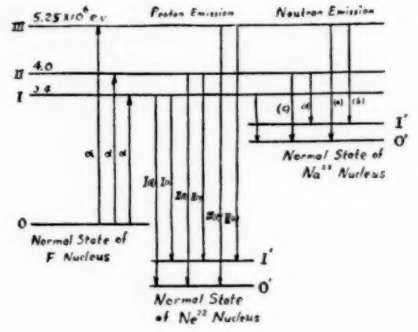

FIG. 1.

such that the four neutron groups should give consistent values of Q_0's and Q_1's. Within the limits of the accuracy of the neutron velocity as calculated from the range-velocity relation for the recoil proton, two assignments are possible,[3] namely: (i) The groups (a), (b) correspond to the disintegration III→O′, III→I′, while the groups (c), (d) to II→O′ and II→I′, respectively. The values of Q_0, Q_1 may be readily calculated by means of Eq. (1) and the data in Table I.

$$Q_0(\text{a})=-2.34\times10^6 \text{ e.v.}; \quad Q_0(\text{c})=-2.10\times10^6 \text{ e.v.}$$

$$Q_1(\text{b})=-2.73\times10^6 \text{ e.v.}; \quad Q_1(\text{d})=-2.54\times10^6 \text{ e.v.}$$

When one considers the sensitiveness of the Q's to the velocities of the neutrons, the consistency of the Q's may be regarded as fair. Using these values of the Q's, we can easily show that the other two neutron groups arising from α-particles entering through the level I would give recoiled

[1] Bonner and Mott-Smith, Phys. Rev. **45**, 552 (1934).

[2] Chadwick and Constable, Proc. Roy. Soc. **A135**, 48 (1932).

[3] The assignment (a) II→O′, (b) II→I′, (c) I→O′, and (d) I→I′ can be left out for it leads to values of Q_0's differing by about 25 percent, and also the Q_1's. The assignment (a) III→O′, (b) III→I′, (c) II→O′ (d) I→O′ is first thought to be not likely the case; for a rough calculation shows that the neutron of the group II→I would have a velocity of about 1.3×10^9 cm/sec. corresponding to a recoil proton range within the region measured. However, as pointed out to the writer by Professor Mott-Smith, this group may appear together with the group I→O′ as a single group in the measurement. Thus the above alternative is not impossible.

protons having ranges of about 1.4 and 0.5 cm. (ii) The groups (a), (c) correspond to the disintegration II→O′ and II→I′, while the groups (b), (d) to I→O′ and I→I′, respectively. On this assumption, we find

$$Q_0(\text{a}) = -1.24\times10^6 \text{ e.v.}; \quad Q_0(\text{b}) = -1.08\times10^6 \text{ e.v.}$$

$$Q_1(\text{c}) = -2.1\times10^6 \text{ e.v.}; \quad Q_1(\text{d}) = -2.01\times10^6 \text{ e.v.}$$

With these values of the Q's, one finds that the ranges of the recoiled protons of the neutrons arising from α-particles entering through level III are roughly 22 and 13 cm. If the idea of these assignments is correct at all, the detection of either two short groups or two long groups will decide between the two possibilities. Professor Mott-Smith kindly communicated to the writer that while they found no evidence for such long groups, they actually found a group of 1.5 cm range. Thus the first assignment above seems very probable. The consistency of this assignment lends further support to the results of Chadwick and Constable and it seems very desirable to carry out a similar investigation on the neutrons from Al whose proton emission has been studied by many investigators with not entirely identical results.

It is of some interest to estimate the mass of Na_{11}^{22} as the result of the disintegration

$$F_9^{19}+He_2^4\rightarrow Na_{11}^{22}+n_0^1. \tag{2}$$

For this purpose one needs the mass of F_9^{19} which may be calculated from the data in Table I for the disintegration

$$F_9^{19}+He_2^4\rightarrow Ne_{10}^{22}+H_1^1. \tag{3}$$

Taking H = 1.0072, Ne = 21.9893, He = 4.0011, Q = 0.0018, then for the three long-range groups I(l), II(l), III(l), one finds for the nuclear mass of F 18.9972. Using this in Eq. (2) and taking n_0 = 1.0065, one gets for the scheme (i) the nuclear mass of Na_{11}^{22} 21.9942, the mean value of $Q_0 = -2.22\times10^6$ e.v. being used. The negative sign of the Q_0's shows that part of the K. E. of the α-particle goes into the mass of Na_{11}^{22} which may be radioactive with positron emission.

TA-YOU WU

Department of Physics,
University of Michigan,
May 12, 1934.

The Prediction of Isotopes

As a result of the work of Aston[1] and others, we now have extensive information about the isotopes associated with the various chemical elements. The writer[2] has attempted to explain the regularities observed for the lighter nuclei. For nuclei of mass number $M>36$, it is known[3] that regularities exist, but the general character of the pattern is still much of a mystery. It is the purpose of the present note to point out further regularities, and to attempt to put the prediction of new isotopes on a somewhat more systematic basis than it is at present.

Beck[4] has emphasized that there are many sequences of isotopes such that, between two successive members of a sequence, $\Delta Z=2$ and $\Delta M=4$. If a member of the sequence be missing, then it may be supposed that this is merely a stable isotope which remains to be discovered. That is, one may interpolate with some degree of confidence.

The isotope pattern is, however, a two-dimensional affair and the above sequences run in one direction only. Since H 3 particles are known to be stable (and might conceivably have an independent existence within the nucleus), it has seemed worthwhile to investigate the sequences of the type $(\Delta M/\Delta Z)=3$. In fact, a very convenient way of representing the isotope pattern is by means of a plot in which the sequences $(\Delta M/\Delta Z)=2$ run vertically, and the sequences $(\Delta M/\Delta Z)=3$ run horizontally. (A "sequence" will be supposed to contain at least three members.)

The horizontal sequences contain, as a rule, more members than do the vertical sequences, and should, therefore, be more useful for the purposes of prediction. Some of them follow: S 34, Cl 37, A 40; A 36, K 39, (Ca 42), Sc 45, Ti 48, V 51, Cr 54; Cr 52, (Fe 58), (Ni 64), Zn 70, Ge 76, Se 82; Fe 56, Co 59, (Ni 62), Cu 65, Zn 68, Ga 71, Ge 74; Ni 60, Cu 63, Zn 66, Ga 69, Ge 72, As 75, Se 78, Br 81, Kr 84, Rb 87, (Sr 90); Ni 58, Zn 64, Ge 70, Se 76, Kr 82, Sr 88, Zr 94, Mo 100, (Ru 106), (Pd 112), Cd 118, Sn 124, Te 130, Xe 136; Mo 94, (Ma 97), Ru 100, (Rh 103), (Pd 106), Ag 109, Cd 112, In 115, Sn 118, Sb 121, Te 124, I 127, Xe 130, Cs 133, Ba 136, La 139, Ce 142; and Ru 96, (Pd 102), Cd 108, etc., clear to Pb 210. The others may be read from the pattern—the ones above are given to show that the sequences do extend over a wide range. (The parentheses indicate elements predicted). The sequence from Ru 96 to Pb 210 has only seven gaps, namely, Pd 102, Te 120, Ba 132, Ce 138, Sm 150, Hf 180, and Pt 198. Palladium, hafnium and platinum have not been analyzed, so that there may be only four gaps in the sequence of twenty members.

On the basis of this two-dimensional interpolation method, one may predict the following isotopes as reasonably probable (for $M>36$): Ca 42; Fe 57, 58; Ni 61, 62, 64; Sr 84, 90; Zr 91; Ma 97, 99; Pd 102, 104–8, 110, 112; Rh 101, 103; Ru 106; Te 118, 120; Ba 130, 132, 134, 140; La 137; Ce 136, 138, 139, 141, 144; Pr 143; Il 145, 147; Nd 148; Sm 150, 151; Gd 154; Tb 157; Dy 160; Ho 163; Hf 176–180; Ir 191, 193; Pt 192–196, 198; and Au 197, 199. It may be that more than this number will be found, but the writer believes this to be a fairly conservative estimate.

JAMES H. BARTLETT, JR.

Department of Physics
University of Illinois,
May 15, 1934.

---

[1] F. W. Aston, *Mass Spectra and Isotopes*, 1933; Nature **132**, 930 (1933) and **133**, 327 (1934).
[2] J. H. Bartlett, Jr., Nature **130**, 165 (1932) and Phys. Rev. **41**, 370 (1932).
[3] H. A. Barton, Phys. Rev. **35**, 408 (1930).
[4] Guido Beck, Zeits. f. Physik **47**, 407 (1928).

Some Observations of the Sky Polarization During the Total Solar Eclipses of August 31, 1932 and February 14, 1934

In connection with my photographic and visual observations of the polarization of the corona during the 1932 and 1934 total solar eclipses, the polarization of a point in the sky was observed at a distance of 8 degrees from the sun at mid-totality. A Martens polarization photometer was used in the Gray, Maine, eclipse, and a Schmidt and Haensch half-shadow polarimeter at Losap Islands, in the South Seas. The instruments were mounted rigidly. Polarization curves were obtained during the eclipse days, and two days each for comparsion.

Both eclipses were observed under perfectly clear skies. It was found that the polarization of the 8° points shows smooth curves for the comparison days, the polarization changing according to the position of the sun. A considerable, sudden *increase of the polarization* was observed during totality for the 8° points, both in 1932 and 1934. After totality the polarization follows again curves similar to those of the comparison days, see Fig. 1.

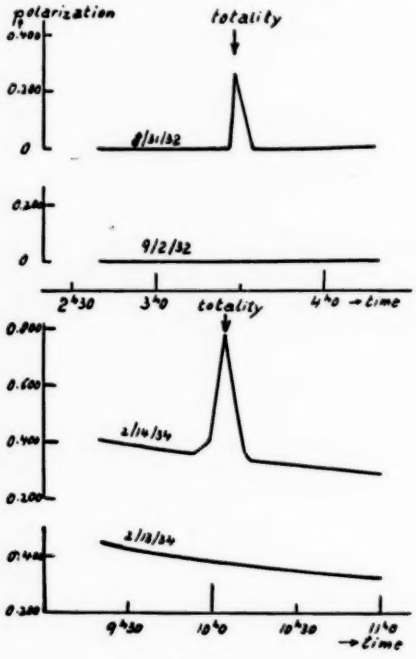

FIG. 1.

The plane of polarization of the 8° points changed during the comparison days according to the position of the sun. During totality, however, the plane of polarization *deviates by several degrees* from the strictly radial polarization observed otherwise.

The increase of sky polarization during totality may be set in parallel with the increase of polarization observed frequently a short time after sun-set, and explained by the Tyndall-Rayleigh- or a similar law, see Tichanowsky.[1] The deviation of the plane of polarization cannot be explained, however, by the Tyndall-Rayleigh- or a similar theory. An explanation may be based on the assumption that the light of the sky contains two components: Scattered light of the sun, and self-luminescence. The latter may be excited by electron impact of gases in the atmosphere, such as found in my recent experiments.[2]

In conclusion, the author wishes to express his thanks to Professors A. C. Hardy of Massachusetts Institute of Technology and C. L. A. Schmidt of the University of California for loan of the instruments, and to Mrs. R. N. Mayall of Harvard College Observatory, Mrs. W. M. Cohn, and Mr. T. Hirai of Kyoto Imperial University, Astronomical Institute, for their able assistance in this work. The 1932 program was supported by grants from the Rumford and Permanent Science Funds of the American Academy of Arts and Sciences. My thanks are due to the Imperial Japanese Government for transportation facilities between Japan and Losap Islands and for many courtesies shown.

WILLI M. COHN

Berkeley, California,
April, 1934.

[1] J. J. Tichanowsky, Meteorologische Zeits. **41**, 352 (1924).
[2] W. M. Cohn, Zeits. f. Physik **75**, 544 (1932).

On the Scattering of X-Rays from Nitrogen at Small Angles and High Pressure

It has long been known[1] that the intensity of x-rays scattered from solids and liquids rapidly diminishes as small angles of scattering are approached. This has been by some ascribed to the crystalline or pseudo-crystalline nature of the scatterer from which it might be inferred that the effect would not occur in the case of a truly amorphous substance such as a gas. But as pointed out by Warren[2] this decrease in scattering need not necessarily imply a crystalline structure but merely that the atoms in the scatterer are close together. Indeed, Debye[3] showed a number of years ago that even in the case of a gas there should be a decrease in scattered intensity as zero angle of scattering is approached. For this decrease to become noticeable, however, it is necessary to measure the scattering at rather high densities such that the volume of the molecules of the gas is not negligible compared to the volume occupied by the gas. If this is the case then the intensity $\sim\phi$ curve should exhibit a maximum at an angle ϕ_m given approximately by the Ehrenfest-Keesom relation[4]

$$\sin \phi_m/2 = \lambda/0.814\times 2a, \qquad (1)$$

where a is the average distance between molecules and on

[1] P. Debye and P. Scherrer, Gött. Nachr. 1 and 16 (1916); C. W. Hewlett, Phys. Rev. **20**, 688 (1922).
[2] B. E. Warren, Phys. Rev. **44**, 969 (1933).
[3] P. Debye, J. Math. and Phys. **4**, 133 (1925); Phys. Zeits. **28**, 135 (1927).
[4] P. Ehrenfest, Versl. Kon. Akad. Amsterdam **17**, 1184 (1915); W. Keesom and J. deSmedt, ibid. **25**, 118 (1922).

the assumption of close packing of spheres is given by $a=1.33(M/\rho)^{\frac{1}{3}}$ where M is the molecular weight ρ the density and a is in Angstroms. At smaller angles the intensity should drop, approaching a finite value as $\phi \rightarrow 0$.

With this in mind filtered Mo $K\alpha$ radiation has been scattered from nitrogen at a pressure of 1270 lbs./in.^{2} at 21°C. This corresponds to a density of 0.10 g. cm^{-3}. According to Eq. (1) ϕ_m should be about 5° 45′ at this density. A very definite angle of scattering was obtained by the use of crossed Soller slits in both the primary and scattered beams, giving a maximum angular divergence of about 0.5°. This, of course, greatly reduces the intensity. A further difficulty is the fact that for the windows of the scattering cell to be strong enough to withstand the pressure they must also be so thick that the scattering from the windows is comparable in intensity with that from the gas, and as the scattering from the windows can enter the ionization chamber at small angles the background is rather large.

Although the intensity was excessively weak it has been possible to show that there definitely is a rather flat maximum at about 6° below which the scattering decreases somewhat, apparently approaching a finite value at very small angles, in (at least qualitative) agreement with Debye's theory. The scattering has not been measured below 1.5°.

The work is being continued and more complete details will be given later with, it is hoped, data at both higher and lower pressures.

G. G. HARVEY*

Ryerson Physical Laboratory,
University of Chicago,
May 15, 1934.

* National Research Fellow.

The Acceleration of Electrons to High Energies

The general method of accelerating ions to high velocities[1] by means of electrical fields that effectively move with the same speed as the ion has been adapted to the special case of the acceleration of electrons. In the previous work the ions were accelerated with "moving fields" obtained by connecting a series of short cylindrical electrodes, mounted in a long evacuated discharge tube, to points on a transmission line in such a way that a potential surge travelling on the transmission line was applied to the electrodes in succession. The transmission line was so designed that the electric field, produced between each pair of electrodes in succession by the potential surge on the line, travelled with effectively the same speed as the ion being accelerated along the axis of the tube. By this means protons with energies corresponding to several million volts have been obtained without the use of very high electrical potentials.

The acceleration of electrons by this method presents a somewhat unique problem because of the very high speed they attain in falling through comparatively modest potentials. For example, a 10^5 volt electron moves 1.65×10^{10} cm/sec. while a 10^6 volt electron moves over 94 percent the velocity of light. Therefore after the energy of the electron has attained say a million volts a transmission line should be used that will permit the potential surge to travel with almost the velocity of light. This of course necessitates a line with very small "loading" or "tapering." Attempts are under way in this laboratory to test the feasibility of this general type of line. Fortunately there exists a quite obvious and simple extension of the above method that can make an electric field "move" down the discharge tube with an effective velocity even greater than the velocity of light if such were desirable. Instead of applying the potential surge to the electrodes in the discharge tube in succession by a single transmission line the potential may be applied by means of a number of different transmission lines of increasing lengths each attached to a separate electrode. In our present apparatus 4 cylindrical aluminum electrodes 5 cm long and 1 cm internal diameter are mounted along the axis of a glass tube 2.2 cm in diameter at intervals of 60 cm. One end of the tube is sealed by a metal cap in which is mounted a tungsten filament heated by an insulated storage battery. The electrons from the hot filament (field emission might also be used) are accelerated along the axis of the tube through the 4 electrodes and into a grounded chamber where they impinge upon a fluorescent screen. Their velocity is measured by their deflection in a uniform magnetic field. The McLeod gauge showed a "sticking vacuum." The source of potential consisted of a small Van de Graaff generator constructed according to a design of Tuve. This generator applies a potential across a condenser, one side of which is grounded, until a discharge occurs between two metal spheres 25 and 40 inches in diameter (it may be noted that a Marx or impulse generator should serve equally well for the source of potential). The electric impulse or surge produced by the discharge between the spheres is applied simultaneously to five transmission lines. The end of the first transmission line is attached to the metal cap in which the hot filament is mounted while the ends of each of the 4 other lines are attached to the respective remaining cylindrical electrodes. A negative potential surge upon its arrival at the end of the first line lowers the potential of the filament and produces a field that accelerates the electrons toward the first cylindrical electrode. When the "blast" of electrons reaches the first cylindrical electrode the negative potential surge on the second transmission line is made to arrive at this same electrode. This in turn produces a field between the first and second cylindrical electrodes so that the electrons are again accelerated. The remaining three transmission lines were so adjusted that the potential surge was applied to the second, third, and fourth cylindrical electrodes,

[1] Beams and Snoddy, Phys. Rev. **44**, 784 (1933); **45**, 287 (1934); Ham and Beams, Washington Meeting, 1934.

respectively, at the proper times to give the moving electrons maximum acceleration. The end of the last line was grounded through a resistance to prevent "floating" while the ground wires were attached to the grounded side of the condenser. By means of the above arrangement with a spark gap distance between the spheres corresponding to 300,000 volts we have obtained electrons with energies of 1.3×10^6 volts, i.e., each transmission line effectively adds 260,000 volts to the energy of the electrons or 86 percent of the spark gap voltage. In view of these first results we believe that with an extension of this method in which a larger number of transmission lines are used it may be possible to secure electron energies of many times that already obtained. However, it should not be overlooked that the potential surge or wave produced by a spark in air has a finite slope and that the total effective surge impedance of the lines decreases with increasing number of lines so that for the present condenser spark gap system the number of lines cannot be advantageously increased beyond a certain limit. Yet on the other hand the potential increases at reflection at the end of each line. Also some recent measurements made by Mr. J. W. Flowers in this laboratory indicate that potential surges many times steeper than those produced by an ordinary spark in air can be obtained.

It is a pleasure to record our indebtedness to Dr. L. B. Snoddy for many helpful discussions and to the Virginia Academy of Sciences for a grant that made possible the construction of the Van de Graaff generator.

J. W. Beams
H. Trotter, Jr.

Rouss Physical Laboratory,
University, Virginia,
May 17, 1934.

The Mass of the Neutron from the Nuclear Reaction $H^2+H^2\rightarrow He^3+n^1$

In recent experiments by Oliphant, Harteck and Rutherford,[1] and by Dee,[2] compounds containing H^2 were bombarded with deutons of energies up to 0.1 m.e.v. In addition to two groups of charged particles, neutrons were observed in large numbers. This neutron emission was best accounted for by assuming the process

$$H^2+H^2\rightarrow He^3+n^1. \qquad (1)$$

The He^3 was not detected; however momentum considerations based upon the measured neutron energy lead to an expected range for the He^3 particles of only 5 mm, a range too short to be observable in these experiments.

One notes that the mass-energy relation of Eq. (1) may be used for a determination of the mass of the neutron. Thus:

$$n^1=2H^2-He^3+T(H^2)-T(He^3)-T(n^1). \qquad (2)$$

The mass of He^3 has been obtained[1, 3] from the reaction

$$Li^6+H^1\rightarrow He^3+He^4. \qquad (3)$$

Hence, if we assume the validity of process (1), the measurement of the mass of He^3 from (3), the absence of gamma-ray emission in both (1) and (3), and an accurate measurement of the neutron kinetic energy, reaction (1) yields an accurate value for the mass of the neutron.

However, Oliphant, Harteck and Rutherford obtained two different values of the He^3 nuclear mass;

(a) $He^3=3.0155$ if the Li^6 nuclear mass equals 6.0129 ±0.0003 as obtained by Bainbridge,[4]

(b) $He^3=3.0167$ if the Li^6 nuclear mass equals 6.0141[5] as obtained from the data[6] of the reaction

$$Li^6+H^2\rightarrow 2He^4. \qquad (4)$$

The maximum neutron energy was measured by Oliphant, Harteck and Rutherford, and by Dee as about 2 m.e.v. From momentum considerations, neglecting the impulse of H^2, the kinetic energy He^3 equals 0.7 m.e.v. The mass of H^2 is 2.0131; its kinetic energy is 0.1 m.e.v. The mass of the neutron is, therefore,

(a) 1.0079 if Bainbridge's Li^6 is used,

(b) 1.0067 if the Li^6 is taken from (4).

The emission of gamma-radiation from lithium bombarded by protons has been observed.[7] If this is associated with (3), the mass of He^3 may be lowered and that of the neutron raised. No study of gamma-ray emission for (1) has yet been reported.

The purpose of this letter is not to stress the specific values of the neutron mass above, but to point to the likelihood that reaction (1) may lead to a reliable value of the neutron mass.

H. H. Goldsmith
Victor W. Cohen

Columbia University,
New York, New York,
May 17, 1934.

[1] Oliphant, Harteck, and Rutherford, Nature **133**, 413 (1934): Proc. Roy. Soc. **A144**, 692 (1934).
[2] Dee, Nature **133**, 564 (1934).
[3] Wu and Uhlenbeck, Phys. Rev. **45**, 553 (1934).
[4] Bainbridge, Phys. Rev. **44**, 56 (1933).
[5] The probable error is not given by *O*, *K*, *R*, but we estimate it from their data to be about ±0.0002 m.u.; hence we retain both values of the mass of He^3 in the calculation.
[6] Oliphant, Kinsey, Rutherford, Proc. Roy. Soc. **A141**, 722 (1933).
[7] R. v. Traubenberg, Eckardt, and Gebauer, Naturwiss. **21**, 694 (1933); Crane and Lauritsen, Phys. Rev. **45**, 63 (1934).